THE UNIVERSITY OF MICHIGAN

INDUSTRY PROGRAM OF THE COLLEGE OF ENGINEERING

THE CONSTANT VOLUME HEAT CAPACITIES OF GASEOUS TETRAFLUOROMETHANE, CHLORODIFLUOROMETHANE, DICHLOROTETRAFLUOROETHANE, AND CHLOROPENTAFLUOROETHANE

Yu-Tang Hwang

A dissertation submitted in partial fulfillment
of the requirements for the degree of
Doctor of Philosophy in The
University of Michigan
1961

February, 1961

IP-496

ACKNOWLEDGMENTS

The author wishes to express his gratitude to those who helped him in this research.

Professor Joseph J. Martin, his committee chairman, gave substantial help in many respects. Without his advice and encouragement, the completion of this project would not have been possible. The other members of his committee, Professors D. W. McCready, D. V. Ragone, G. J. Van Wylen, and E. H. Yound also gave freely their advice and help.

Dr. Noel de Nevers, who preceded the author on this project, supplied a great deal of useful information and many constructive suggestions. Mr. Lynn E. Paul, Associate Research Engineer of Electrical Engineering Department, helped with the design and fabrication of the electrical seals, and many persons in the machine shop of the Department of Chemical and Metallurgical Engineering assisted with other mechanical details.

The Esso Research Grant provided part of the funds for this research. The University of Michigan and the Nationalist Government of China supported the author by means of fellowship and scholarship. E. I. du Pont de Nemours and Company and Precision Rubber Products Corp. supplied materials without charge.

TABLE OF CONTENTS

TABLE OF CONTENTS (CONT'D)

LIST OF TABLES

LIST OF FIGURES

LIST OF FIGURES (CONT'D)

LIST OF FIGURES (CONT'D)

NOMENCLATURE

A	Work content, Helmholtz free energy
$A,B,C,$	Used as arbitrary constants in various equations
A_1,B_1,C_1 A_2,B_2,C_2 A_3,B_3,C_3 A_4,B_4,C_4 A_5,B_5,C_5	Constants used in the Martin-Hou equation of state
b	Constant used in the Martin-Hou equation
c	Speed of sound or speed of light
C_{calr}	Heat capacity of the calorimeter
C_p	Constant-pressure heat capacity
C_v	Constant-volume heat capacity
C_v^*	Constant-volume heat capacity at zero pressure
C_{gross}	Gross heat capacity of calorimeter and contents
$C_{sat}^{g,l}$	Heat capacity of two-phase mixture at constant volume
C_{sat}^{l}	Heat capacity of the saturated liquid
d	Differential operator
exp	Exponential operator
E	EMF
f g h	Functions
h	Planck constant

I	Electric current
k	Constant used in the Martin-Hou equation
k	Boltzman constant
ln	Natural logarithm
m	Mass
P,p	Pressure
Q	Quantity of energy
q	Rate of energy input
R	Resistance
R	Universal gas constant
r	Radius
S	Entropy
T	Temperature
t	Temperature
V	Volume
z	Compressibility factor

Greek Letters

$\alpha,\beta,\gamma,\delta$	Arbitrary constants used in various equation
Δ	Finite increment
θ	Time
ρ	Density
Ω	Ohms
ν	Vibrational frequency
ω	Wave number

Subscripts

c	Critical
corr	Correction
i	Summation index
mean	Mean value over some interval
R	Reduced
sat	Saturated
1	At the start of the heating period
2	At the end of the heating period

Superscripts

*	At the zero pressure
g	Gas phase
l	Liquid phase

THE CONSTANT VOLUME HEAT CAPACITIES OF GASEOUS TETRAFLUOROMETHANE, CHLORODIFLUOROMETHANE, DICHLOROTETRAFLUOROETHANE, AND CHLOROPENTAFLUOROETHANE

Yu-Tang Hwang

ABSTRACT

Constant-volume heat capacity (C_v) data have been determined for four common refrigerants, tetrafluoromethane, chlorodifluoromethane, dichlorotetrafluoroethane and chloropentafluoroethane, as a function of temperature and density in the range of 70-400°F and 100-500 psi. Ideal-gas heat capacities (C_v^*) were obtained by extrapolating the C_v data to zero density and the results compared with values obtained by the method of statistical mechanics. The variation of the experimental heat capacities with density were compared with the variations predicted by equations of state. The applicability of the law of corresponding states to the C_v-C_v^* data was also considered.

A thin-wall large-volume adiabatic calorimeter was used. This type of calorimeter, first developed by N. H. de Nevers, was improved in this research in the following ways: (1) Safety provisions were greatly increased; (2) The maximum working temperature was raised from 150 to 200°C; (3) Fluctuations of data were minimized and the over-all accuracy was enhanced by a better designed adiabatic shield and by a newly developed method for calibrating the calorimeter heat capacity.

Comparison of the experimental C_v^* with those calculated statistically has revealed that, except for tetrafluoromethane for which agreement was unusually good, the currently available assignments

of fundamental frequencies for chlorodifluoromethane, dichlorotetrafluoroethane, and chloropentafluoroethane, are generally inadequate.

Comparison of the experimental $C_v-C_v^*$ data with those predicted by the Martin-Hou equation of state shows that the equation neither predicts the isotherms with the right curvature at a low density range nor represents the isometrics ($C_v-C_v^*$ vs. temperature) with a sufficient curvature. However, the Martin-Hou equation does correctly predict the small $C_v-C_v^*$ at high temperatures.

The law of corresponding states has been shown to be applicable to $C_v-C_v^*$ if the gases are similar in their molecular structures.

I. INTRODUCTION

I-1 Objectives of this Research

The accurate constant-volume heat capacity (C_v) measurements, at several densities and over a range of temperature, are useful in at least wo ways. (1) Ideal gas heat capacity (C_v^*) may be determined by extrapolating isotherms to zero density on the C_v vs. density plane. A set of C_v^* thus obtained may be utilized to shed light on the questions of molecular structure or the assignment of the fundamental frequencies. (2) Through exact thermodynamic relations, C_v may be related to the data of state. If the first or second derivatives of the pressure-volume temperature (PVT) data are involved in the corresponding expression, the chances are that C_v data may be more accurate than the same quantities calculated from the state data. This provides an opportunity to check or improve existing equations of state.

In 1958, Noel de Nevers[12] constructed a thin-wall large volume adiabatic C_v calorimeter and collected C_v data for propylene and perfluorocyclobutane at several densities and over a range of temperature from room temperature up to 150°C. This was the most recent effort in the field of constant-volume calorimetry. Although his calorimeter exploded at the estimated pressure of 860 psi, it certainly excelled previous calorimeters in many respects. For this reason, the present author decided to construct a similar but improved calorimeter, intended to achieve the following:

(1) An increase of the safety provisions to minimize the accidental damage to the instruments and operator.

(2) A raise of the maximum workable temperature from 150°C to 200°C (approximately 400°F).

(3) A better designed adiabatic shield to minimize fluctuations of data and enhance the over-all accuracy.

The main objectives of this research were:

(1) To collect C_v data for four common refrigerants as a function of temperature and density in the range of 70-400°F and 100-500 psi so that tables of thermodynamic properties may be calculated.

(2) To determine the ideal gas heat capacities by extrapolating the C_v data to zero density, and to compare them with the statistical calculations.

(3) To compare these experimental data with the available state data and the existing equations of state.

I-2 Constant-Volume Versus Constant-Pressure Calorimetry

Although the constant-volume heat capacity of gases is one of the most important thermodynamic properties, the basic technique for measuring C_v has not been as fully developed as constant pressure calorimetry. For instance, Osborne, Stimson, and Sligh[36] constructed a flow calorimeter in 1924 which produced C_p data reliable to plus or minus 0.1%. No comparable constant-volume calorimeter has been built.

In a flow calorimeter, a steady flow of gas passes through an apparatus where a known amount of heat is added to the gas. All measurements are made only when the entire system is at steady state. The net result is that only the gas changes the temperature, and the heat capacity of the apparatus is not involved in the calculation of C_p of the gas. In

the C_v measurement, however, the gas must be confined in the closed vessel of fixed volume which also changes its temperature with the gas when a known amount of heat is added. Thus the heat capacity of the calorimeter enters into the calculation and affects the accuracy of the results.

Reducing the heat capacity of the calorimeter is clearly a good approach to the problem; the concept resulted in the pioneering work of de Nevers and Martin[13] for the construction of a thin-wall large-volume C_v calorimeter.

I-3 Constant-Volume Heat Capacity Calculated by the Method of Statistical Mechanics

If sufficient data are available on the spectrum and structure of the complex molecule, C_v^* calculated by the method of statistical mechanics is often more accurate than the experimental C_v^*. Also, values can be determined over a temperature range far greater than the experimental range. Unfortunately, assigning fundamental frequencies and other necessary molecular constants still requires either largely empirical work or guessing. The experimental C_v data are often extrapolated to zero density to obtain C_v^*, as a guide to the selection of the fundamental frequencies. Once a reliable set of fundamental frequencies is worked out, C_v^* may be calculated over a wide temperature range.

The calculations are based on the assumption that the heat capacity may be divided into translational, rotational, and vibrational components. The translation and external rotation are independent of the nature and size of the molecule, and contribute R/2 per degree of

freedom per mole or a total of 3R for non-linear molecules. The total vibrational contributions are obtained as a sum of the contributions of all individual degrees of vibrational freedom, each corresponding to a particular value of the fundamental frequency ν_i, as follows:

$$(C_v^*)_\omega = R \sum_{i=1}^{n} \frac{x_i^2 e^{x_i}}{(x_i - 1)^2} \qquad (1\text{-}1)$$

where $X_i = \frac{h\nu_i}{kT} = \frac{hc\omega_i}{kT} = \frac{1.43868\omega_i}{T}$, n is the number of vibrational degrees of freedom (n = 3m-6 for non-linear molecules where m = number of atoms), T is in degrees Kelvin, and ω is in cm^{-1}. Equation (1-1) assumes harmonic vibrations. A correction may be added for anharmonic effects which are estimated by various empirical equations. For instance, McCullough, et al.[33] presented the semi-empirical equation for the total anharmonic contribution as follows:

$$C^*_{(anh)} = Z\left\{\frac{C^*}{R}\right\}\left\{3\left(\frac{C^*}{R}\right)/U - \left[1 + \frac{2}{U}\right]\left[\frac{H^* - H_o^\circ}{RT}\right]\right\} \qquad (1\text{-}2)$$

where $U = \frac{hc\omega}{kT}$, and the values (C^*/R) and $\frac{H^* - H_o^\circ}{RT}$ are those for an anharmonic oscillator of frequency ν. The adjustable parameters ν and Z are an arbitrary frequency and a term involving an arbitrary anharmonicity coefficient, respectively. If the experimental data and a reliable set of fundamental frequencies are available, two adjustable parameters ν and Z may be evaluated by assuming that the anharmonic contribution is the difference between the experimental C_v^* and the calculated C_v^* based on harmonic vibration. Mathematically, only two sets of conditions ($C^*_{(anh)}$ and corresponding temperature) will be required for evaluation of two arbitrary constants. The better results, however, may be obtained by evaluating two parameters from experimental values of C_v^* at three or

more than three temperatures, using an appropriate mathematical procedure.

I-4 Constant-Volume Heat Capacity and the State Behavior

The constant-volume heat capacity is related to the state data through the following exact thermodynamic relation, valid for the single phase of a pure substance:

$$\left(\frac{dC_v}{dV}\right)_T = -\rho^2 \left(\frac{dC_v}{d\rho}\right)_T = T\left(\frac{d^2P}{dT^2}\right)_V \qquad (1\text{-}3)$$

where V is the specific volume, T is the absolute temperature, P is the pressure, and ρ is the density. In the integral form, Equation (1-2) may be modified as follows:

$$C_v - C_v^* = -\int_V^\infty T\left(\frac{d^2P}{dT^2}\right)_V dV \qquad (1\text{-}4)$$

or

$$C_v - C_v^* = -\int_o^\rho \frac{T}{\rho_2}\left(\frac{d^2P}{dT^2}\right)_\rho d\rho \qquad (1\text{-}5)$$

Equations (1-3), (1-4), or (1-5) are frequently used as a check on state data and equation of state, since the second derivative of P with respect to T, or the curvature of the isometrics in P versus T plane, is not known with high accuracy. Each differentiation magnifies the fluctuation of data and the second derivative may present a considerable error, even though the PVT data are accurate within 1%. In other words, the check on the second derivative is a very severe test on the equation of state.

The general behavior of PVT relations has been discussed by various authors. Martin and Hou[27] pointed out the general characteristics

of the isometric and P versus T plot as follows:

$$\left(\frac{d^2P}{dT^2}\right)_V = 0 \quad \text{as } P \to 0 \tag{1-6}$$

$$\left(\frac{d^2P}{dT^2}\right)_V = 0 \quad \text{at } V = V_c \tag{1-7}$$

$$\left(\frac{d^2P}{dT^2}\right)_V = 0 \quad \text{for high T} \tag{1-8}$$

$$\left(\frac{d^2P}{dT^2}\right)_V < 0 \quad \text{at } V > V_c \tag{1-9}$$

$$\left(\frac{d^2P}{dT^2}\right)_V > 0 \quad \text{at } V < V_c \tag{1-10}$$

Later, Martin, Kapoor, and de Nevers[29] pointed out another condition, as follows:

$$\left(\frac{d^2P}{dT^2}\right)_V = 0 \quad \text{at } V = \frac{V_c}{n} \tag{1-11}$$

where n lies between 1.5 and 2.0. If the conditions represented by Equations (1-6) through (1-11) are substituted into Equations (1-4) or (1-5) in an appropriate order, it can be seen that for an isotherm of not too high temperature $C_v - C_v^*$ as a function of density starts from zero at zero density, increases gradually to a maximum at the critical density, then decreases to a certain point, and flattens at about 1.5 to 2.0 times the critical density.

It is interesting to compare the result of the above analysis with the isotherms predicted by various equations of state. The following are the analytical expressions of $C_v - C_v^*$ by various equations of

state as derived by de Nevers.[12]

Berthelot equation:[15]

$$C_v - C_v^* = \frac{2a}{T^2}\int_0^\rho d\rho = \frac{2a\rho}{T^2} = f(T)\rho \qquad (1\text{-}12)$$

Beattie-Bridgeman equation:[5]

$$C_v - C_v^* = \frac{6CR}{T^3}\left[\rho + \frac{B_o\rho^2}{2} - \frac{B_o b\rho^3}{3}\right] \qquad (1\text{-}13)$$

Benedict-Webb-Rubin equation:[6]

$$C_v - C_v^* = \frac{6}{T^3}\left[C_o\rho + \frac{C}{2\gamma}\{2\exp(-\gamma\rho^2) - 2 + \gamma\rho^2\exp(-\gamma\rho^2)\}\right] \qquad (1\text{-}14)$$

Martin-Hou equation:[27,29]

$$C_v - C_v^* = T\left(\frac{k}{T_c}\right)^2 \exp\left(\frac{-kT}{T_c}\right)\left[\frac{C_2\rho}{(1-\rho b)} - \frac{C_3\rho^2}{2(1-\rho b)^2} + \frac{C_5\rho^4}{4(1-\rho b)^4}\right] \qquad (1\text{-}15)$$

where all letters other than T and ρ are arbitrary constants, all of which are positive. de Nevers[12] has fully discussed the shape of isotherms on the $C_v - C_v^*$ versus ρ plot, and has shown that the Berthelot equation predicts the straight line through the origin; the Beattie-Bridgeman equation predicts the upward curvature at low density and the downward curvature at the high density; the Martin-Hou equation and the Benedict-Webb-Rubin equation predict the downward curvature at low densities and upward curvature at the very high densities. The latter three equations all predict (d^2P/dT^2) is zero at the critical density, and therefore, the isotherm reaches a maximum at the critical density. Figure 1-1 is a summary of de Nevers' conclusions and is reproduced from his thesis.

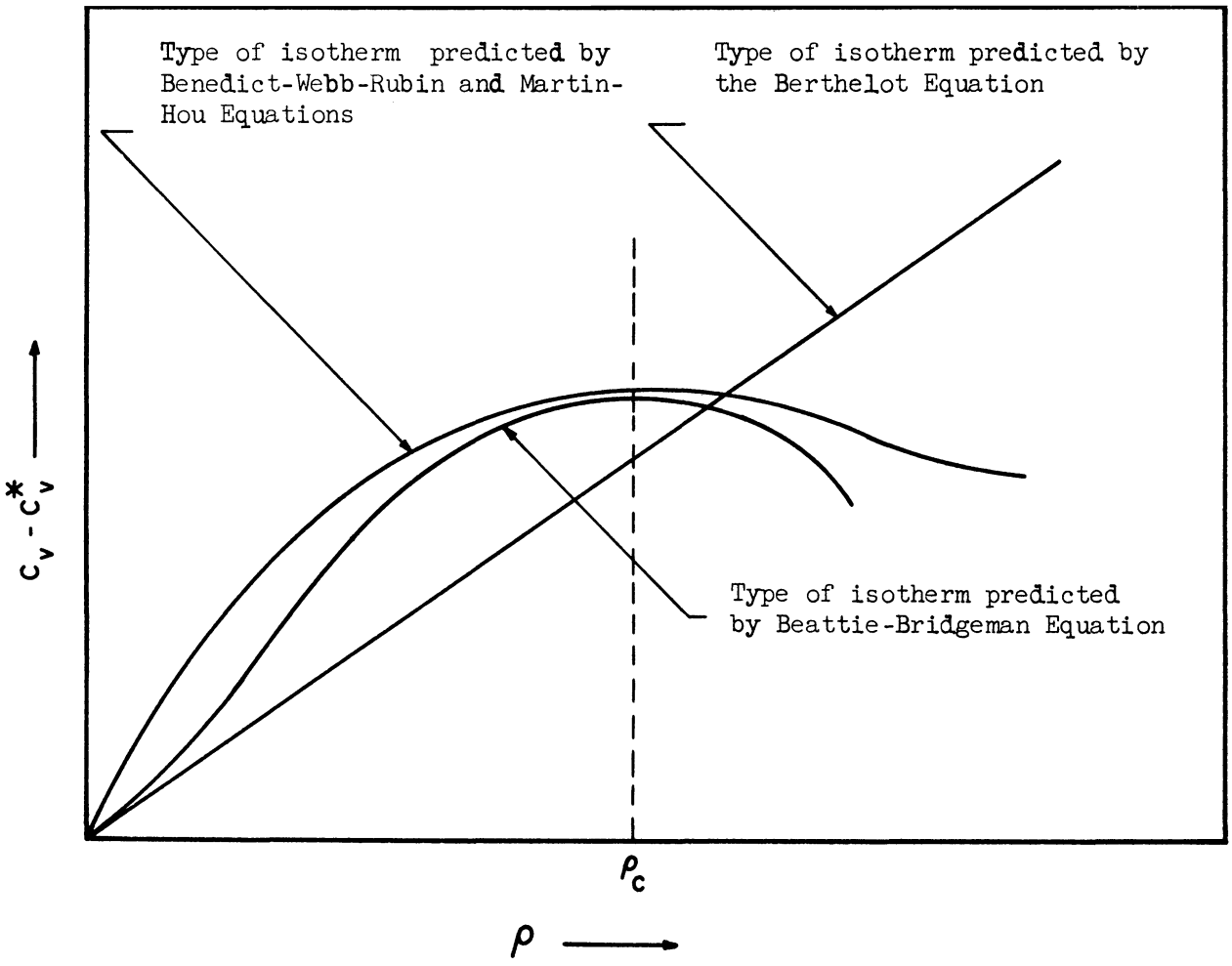

Figure 1-1. Types of Isotherm on a C_V-C_V* vs. Density Plane Predicted by Several Equations of State. (This figure is reproduced from de Nevers' thesis, p. 11.[12])

I-5 Constant-Volume Heat Capacity and the Speed of Sound

The constant-volume heat capacity is also related to the speed of sound by the following exact thermodynamic relation, valid only for the single phase of one component:

$$c = V\left(\frac{dP}{dT}\right)_V \left(\frac{T}{C_V}\right)^{1/2} \left\{1 - \frac{\left(\frac{C_V}{T}\right)\left(\frac{dP}{dV}\right)_T}{\left(\frac{dP}{dT}\right)_V^2}\right\}^{1/2} \qquad (1\text{-}16)$$

where c is the speed of sound. By Equation (1-16), C_V may be evaluated if the speed of sound and the state data are known. However, since the first derivative of P with respect to T or V is generally less accurate than PVT data itself, it is to be expected that C_V thus calculated may have a considerable error.

II. PRIOR WORK IN CONSTANT-VOLUME CALORIMETRY

II-1 Calorimetric Measurements of Constant-Volume Heat Capacity

Joly's[22] work on carbon dioxide in 1894 was probably the earliest attempt in this field. His apparatus was a differential steam calorimeter, and data were collected over a temperature range from room temperature to 100°C, at low pressure. Although his data were superseded by later work, he correctly concluded that C_v increased with increasing temperature and increasing density for the range he studied.

In 1903, Dieterici[14] measured the heat capacity of carbon dioxide and isopentane using a Bunsen ice calorimeter. He worked on the two-phase system, but convered his two-phase saturated heat capacity, $C^{g,l}_{sat.}$, into the heat capacity of the saturated liquid C^{l}_{sat} and C_v of gas by means of the PVT data of Young.[46]

In 1905, Reinganum[39] compared Dieterici's data with those calculated from the PVT data of Amagat[2] and Young,[46] and came to the postulate that C_v as a function of density at a constant temperature would exhibit a maximum near the critical density. On the basis of more extensive PVT data later available, his postulate has been confirmed by subsequent investigators. Most modern equations of state also show this behavior (see Figure 1-1).

To test Reinganum's postulate, Bennewitz and Splittgerber[7] constructed a calorimeter in 1928 to measure the C_v of carbon dioxide near the critical point. Their calorimeter consisted of a steel vessel placed in the evacuated space and surrounded by a water bath of constant temperature. The resistance thermometry and electrical heating method

were used in their calorimeter. Their data were mostly taken in the two-phase region below the critical temperature, but they computed the C_v of the liquid and C_v of the gas by means of the PVT data. They concluded that $(dC_v/dV)_T$ was zero at the critical point, and that just below the critical temperature both the C_v of the liquid and that of the gas had a negative values. Keenan's[23] reasoning on the impossibility of negative values of C_p in the stable system can also be applied to C_v, and it is logical to conclude that Bennewitz and Splittgerber's work must have been in error.

In 1928, Eucken and Hauck[16] measured C^l_{sat} and C_v for argon, carbon dioxide, ethane, and air in the liquid and supercritical region, using an adiabatic calorimeter, simply "to increase our deficient knowledge of heat capacities in this region." The heat capacity of their calorimeter was five to eight times that of its contents.

Interested in the "hysterisis" effects near the critical state, Pall, Broughton, and Maass[37] measured the C_v of ethylene in 1938, using the adiabatic calorimeter. They measured the C_v as a function of temperature for only the critical density, and found that the C_v might differ by as much as 3% at a particular temperature of measurement, depending on the past history of the gas: whether it had been heated up to the experimental temperature from below the critical state or had been cooled to the same temperature from well above the critical temperature before the experiment. The heat capacity of their calorimeter was 5 to 8 times the heat capacity of its contents.

In 1950 Hoge[20] measured the $C^{g,l}_{sat}$ and C_v of oxygen in apparatus originally designed for vapor-pressure measurements. He wished to assess

the possibility of determining the two-phase boundary by measuring the liquid and gas heat capacities, perhaps a more accurate method than the PVT measurements. He came only to the tentative conclusion that $C_{sat}^{g,l}$ and C_v measurements should be as reliable as PVT measurements for determining the two-phase boundary, and that the former would be much easier. The heat capacity of his calorimeter was about twenty times that of its contents.

Up to 1951, Sage and various co-workers[10] had made a series of measurements of $C_{sat}^{g,l}$ to determine saturated-liquid heat capacity C_{sat}^{l}. They adjusted the sample of two-phase mixture so that the correction for the gas-phase heat capacity and that for the heat of vaporization were always small. Their calorimeter was the first one of its kind which utilized mechanical stirring for obtaining temperature uniformity. All others merely relied upon conduction of heat through their heavy metal walls and natural convection by their contents. In one of the calorimeters used by Sage et al., the stirrer was driven by the external motor whose shaft entered the calorimeter through a rotary seal; in the other one, the entire calorimeter was rocked to cause the liquid to move within. The heat capacity of their calorimeter was about one-half that of its contents.

In 1952 Michels and Strijland[35] constructed a differential calorimeter which consisted of two identical containers, of which only one was filled with the gas. An identical amount of electrical energy was added to both containers, and the C_v calculated from the resulting difference in their temperature rise. They collected the C_v of carbon dioxide over a considerable range of temperature and density, and

presented the comprehensive picture of the relation among these variables. Comparison of their experimental results with those computed from the PVT data indicated that the agreement was good for temperatures and densities well removed from the critical point, but that near the critical point, experimental C_v was much larger than what could be predicted from the state data.

In 1958 de Nevers[12] constructed an adiabatic calorimeter, using the thin-wall large-volume stainless-steel sphere. The heat capacity of his calorimeter was about 1/3 to 1.5 times that of the contents depending on the loading density. The special feature of his calorimeter was an inclusion of a tiny motor-stirrer into the calorimeter to avoid the complexity of the externally driven stirrer. He collected C_v data for propylene and perfluorocyclobutane over a considerable range of density from saturation temperature to 150°C. Comparison of his experimental results with those predicted from the available PVT data indicated that in the C_v vs. ρ plane the experimental isotherms presented an upward curvature at the low densities and then changed to the downward curvature at the higher densities, while the Martin-Hou equation and Benedict-Webb-Rubin equation all predicted the downward curvature starting from the zero density.

II-2 Constant-Volume Heat Capacity from Speed of Sound

The speed-of-sound measurement has been utilized by various authors to determine C_v, mainly for helping the selection of fundamental frequency or the determination of some molecular constants, for instance a potential barrier. It has not been common to use this method for measuring the C_v itself as a single purpose.

In view of the excessively high values of C_v at the critical point as measured by the calorimeter, Curtiss, Boyd, and Palmer[11] tried to verify these results by the measurement of the speed of sound. They assumed that $(dP/dV)_{T_c}$ was zero at the critical point, and simplified Equation (1-16) as follows:

$$c = V_c \left(\frac{dP}{dT}\right)_{V_c} \left(\frac{T_c}{C_v}\right)^{1/2} \qquad (2\text{-}1)$$

Curtiss et al. measured the speed of sound at the critical point for carbon dioxide and ethylene, and, together with the available data on the critical volume, critical temperature, and the slope of the vapor pressure curve at the critical point, calculated C_v according to Equation (2-1). Their computed values were less than one-half of those calorimetric values for both compounds.

Schneider and Chynoweth[41] explained the above discrepancy by pointing out the inadequacy of assumption used in the derivation of Equation (2-1). Although $(dP/dV)_{T_c}$ is indeed zero at the critical temperature for the static measurements, it is not zero for the small adiabatic pressure changes caused by the sound wave. So they maintained that the assumption $(dP/dV)_{T_c} = 0$ was not justified and consequently that Equation (2-1) was not reliable, although Equation (1-16) was valid.

II-3 Other Methods of Measuring Constant-Volume Heat Capacity

For a gas at subatmospheric pressure, two methods have been proposed for C_v measurement. One of them, proposed by Trautz and Grosskinsky,[44] is as follows: An identical amount of heat is added to the gases of both known and unknown heat capacity. By comparing

their pressure increases, the C_v of the gas of unknown heat capacity is computed. But the numerous assumptions involved in this method lessen its reliability. Another method, proposed by Schaefer,[40] is based on measurement of the rate of heat loss from a wire electrically heated. However, no data obtained through this method have been published.

III. EXPERIMENTAL APPARATUS

III-1 General Discussion

It is apparent that a slight error, say 1%, in the gross heat capacity will be magnified to an intolerable extent in the final results if the heat capacity of the metal container is several times greater than that of the contents. This is the basic difficulty inherent in the constant-volume calorimetry.

There are two ways to overcome this difficulty: (1) By reducing the weight of a container to an extent that the apparatus is operated at marginal safety, we may optimize the ratio of heat capacity of contents to that of a container. (2) By improving the design of the apparatus, we may enhance the accuracy of gross heat-capacity data and, consequently, suppress the fluctuation in the final results.

Along the first line, de Nevers[12] pioneered in the development of the thin-wall large-volume calorimeter, which proved practical when the density of gas was considerably high. But effort in this direction has an inevitable limitation due to the possible deformation when the wall of a container gets too thin.

On the other hand, de Nevers' work left much room for improvement along the second line. Work in this direction appeared to offer the only way to achieve the projected goal, to determine the ideal gas constant-volume heat capacity, C_V^*, by the extrapolation of C_V data at reasonably low densities.

It was known from experience that the fluctuation was mainly caused by the poor temperature control between the calorimeter and the

shield. In other words, the radiational heat transfer was not negligible in this type of calorimeter. The convectional heat transfer was not so important in an evacuated surrounding of about 0.03 mm-Hg. The conductional heat transfer was significant but could be estimated with a reasonable accuracy based on the drift measurements before and after the heating period.

Thus it was apparent that the shape of the radiation shield, smoothness of its surface, and the number of thermocouples attached to it for the temperature control all had significant effects on the fluctuation of data.

Since the calorimeter was to be operated with the marginal safety factor at the most severe condition, the appropriate safety device was also provided.

III-2 The Calorimeter

The calorimeter proper was actually a thin-wall spherical gas container which accommodated a tiny d-c motor-stirrer and a resistance thermometer-heater. Figure 3-1 shows the cross section of the calorimeter. The fabricated calorimeter is shown in Figure 3-2 at its operating position relative to the other parts of the experimental apparatus.

Except for a few improvements or necessary modifications, the idea of the first successful model as developed by de Nevers[12] has been generally followed by the present author. For completeness of presentation, de Nevers' descriptions will be briefly recapitulated, emphasizing details of improvement and modification.

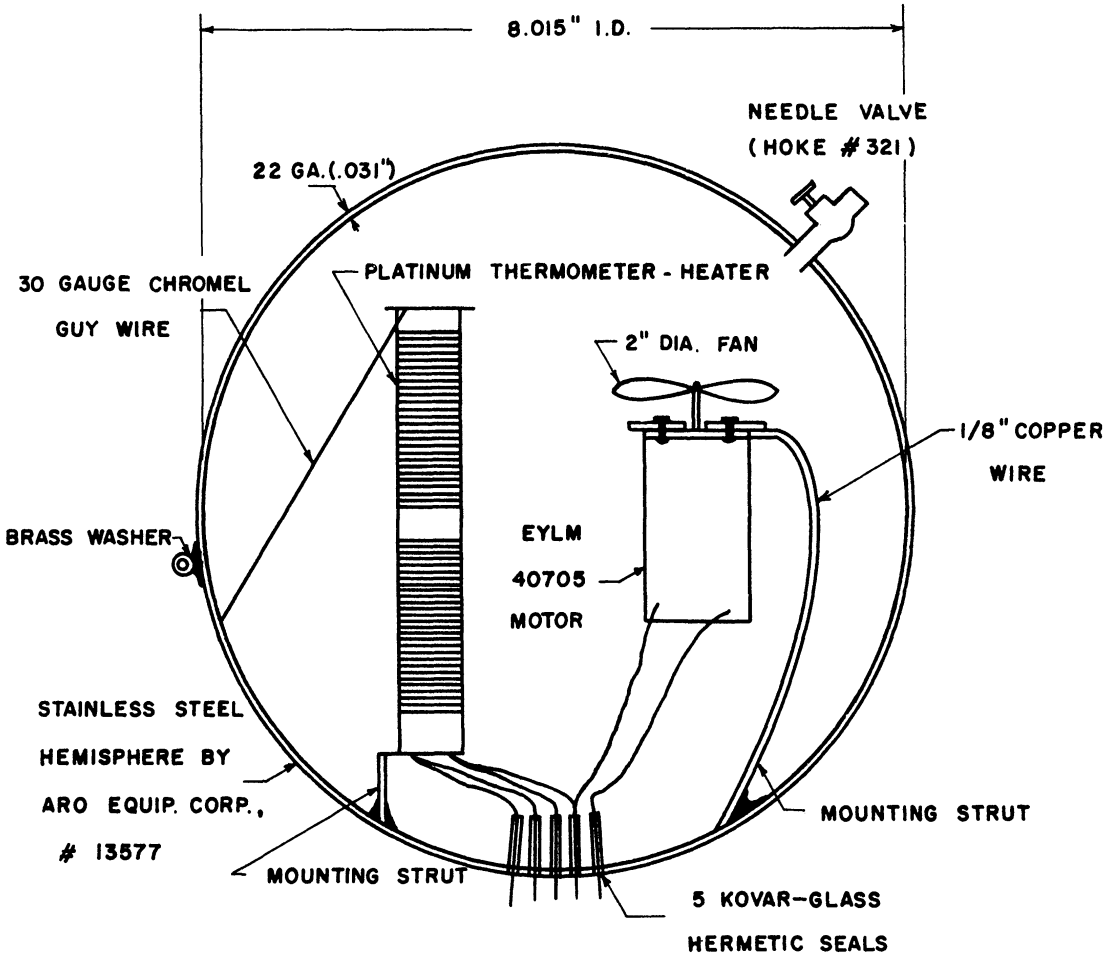

Figure 3-1. Cross Section of the Calorimeter.

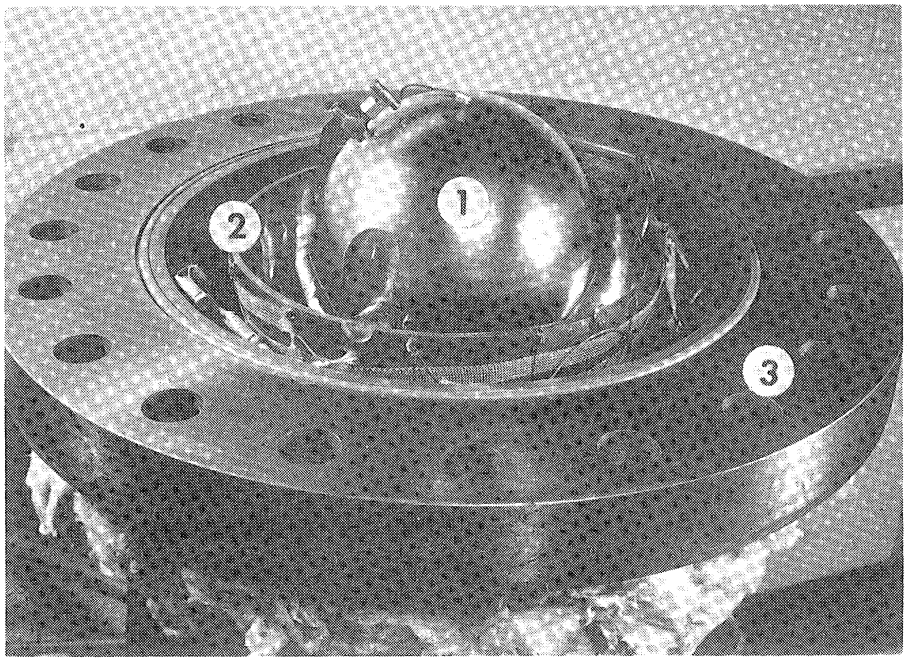

Figure 3-2. Calorimeter, Shield, and Vacuum Container in Their Relative Positions.

(1) Calorimeter, showing the thermocouple well on the top, valve, and also the suspension Fiberglas strings.

(2) Adiabatic shield, showing three baffle pieces which also serve as the suspension frame for the calorimeter.

(3) Vacuum container, showing a silicone rubber "O"-ring in the groove, and Fiberglas insulation outside the container.

The spherical shape was chosen because it demanded the lowest mass of container material for a given volume and allowable stress. The calorimeter shell was fabricated with two 8.015-in. I.D., 0.031-in.-thick stainless-steel hemispheres, Aro Equipment Corporation No. 13577, which were cold-drawn from sheets of type 304 extra-low-carbon stainless steel. After fixing all necessary fittings and essential parts into the upper and lower hemispheres, respectively, the two hemispheres were jointed by Heliarc fusion welding (actually in the argon atmosphere). After welding, the exterior of the sphere was copper plated for the purpose of reducing heat transfer by radiation. The welding and copper-plating were done by Aro Equipment Corporation. The stress analysis showed that the tensile stress was 64,500 psi at a pressure of 1,000 psi. However, considering that de Nevers' calorimeter exploded at about 860 psi, it was decided to operate the calorimeter up to 500 psi and by no means to exceed 550 psi.

For loading and unloading the calorimeter, a small stainless-steel needle valve, Hoke No.321, was silver-soldered into the top hemisphere. Also, three small brass washers were silver-soldered to the bottom hemisphere along a line roughly one inch below the welding seam, for mounting purposes.

It is to be emphasized that in the de Nevers' calorimeter the inclusion of the motor-stirrer was, in fact, a key to the success achieved. It was reported that natural convection alone was not able to yield a sufficiently uniform temperature distribution. Even with a forced convection by means of the motor-stirrer, the temperature difference was still observed; but the difference was so small that the heat leakage to the surrounding could be reasonably controlled. The motor was a

No. EYIM 40705 d-c motor by Barber Colman Company and was specially designed to operate in the ambient temperature of 400°F or approximately 200°C. The Delco No. 5074368 motor was used in de Nevers' calorimeter, which was operated up to 150°C. Since the motor was a limiting factor in the temperature range, this meant the substantial increase of 50°C in the workable temperature range. The EYIM 40705 motor was 1.38 in. in diameter, 2 in. long and weighed 0.31 lb. It was operated on 6 to 12 volts d-c (see Figure 3-3). The motor speed varied with the voltage, gas density, gas viscosity, etc. Since neither density nor viscosity was adjustable, the applied voltage alone was adjusted to limit the temperature difference between any two control points within 0.2°C. To reduce the weight, a part of the protective shell was removed, and eight 1/8-in. diameter holes were drilled into the rest of the shell to improve the heat transfer between the motor and the gas. The stirrer was a 2-inch-long propeller made of a 3/32-inch-thick stainless-steel sheet, with a 1/4-inch stainless-steel rod for a hub. The motor was mounted on an 1/16-inch thick brass plate, which was supported by two 1/8-inch-diameter copper wires, which in turn were silver-soldered to the inside of the lower hemisphere.

In this calorimeter, the thermometer was also used as a heater during the heating period for its simplicity in design and construction of the calorimeter. The thermometer-heater was essentially 10 ft. of 36-gauge platinum wire wound bifilarly on a mica cross (see Figure 3-3). The cross was made of four pieces of 3-inch long, 7/8-inch-wide mica. All pieces were appropriately slotted and inserted into matching slots to make 5 1/2-inch-long cross. They were secured together with 30-gauge

chromel wire for strength and rigidity. Before assembly all mica pieces were appropriately notched for the winding purpose. The notches, 1/16 inch deep and divided into two sections of 2 inches each, were made by clamping the mica sheet between two notched brass templates and filing away the excess mica. To increase the strength of the structure, a mica disc, 1 1/8 inch in diameter, was attached to each end of the cross by 30-gauge chromel wire. Four 24-gauge copper wires were anchored to the base disc. These were joined, in pairs, by silver-soldering to the ends of the platinum wire, to form the four leads of the four-terminal type thermometer. Figure 3-3 shows many of the details hitherto described.

Before winding on the mica cross, the platinum wire was annealed to reduce the stiffness by connecting it across a 110 volt a-c for 30 minutes. After winding the wire on the mica cross, it was again annealed by the same procedure for 48 hours to remove the strains imposed by the winding. Annealing was repeated three times, followed each time by the measurement of the resistance at the ice point to make sure that the resistance was not significantly changed by the further annealing. After this treatment, the resistance of the thermometer-heater as a function of temperature was calibrated according to the method discussed in Appendix B.

The thermometer was mounted on the strut made of 1/8-inch copper wire, and was secured firmly by three 30-gauge chromel guy wires. Both the strut and the three guy wires were silver-soldered to the inside of the bottom hemisphere.

The six electrical leads (4 from the thermometer, 2 from the motor) left the calorimeter through five kovar-glass seals. Formerly

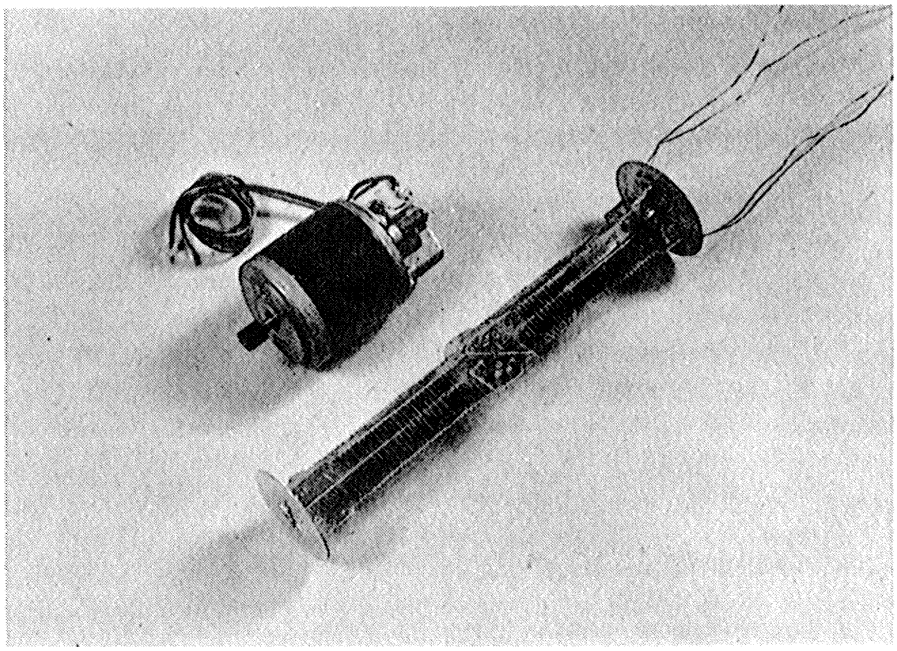

Figure 3-3. The Platinum Resistance Thermometer and High-Temperature Motor Used Inside the Calorimeter.

six seals were used, but since the motor and thermometer-heater were connected electrically in series, one lead from the motor did not have to leave the calorimeter but was simply connected to one of the four thermometer leads. The omission of one seal resulted in the reduction of the total weight of the calorimeter, and was highly desirable in this type of calorimeter. The cross section of one of the electrical seals, which were all made by the Electron Tube Laboratory of the University of Michigan, is shown in Figure 3-4.

The ruggedized cable end seals, ADVAC No. ES-250, available from the Advanced Vacuum Products Company, were also tried. Although the specification was excellent, their use was finally rejected for two reasons: (1) They weighed considerably more than the "home-made" kovar-glass seals and roughly increased heat capacity of the calorimeter by 8%. (2) They were not 100% reliable; of six seals tried, one was found to leak seriously.

The kovar-glass seals were silver-soldered into the wall of the calorimeter with a long part of the seals inside the calorimeter. This orientation was intended to produce the compressive stress in the glass. The reversed orientation would have produced a tensile stress in the glass which would have been less satisfactory.

All electrical connections within the calorimeter were done by silver-soldering. Except the motor leads and one of the longer leads, no insulation was made on any wire.

III-3 The Adiabatic Shield

The adiabatic shield in de Nevers' calorimeter was cubical in shape, and thus obviously had more geometrical nonuniformity than the spherical form. Therefore a spherical form was employed in this

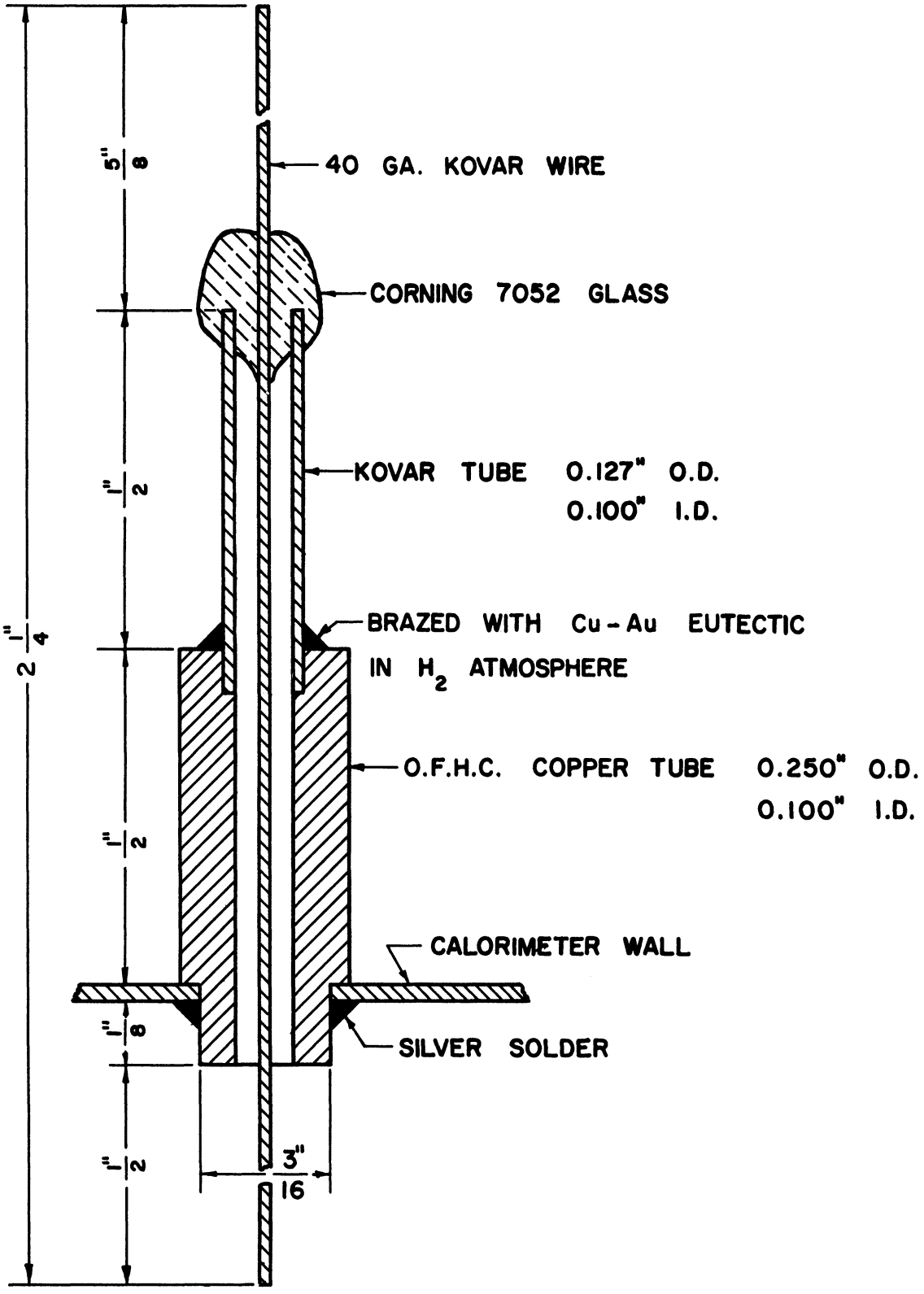

Figure 3-4. Cross Section of the Hermetic Electrical Seal.

project. The adiabatic shield consisted of two 12-inchI.D., 1/4-inch-thick copper hemispheres. Three 7/8-inch-diameter holes were carved off along the contact edges of two hemispheres to facilitate the evacuation. Three baffle plates, made of copper sheets, 1 1/2-inch wide, 2 1/2-inch long, and 1/16-inch thick, were placed in front of these holes to serve as a radiation shield and also as a frame for suspending the calorimeter. The base of a baffle plate was appropriately bent so that the clearance between the baffle and the adiabatic shield was approximately 3/8-inches. The base of the baffle plate was fixed to the inside of the bottom hemisphere of the adiabatic shield by two 1/8-inch brass screws. Close to the top of each baffle plate, a 1/8-inch diameter hole was drilled for hooking the calorimeter. The interior of the adiabatic shield was hand-polished to a mirror-like smoothness to reduce the heat transfer by radiation. Three legs, made of 1/2-inch-diameter brass rod, were brazed to the lower shield to locate the shield in the concentric position with the vacuum container. Two handles made of 1/8-inch steel wire were attached on the top adiabatic shield for lifting. To avoid the dislocation of the top shield from the bottom one, three small pieces of copper block were attached to the bottom hemisphere with 1/8-inch screws; each was located just between two adjacent 7/8-inch holes. Twenty-four small brass washers were brazed to each hemisphere for mounting the heating tapes. All details described above can be seen in Figures 3-2 and 3-5.

The adiabatic shield was heated by six 1/2-inch by 6-ft "Briskeat" flexible heating tapes which were attached to its outer surface. The heating rate of these heating tapes was 288 watts per tape at 115 volts.

Three heating tapes were uniformly distributed on each hemisphere of the adiabatic shield. The actual distribution of the heating tape was as follows. The total area of the hemisphere was divided into two parts: a top circular space, 1/3 of the total area, and the rest of the hemisphere. One heating tape was attached to the top circular area in a zig-zag pattern, and two heating tapes were attached to the side ring in a spiral fashion. All tapes were fixed by 20-gauge copper wire which ran between two washers. These washers were arrayed in two rings, one close to the edge and the other along the dividing line as mentioned above. Most of the details can be seen in Figure 3-5. No special attempt was made to cement or glue the heating tapes to the copper shield. Six heating tapes were grouped into three pairs for the regional temperature control, i.e., top, side, and bottom respectively. The power was supplied to each heating tape in parallel through three "Powerstat" variable voltage transformer, one for each pair of tapes. The circuit diagram of the heaters is shown in Figure 3-6.

The calorimeter was held in the center of the spherical adiabatic shield by three glass strings, to the ends of which steel hooks of convenient shape were attached. These strings ran from the three brass washers silver-soldered to the bottom hemisphere of the calorimeter to three holes drilled into three baffle plates bolted to the bottom hemisphere of the adiabatic shield.

III-4 The Thermocouples

As mentioned in Section III-1, the temperature control was of great importance to the accuracy of data. From a practical point of view, however, only a few points might be selected for the control purpose.

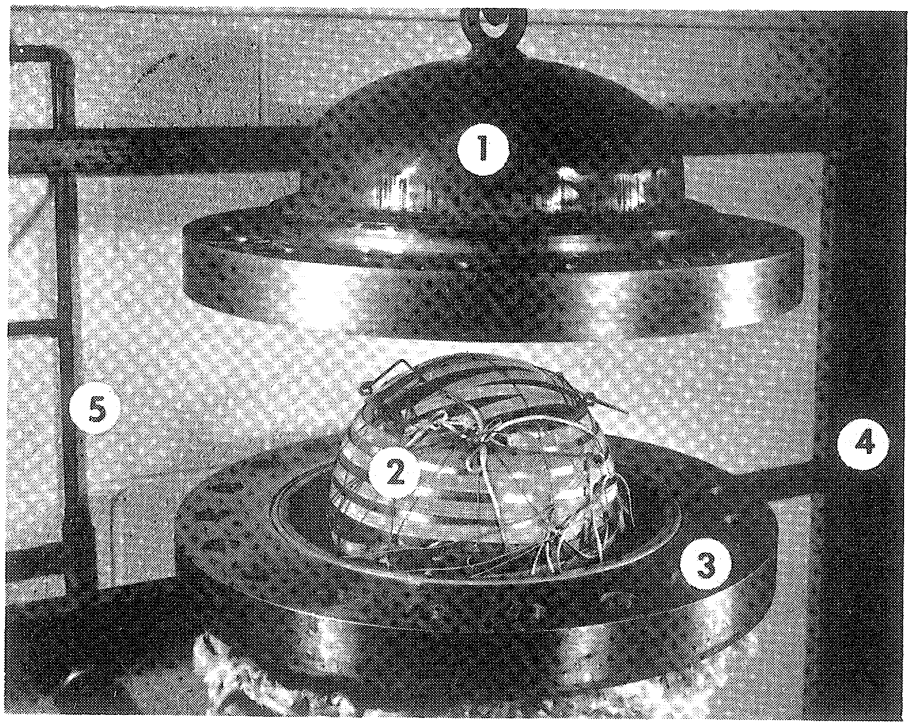

Figure 3-5. Vacuum Container and Adiabatic Shield.

(1) Lid of the vacuum container, suspended by a chain hoist.

(2) Adiabatic copper shield, showing "Briskeat" heating tapes, small brass washers, handles for lifting, holes for facilitating evacuation, and small pieces of edge guide.

(3) Vacuum container, showing silicone rubber "O"-ring in the groove, and Fiberglas insulation outside.

(4) Part of safety cabinet.

(5) Part of vacuum system.

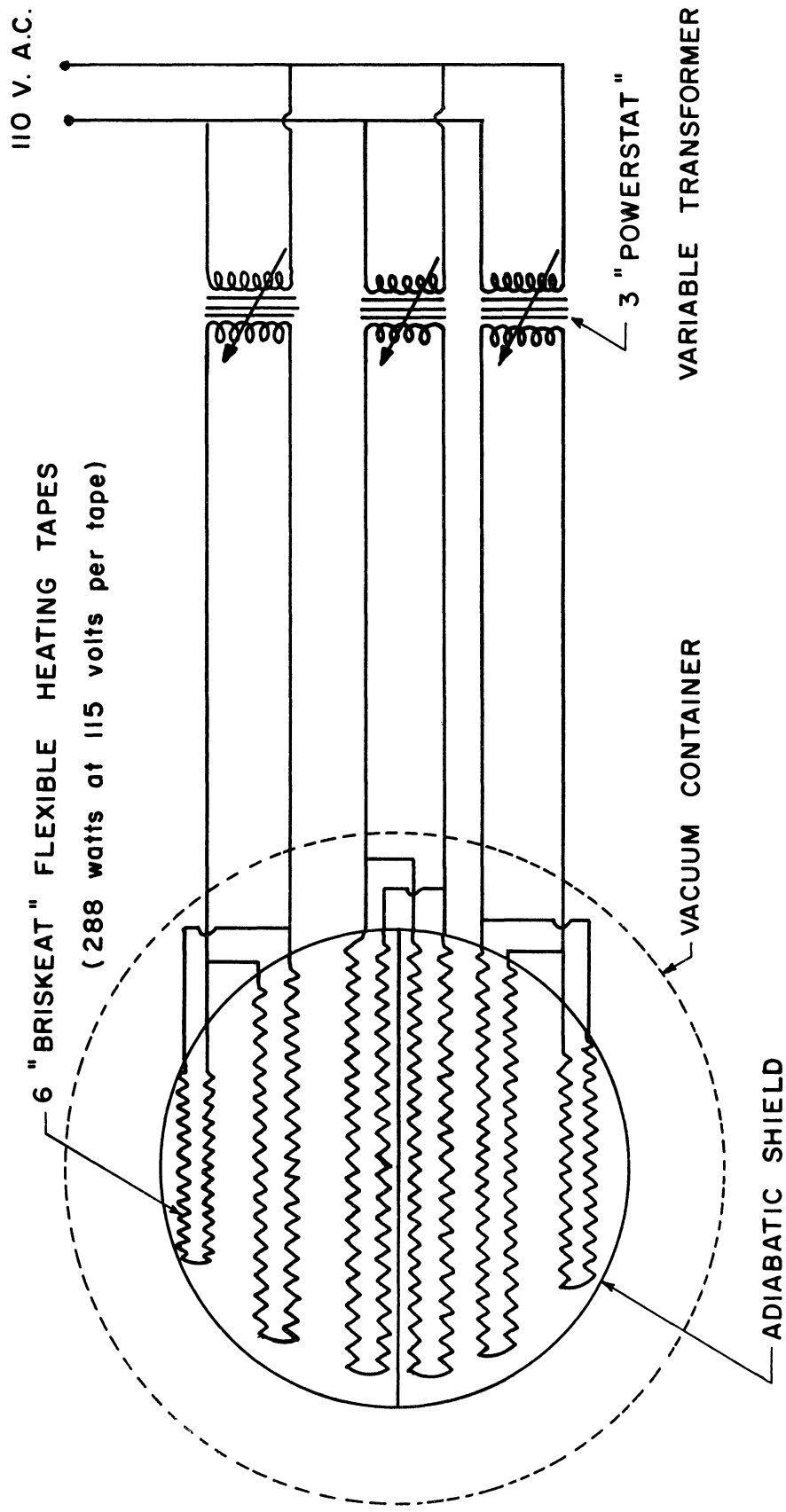

Figure 3-6. Circuit Diagram of Heaters.

Three points (top, side, and bottom) were selected on the surface of the calorimeter, and corresponding points were also selected on the adiabatic shield except the side. For the side of the shield, two points were selected instead of one since this region did not consist of a single piece of copper. Across the contact edge, two points were located closely but on different hemispheres.

The temperature difference between any two points was indicated by means of copper-constantan differential thermocouples. Seven thermocouples were installed at seven control points and all constantan wires were brought to a common junction, at a point within a vacuum container. The seven copper wires left the vacuum system through the electrical junction box. After that, all copper wires were brought to a junction board, from which eight combinations were selected (see Figure 3-7 for these combinations). By measuring EMF between any two copper wires, it was possible to determine the temperature difference between any two of the seven control points. In practice, no definite value of EMF was measured but the desired combinations were led to an eleven-point, double-pole, rotary switch, Leeds & Northrup type 8240, No. 1210525, from which they were directly connected to the moving coil galvanometer, Leeds & Northrup No. 1193782.

To adjust the sensitivity of the galvanometer, three extra resistors of 1,000, 10,000, and 100,000 ohms were arranged in series with the galvanometer. These resistors were seldom used unless the temperatures were excessively off balance. The circuit diagram of the entire thermocouple system is shown in Figure 3-7. The circuit involved no reference junction since only the temperature difference

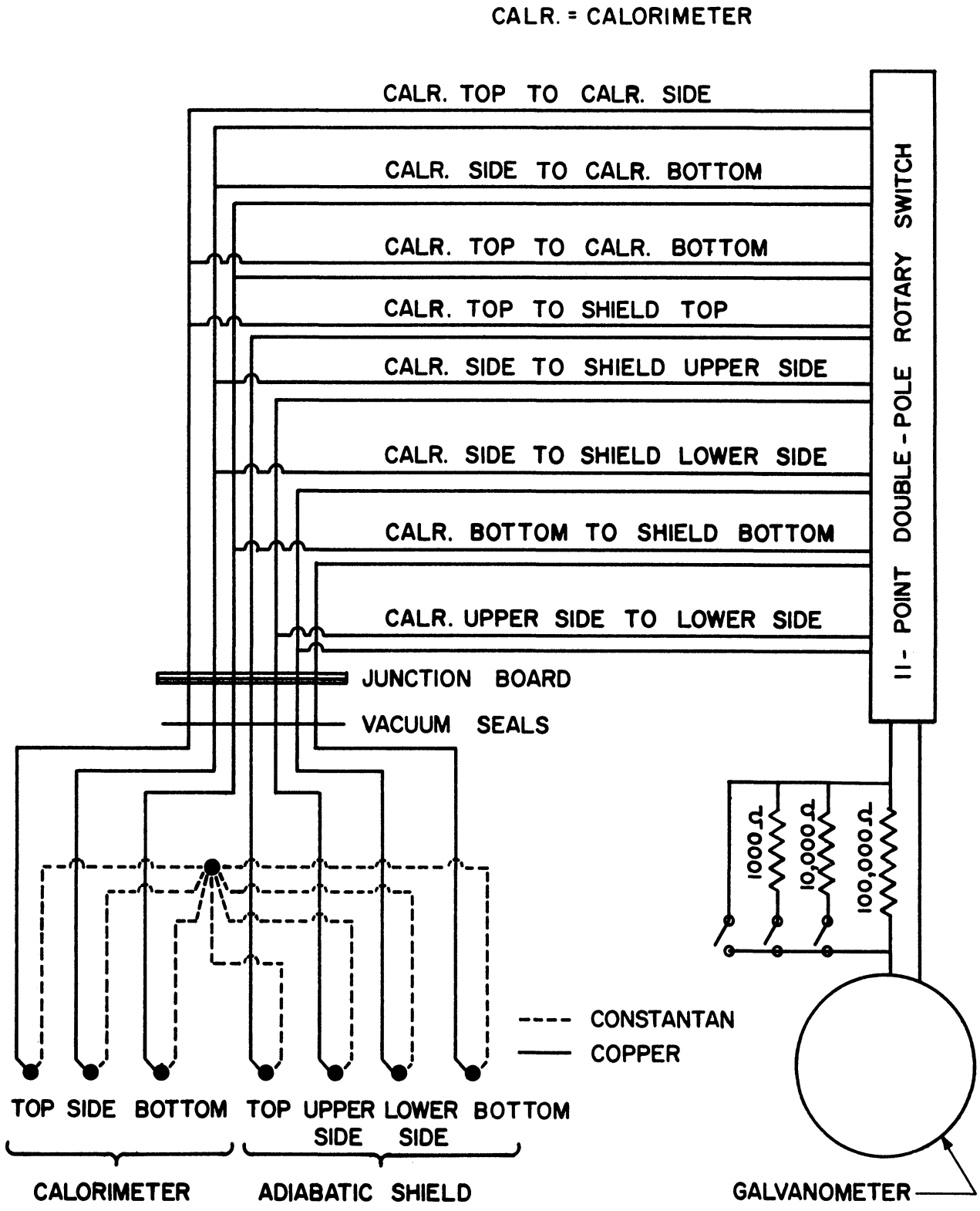

Figure 3-7. Circuit Diagram of Thermocouples.

was of interest. The galvanometer was of a null-type and no accurate EMF might be observed, but the rough temperature difference might be estimated based on the published data for a copper-constantan thermocouple and galvanometer. It was estimated that one centimeter of deflection on the galvanometer scale corresponded to 1/100°C.

To place the thermocouple in thermal contact but not in electrical contact with various surfaces, insulated thermocouple wells were employed at all control points. The wells were made of 20-gauge copper tubing (0.125-in. O.D., . 0.0635 in. I.D., and 1/2 in. long), and were soldered to the places by silver-solder or high melting solder (melting point 710°F). The Teflon tubing (0.052-in. O.D. and 0.030-in. I.D.) was coated with vacuum grease and forced into the copper tube. The Teflon tubes were again filled with vacuum grease using a hypodermic syringe, and the thermocouples were then forced into them.

III-5 The Vacuum Container

The purpose of the outer container was two-fold: (1) to provide an evacuated space for housing the calorimeter and radiation shield with an aim of eliminating the heat transfer by convection; and (2) as a safety device to contain various parts of the calorimeter from flying in every direction in case of rupture of the calorimeter. For these reasons the container demanded not only a good vacuum seal but also quite heavy construction.

The vacuum container consisted of two identical parts, each of which was fabricated by welding a "Taylor Forge" 16-inch Schedule 80 welding cap to a "Taylor Forge" 16-inch 300# slip-on flange. The thickness of the container was 0.843 inches and the flange was 2 1/4-inches

thick. The total weight of the vacuum container was about 680 lb. Figure 3-5 shows the lid of the container being lifted by a chain hoist. After welding, it was found that the flanges were slightly warped and gave about 3/16-inches clearance at the outer edge. Three legs, each made of 3 x 1-1/2 x 2-1/2 in. channel, were welded to the bottom of the vacuum container and bolted on the other end to the concrete slab which formed a basis for the safety cabinet.

A silicone rubber "O"-ring was used as a vacuum seal between two flanges. The "O"-ring was provided by Precision Rubber Products Corporation (PRP6543, I.D. 17.000 in. CS .275 in. Compound 1130-80). The matching "O"-ring groove was machined on the lower flange, with the following dimensions: grove I.D.: 17.000-.005 + .000 in; groove depth: .225 $\pm$ .005 in; groove width: approximately .375 in. The bottom of the container was connected to the vacuum system through 7/8-inch copper tube. Two flanges were bolted together by twenty 1-1/4 x 6-in.machined bolts. An iron ring was welded to the top of the vacuum container for lifting the lid with a 1/2-ton chain hoist equipped with a sliding roller. The heating tape leads left the vacuum container through the Stupakoff Multi-terminal Header, No. 95.4003. The multi-terminal header was silver-soldered to a 2 inch-long stainless-steel tube, which in turn was welded directly to the wall of the container. The calorimeter leads left the vacuum container through a 6-ft-long Tygon tube to the junction box. The lower half of the container was insulated by approximately 2-inch-thick Fiberglas. A removable canvas-covered mat of Fiberglas was placed on the top of the container after the flanges were bolted together.

As an additional safety measure, a steel cabinet was built to house the entire vacuum container and vacuum system. The steel cabinet, roughly 8 x 3-1/2 x 8 ft in size, was bolted to the concrete slab, cast into the rectangular frame made of 6 x 2 inch channel. The frame of the cabinet was made of 2 x 2 x 3/8 inch angles on which were attached 1/4 inch hot-rolled steel sheets. The front of the cabinet consisted of two doors of 4 x 8 ft, each fixed to the side of the cabinet by four 7 1/2-inch hinges. The doors were secured to the place by four 3/4-inch bolts and a latch made of 2-inch pipe. No steel sheet had been attached to the rear side of the cabinet, which faced the windows directly. Naturally it was expected to blow into the direction of the window when the rupture of the calorimeter should take place. One 6-ft long, 6 x 3-1/2 inch I beam was fixed to the ceiling of the cabinet to slide the roller of the chain hoist.

III-6 Electrical Junction Box

As reported by de Nevers[12] thermal EMF would be induced in the Stupakoff multi-terminal headers if the headers were soldered directly to the wall of the vacuum container, because of the irregular temperature gradient across the wall. To avoid this difficulty, the header was installed in a separate junction box which was connected to the vacuum container by a 6-ft long piece of Tygon tubing. By this separation the heating elements did not affect the headers and the temperature gradients were usually negligible (see Figure 4-1).

The junction box consisted of a 500-cc stainless-steel beaker, to the bottom of which was silver-soldered a piece of stainless-steel

tubing and to the top of which was silver-soldered a 1/8-inch-thick, 1-inch-wide steel flange. The matching brass plate was bolted to this flange with eight 1/4-inch bolts. An "O"-ring was used between them as a vacuum seal. Two Stupakoff eight-terminal kovar-glass headers No. 95.4003 were soft-soldered into the holes in the brass plate. Of the total 16 terminals, four were for the thermometer, two for the motor, seven for the differential thermocouples, two for spare wires, and one was left unused. All the wires used were 30-gauge copper Formvar - and Fiberglas-insulated.

III-7 The Vacuum and Loading System

A Cenco Hyvac No. 2 mechanical vacuum pump was used to evacuate the vacuum container and also to provide vacuum necessary for loading and unloading the calorimeter. Figure 3-8 is a schematic diagram of this system. Three sizes of tubes were used: 1/8-inch copper tube for the loading and unloading line; 5/8-inch O.D. copper tube for connecting Lippincot-McLeod gauge via flexible Tygon tubing, into which a number of 1/8-inch O.D. 5/8-inch long pieces of glass tubes were inserted to prevent the Tygon tube from flattening during the evacuation; and the main line tubing consisting of 7/8-inch copper tube for fast evacuation. The pump was connected to the heavy-wall rubber tube, approximately 1-ft loog, which, in turn, was connected to the U-shaped cold trap made of 5/8-inch glass tubing. The cold trap was eventually removed from the system because the vacuum pump alone was able to provide sufficient vacuum. It was replaced by an L-shaped glass tube which was connected to the main line by the "O"-ring sealed fitting. This tube served not

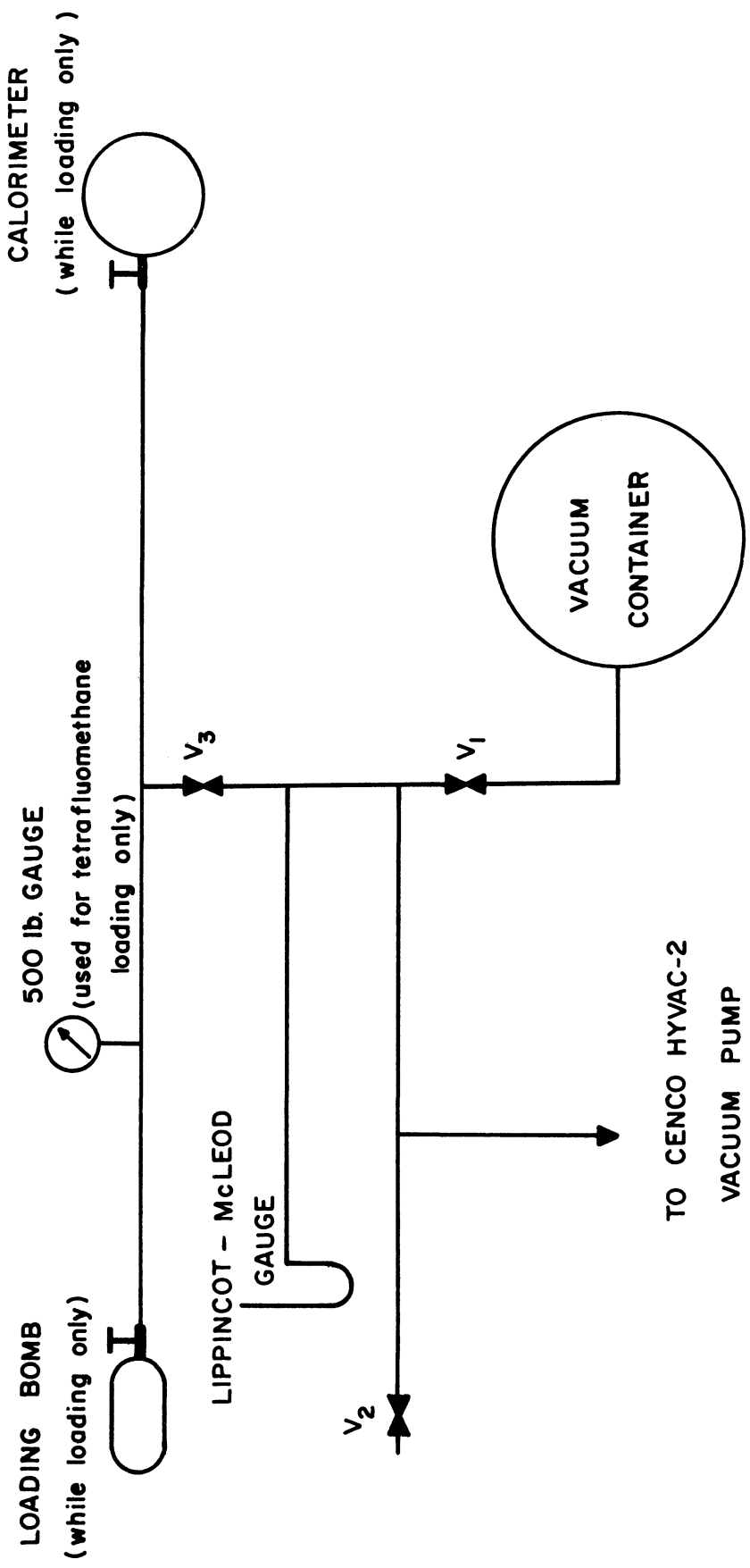

Figure 3-8. Schematic Diagram of the Vacuum and Loading System.

only as the connection but also as a safety measure for keeping high-pressure gas from reaching the pump in case of rupture of the calorimeter. The valves were all Imperial Diaphragm type vacuum valves, except one located near the intersection of the loading line and the main line. This was a Hoke needle valve primarily used as a double check to make sure no sample ever got into the pump. During the loading period, the calorimeter was taken out of the adiabatic shield and placed on the flange of the vacuum container.

III-8 The Measuring System

The measuring system consisted of two parts: the temperature-measuring system and the power-measuring system; the latter included the power circuitry. Figure 3-9 is a circuit diagram of this system, and Figure 3-10 is an over-all view of the measuring and control instruments.

Six electrical leads from the calorimeter reached the 8-pole double-throw master switch via the vacuum junction box described in Section III-6. At this master switch, located on the control and measuring panel, six leads were switched either to the temperature-measuring circuitry or to the power circuitry in accordance with the experimental procedures.

While the master switch was set to the temperature-measuring circuitry, two leads from the motor remained idle and four leads from the platinum resistance thermometer were directly connected to the Leeds & Northrup mercury cup commutator, type #8068, serial No. 1194595, which provided the so-called "potential terminal" type of circuitry to compensate the resistance of the leads as described by Mueller. From this commutator three leads went into the Mueller Bridge, which was essentially

the modified Wheatstone Bridge for measuring the resistance of the platinum thermometer. The bridge was a Leeds & Northrup type C-1, serial No. 1192498. The power for the bridge was supplied by four 1 1/2-volt dry cells in series, using a small rheostat as a potential divider. It was not necessary to know the exact voltage, and the rheostat was adjusted to give the appropriate sensitivity.

A moving-coil galvanometer, Leeds & Northrup type 2284-d, serial No. 1193782, was used as an indicator for the Mueller Bridge. This is the same galvanometer which was used for the thermocouples. It was mounted on a wooden bracket bolted to the wall of the building. A copper guy wire was also used to secure it against accidental dislodgement. The galvanometer was read with a Leeds & Northrup light and ground scale, type 2100, serial No. 223883, located about 1 1/2-meters from the galvanometer. As this is a null-type instrument, the exact calibration of the deflection was omitted. The 11-point double-pole rotory switch was used to relay the signal from the Mueller Bridge to the galvanometer. In general, the signal was transmitted directly, although an extra resistance could be added in series with a galvanometer as mentioned in Section III-4. To prevent too much current from passing through the thermometer and thus slightly increasing the temperature, the zero-ohm key was generally avoided; the 220-ohm key was used mostly.

While the master switch was set to the power-measuring circuitry, one pair of thermometer leads, directly connected to one of the motor leads, reamined idle. One of the thermometer leads, one of the motor leads, the milliammeter, balancing resistor, 0.1-ohm standard resistor, and 30- to 42-volt batteries formed a main power circuit whose current was determined

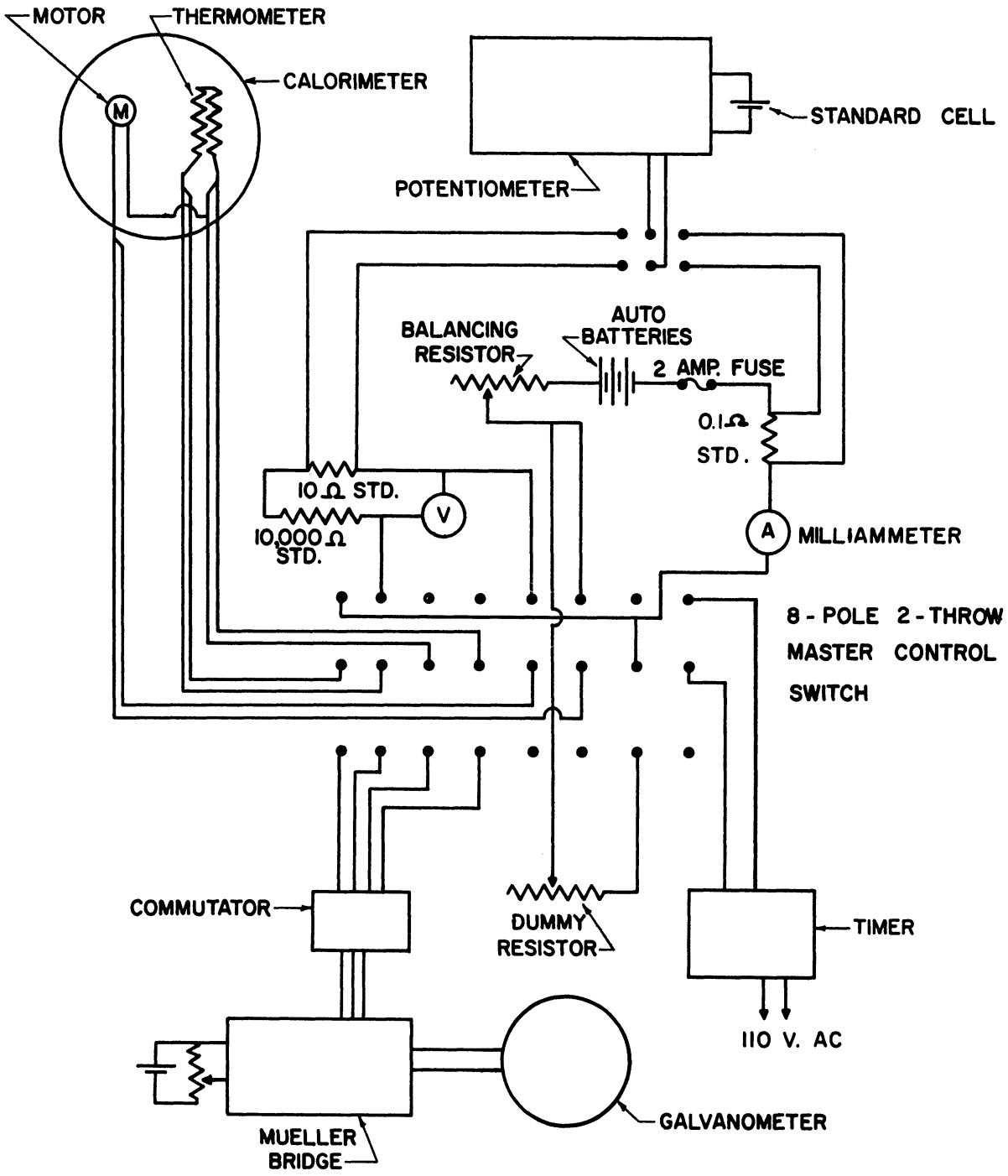

Figure 3-9. Circuit Diagram of the Measuring System.

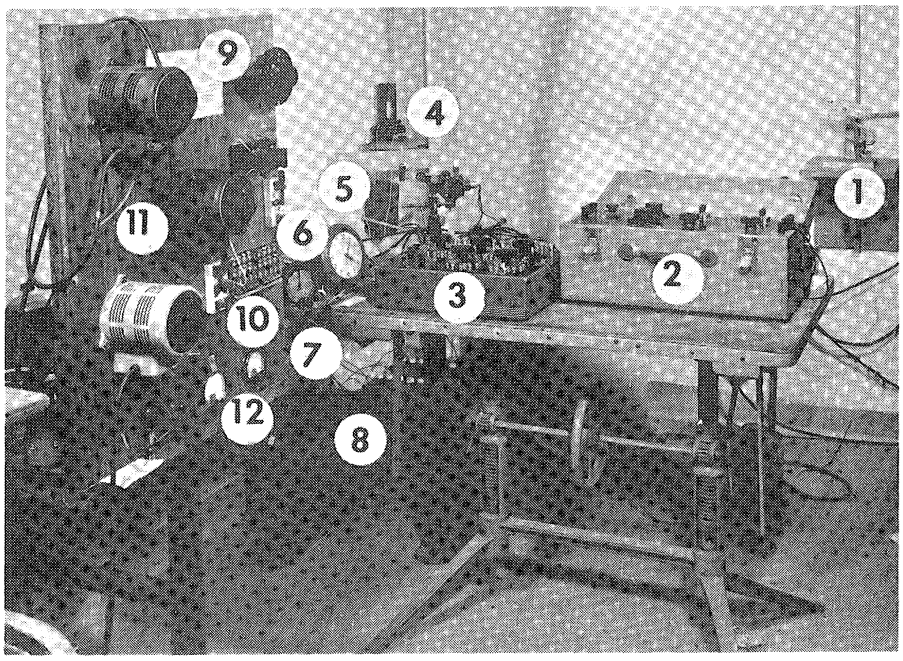

Figure 3-10. Control and Measuring Instruments.

(1) Lippincot-McLeod gauge.

(2) Potentiometer.

(3) Mueller bridge.

(4) Galvanometer, light and scale.

(5) Battery charger.

(6) Clock and timer.

(7) Balancing and dummy resistor.

(8) Lead storage batteries.

(9) 11-point 2-pole selector switch.

(10) 8-pole double-throw master control switch.

(11) Powerstats variable transformers.

(12) Milliammeter and voltmeter.

by measuring the potential drop across a standard 0.100000-ohm resistor, Leeds & Northrup type No. 4221-B, serial No. 1216562. Two remaining leads, one from the thermometer and one from the motor, were connected to a potential divider. A voltmeter was added to the circuit in parallel with the potential divider. The potential divider was essentially a combination of two standard resistors in series, i.e., a standard 10.000-ohm resistor, Leeds and Northrup type No. 4025-B, serial No. 1196149, and a standard 10,000-ohm resistor, Leeds and Northrup type No. 4040-B, serial No. 1201941. All resistors were certified in November, 1956, by the manufacturer with 0.01% accuracy. With this setup the voltage across the thermometer-heater and motor combination was determined by measuring the potential drop across the standard 10.000-ohm resistor. All three of these standard resistors stood in an oil bath: a stainless-steel pan, 10 by 7 by 5 inches deep, filled with 20-weight motor oil.

The potential drop across these standard resistor was determined by means of a Leeds & Northrup No. 8662 portable precision potentiometer, serial No. 1042502. This potentiometer had a self-contained galvanometer, and a standard cell. An external standard cell, Epply No. 425935, however, was used for all measurements considering the accuracy of its calibration. The standard cell was calibrated against Weston standard cell mode 4 No. 15559, whose NBS calibration on October 28, 1958 was available. Power for the potentiometer was supplied by the self-contained dry cell.

A milliammeter reading 0-800 ma and a voltmeter reading 0-25 volts were mounted on the control panel to show the current through and voltage across the thermometer and motor combination (or just a current

through a dummy resistor during the non-heating period). These rough instruments took no part in producing the experimental data, but were simply used for minor adjustments such as a balancing resistor, dummy resistor, or rough potentiometer-reading setup. These instruments also served to warn the operator of malfunctions of the equipment.

Power for the calorimeter, for both thermometer-heater and motor-stirrer, was supplied by lead storage batteries. Two 12-volt and three 6-volt automobile batteries were available for various combinations to yield over-all voltage of 30, 36, and 42 volts. The selection of the voltage was made so that a net voltage across a motor was always more than 6 and less than 10 volts. A battery charger was used to recharge the batteries when they were not in use. Before or after the heating period, the batteries were connected to the dummy resistor, of about the same resistance as the thermometer and motor combination, by simply switching the 8-pole double-throw master switch to the temperature-measuring position. This was to prevent the rapid change of the battery voltage at the start of a heating period.

To minimize the change of power input with changes in thermometer-heater and motor resistance, a balancing resister was connected in series with thermometer-heater and motor. Hoge[21] has given a detailed account of the use of the balancing resistor. Both a dummy and balancing resistors were 100-ohm, sliding-contact "Ohmite" No. 2921-A resistors.

The elapsed time of a heating period was measured by a synchronous timer with an electrically actuated clutch (Standard Electric Time Company model S-6). The clutch was actuated by the 8-pole double-throw master switch which started the heating period simultaneously.

A two-pole double-throw switch was also mounted on the control panel, connecting potentiometer to either 0.1-ohm standard resistor for measurement of current or to 10.000-ohm standard resistor for measuring the voltage.

IV. EXPERIMENTAL PROCEDURE AND MATERIALS

IV-1 Transferring the Material Into the Loading Bomb

Prior to any loading of the calorimeter, the material under investigation was first transferred from its shipping container to one of the light-weight loading bombs. Two types of bombs were used: for the condensable gas whose vapor pressure at room temperature was less than 500 psi, war-surplus, stainless-steel oxygen bottles; for non-condensable gas such as tetrafluoromethane, a specially rated heavy-wall container. The loading bomb of the first type had a capacity of about two liters; its rated pressure was 500 psi. Each bomb was equipped with a needle valve (Hoke #321) and a small aluminum identification tag bearing the name of the contents. The loading bomb of the second type was also cylindrical in shape, had a volume of approximately 1.2 liters, and a rated pressure of 2,000 psi. To transfer the material, the loading bomb and the shipping container were connected to both ends of the loading line, respectively. Then the loading bomb and the whole line were evacuated to less than 10 μ with the main valve close to the vacuum container shut off (see Figure 3-8). Finally, the loading line was isolated from the vacuum system and the valve of the shipping container was opened. The material was transferred either by heating the shipping container or by condensing the gas into the loading bomb with liquid nitrogen.

IV-2 Loading the Calorimeter

First the loading bomb was weighed on the precision balance, Seederer-Kohlbusch serial number 2F-2756, which could weigh quantities

up to 3,000 grams and could be read to 0.01 gram. Then, as shown in Figure 3-8 the loading bomb and the calorimeter were connected to the loading system. With valve No. 1 and No. 2 shut off, valve No. 3 and the calorimeter valve open, the line and the calorimeter were evacuated down to less than 0.010-mm Hg. After this, the loading line was isolated from the vacuum line by closing valve No. 3. As soon as a valve of the loading bomb was opened, the vapor flew into the calorimeter and was condensed there except tetrafluoromethane. This procedure was facilitated by heating the loading bomb with a flexible heating tape. To determine the approximate amount of material loaded, the loading bomb was placed on one pan of a crude 2-kg balance, and the needed weights were placed on the other pan. As the loading proceeded, the weights were removed from the pan gradually until the total weight removed was approximately equal to the desired quantity of loading. At this point the calorimeter valve was closed, and the residual vapor in the line was collected back into the loading bomb by condensing it with liquid nitrogen. At the temperature of the liquid nitrogen, the vapor pressure in the loading bomb was reduced to a negligible value, so material left in the line should also be negligible. Figure 4-1 shows many details hitherto described. The valve of the loading bomb was then closed, the bomb was disconnected, warmed to room temperature, and again weighed to 0.01 gram. The difference between the initial and final weights corresponded to the mass loaded to the calorimeter. The crude balance was able to regulate the loading to about $\pm$ 15 grams.

The calorimeter was then disconnected from the loading line. The surface was carefully polished by "Boyer's Instantaneous Metal Polish",

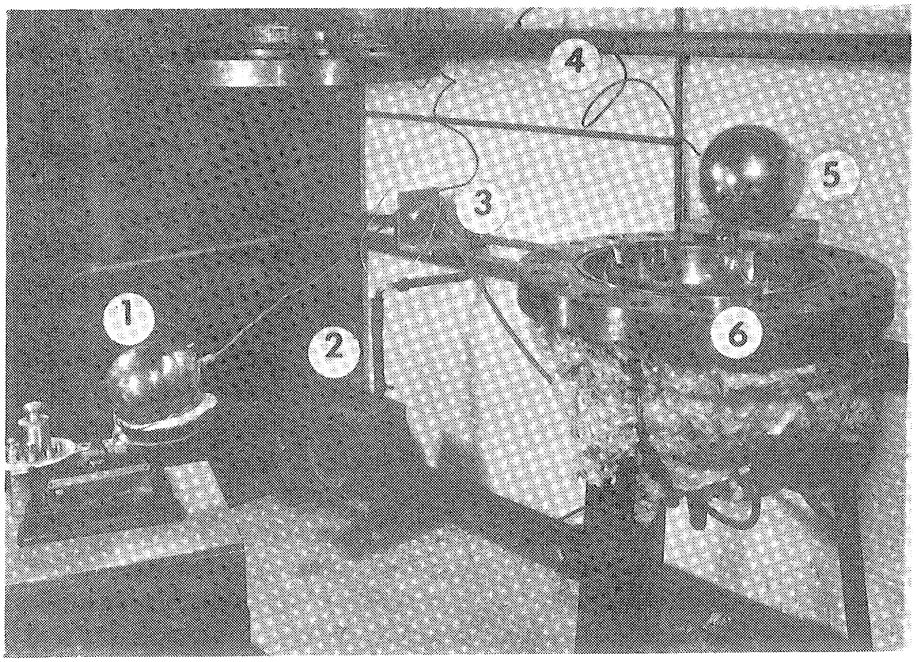

Figure 4-1. Loading the Calorimeter.

(1) Loading bomb resting on the balance pan.

(2) Vacuum pump.

(3) Junction box.

(4) Vacuum manifold.

(5) Calorimeter on a wooden base.

(6) Lower half of the vacuum container and adiabatic shield.

if necessary. The "Instantaneous Metal Polish" was also applied to the adiabatic shield for the best result in reducing the radiation heat transfer. The calorimeter was then suspended in place by the Fiberglas strings. All thermocouples were installed in the corresponding wells, and then the top of the shield was mounted. After the heating tapes were electrically connected, and the "O"-ring was installed, the lid of the vacuum container was lowered to the position and secured by twenty 1 1/4-inch bolts. Finally the Fiberglas mat was placed over the vacuum container, and the system was evacuated.

IV-3 Operating the Calorimeter

The actual calorimetric measurements were not started until the system had been evacuated to about 0.030-mm Hg. Any series of measurements for one particular density was begun at the lowest temperature above which only a single phase existed. Each normal run consisted of the first temperature-measuring period, a heating period, and the second temperature-measuring period. For the successive runs the second temperature-measuring period also served as the first temperature measuring period of the following run.

To begin a run, the shield heaters were controlled by the variable transformers so that the differential thermocouples indicated zero average temperature differences between the control points on the adiabatic shield and those on the calorimeter. In fact, this was the most difficult part in the whole experiment and involved considerable uncertainty if its fluctuation was not limited to a certain value. It was, in practice, adopted as a criterion of acceptance that the galvanometer deflection should always stay within $\pm$ 10 cm on a ground glass

scale during this period. Fluctuations of about 0.1°C were quite common. Before the temperature reading was taken, at least 20 minutes were allowed for thermal equilibrium after the zero average temperature difference had been attained. Temperatures of the calorimeter were measured at 5-minute intervals by means of the platinum resistance thermometer and the Mueller bridge.

Generally four readings were taken to determine the "drift" or the rate of temperature change with respect to time. If the drift thus determined appeared reasonable for the circumstance, the heating period was begun by throwing the 8-pole double-throw master swithc to the heating position. This switched the power from the dummy resistor to the thermometer-heater and motor, and simultaneously engaged the clutch of the synchronous timer. Of course, the Mueller bridge was automatically disconnected from the thermometer at this time to prevent current from flowing through the bridge.

The total length ofthe heating period ranged from 18 to about 30 minutes depending on the contents of the calorimeter and the intended temperature rise. The temperature rise was usually from 10 to 14°C. At the start of the heating period, a burst of power was given to the shield to compensate the slow response of the adiabatic shield to the heat input. Of course, during the heating period, the adiabatic shield was continually controlled to maintain zero average temperature differences between the control points on the surface of the calorimeter and those on the adiabatic shield. The temperature control during this period was much more difficult than that during the temperature-measuring period, and the following criterion was observed: The galvanometer deflection should not exceed the observable scale about $\pm$ 30 cm.

Power supplied to the thermometer-heater was determined twice or three times in each run depending on the duration of the heating period. In general, one reading was taken every 10 minutes. It was determined at times corresponding to 1/4, 1/2, and 3/4 of the heating period if three readings were necessary; otherwise, they were determined at times corresponding to 1/4 and 3/4 of the heating period. First the potentiometer was standardized by the external standard cell. Then with the two-pole double-throw knife switch set to the "current" position, the current was determined by measuring the voltage across the 0.10000-ohm standard resistor, which was in series with the thermometer-heater and motor. Next, with the two-pole double-throw knife switch set to the voltage position, the voltage across the thermometer-heater and motor was determined by measuring the voltage across the 10.000-ohm standard resistor, a part of a circuit which was in parallel with the thermometer-heater and motor. Then the current measurement was repeated. Two current measurements differed slightly due to the change in the resistance as temperature increased. Thus, the average of two current measurements was assumed equal to the instantaneous current reading at the time of the voltage reading. The product of this average current and voltage was regarded as the instantaneous power of the thermometer-heater and motor.

At the end of the heating period, the master control switch was thrown back to the temperature-measuring position. This simultaneously switched the power from the thermometer-heater and motor to the dummy resistor, disengaged the clutch of the timer and reconnected the Mueller bridge. After the time and reading of the timer were recorded, the timer was reset. To prevent the adiabatic shield temperature from

overshooting that of the calorimeter, the power to the shield was cut down substantially one or two minutes before the end of the heating period.

Ten minutes were allowed for the calorimeter to attain the thermal equilibrium while the temperature of the shield was controlled as before to maintain zero average temperature differences between the control points on the surface of the calorimeter and those on the surface of the shield. The temperatures were then recorded at 5-minute intervals as in the first heating period, until the drift had been determined. If another run was planned, the heating period was started immediately; otherwise, the operation ceased at this point.

Due to the large mass of the vacuum container, its temperature increase always lagged behind that of the shield or calorimeter. From the experience, we knew that the greater the temperature difference between the shield and the vacuum container, the higher the value of drifts and the more difficult was the temperature control. In practice, the continuous operations never exceeded three runs, and at high temperatures they were limited to two successive runs each time. With an appropriate power supplied to the adiabatic shield to keep the desired temperature, the whole system was left idle for three or four hours for the vacuum container to attain the same or close to the same temperature as the calorimeter.

The experience also indicated that the best results could be obtained if the shield was controlled by a small adjustment of the voltage of the variable transformer at a greater frequency rather than by operation of "On-Off" switch and a burst of power in an attempt to obtain a quicker adjustment.

IV-4 Unloading the Calorimeter

When sufficient C_v data were collected over the allowable temperature range for a given loading, the contents of the calorimeter were recovered into the loading bomb. The recovery of the material served to check the possible leakage of the calorimeter or the loading line. It also saved the material for the further study. The loading bomb and the calorimeter were connected to the loading line, which alone was evacuated to less than 0.010-mm Hg. Then the loading line was closed off from the vacuum system, and the valves of the loading bomb and calorimeter were opened. With the loading bomb immersed in a dewar of liquid nitrogen, and the calorimeter warmed by a flexible heating tape, if necessary, the material was transferred from the calorimeter into the loading bomb. The completion of the transfer process was indicated by the cessation of the violent boiling of the liquid nitrogen and also by the disappearance of the atmospheric condensation or frost on the bottom of the calorimeter. At the completion of the recovery process, the valves of the loading bomb and calorimeter were closed, and the loading bomb was then disconnected, warmed to room temperature, and weighed on a precision balance.

The loss of material during these two transfer operations was usually less than 0.7 grams for the gases condensable at a normal condition. The loss could reach 1.5 grams for the gases not condensable at a normal condition, for instance, tetrafluoromethane. The loading bomb was always weighed immediately before the recovery process to make sure there was no leakage in the loading bomb itself by comparing it with the weight determined immediately after the loading.

IV-5 Material Used for Investigation

The four compounds selected for the investigation were tetrafluoromethane, chlorodifluoromethane, dichlorotetrafluoroethane, and chloropentafluoroethane. The statistical heat capacities have been calculated for four compounds by various authors, but none of them has been fully tested by the calorimetric measurements. For chloropentafluoroethane, a few data have been determined by measuring the speed of sound.(30) The Martin-Hou equations of state have been developed for chlorodifluoromethane,(26) tetrafluoromethane,(8) and dichlorotetrafluoroethane.(25)

All four compounds were supplied by the "Freon" Products Laboratory of E. I. du Pont de Nemours & Company. These compounds are known commercially as "Freon"* refrigerants. Tetrafluoromethane is known as "Freon-14," chlorodifluoromethane as "Freon-22," dichlorotetrafluoroethane as "Freon-114," and chloropentafluoroethane as "Freon-115."

The purity of the samples was specified by the supplier as follows. Tetrafluoromethane (sample No. J-5452) has a purity of 99.7 + % by volume. It contains 5ppm H_2O, less than 0.01 volume % dichlorodifluoromethane, 0.02 volume % chlorotrifluoromethane, 0.16 volume % air, 0.04 volume % H_2 and no CO. Chlorodifluoromethane (sample No. KCD 2210) has a purity of 99.9 + % by gas chromatography. It contains 3 ppm of moisture and 0.04 volume % of air in the vapor phase. Dichlorotetrafluoroethane (sample No. FCD 909) contains 7 mole % of isomeric CF_3CFCl_2 and no detectable impurities. The minimum detectable amount of probable impurities is as follows:

* Trade name copyrighted by E. I. du Pont de Nemours & Company.

Trichlorotrifluoroethane	0.2	mole %
Isodichlorotetrafluoroethane	0.06	mole %
Chloropentafluoroethane	0.1	mole %
Dichlorotrifluoroethane	0.05	mole %

Chloropentafluoroethane contains no detectable impurities by infrared absorption analysis. It probably contains less than 0.1% of air and moisture. Dichlorodifluoromethane (sample No. KCD-1506) contains no detectable impurities by infrared spectrum. The moisture content is 4 ppm and air content is 0.0008% by volume in the vapor phase.

V. METHOD OF CALCULATION AND ESTIMATED ACCURACY

V-1 Calculation of the Gross Heat Capacity

For the perfectly adiabatic calorimeter, the gross heat capacity may be expressed as follows:

$$C_{gross} = \frac{dQ}{dT} \quad \text{or} \quad C_{gross} = \frac{q d\theta}{dT} \tag{5-1}$$

or in the integral form:

$$\int_{T_1}^{T_2} C_{gross} dT = \int_{\theta_1}^{\theta_2} q d\theta \quad \text{or} \quad \int_{T_1}^{T_2} C_{gross} dT = Q_2 - Q_1 \tag{5-2}$$

where Q is a total heat input, q a rate of heat input, T the temperature, and θ the time. For a small interval of temperature increase, ΔT, the following approximation is valid since q is nearly constant or linear in its change. If we define the mean gross heat capacity $(C_{gross})_{mean}$ as

$$(C_{gross})_{mean} = \frac{\Delta Q}{\Delta T} = \frac{\int_{\theta_1}^{\theta_2} q d\theta}{\Delta T} \tag{5-3}$$

it follows that

$$(C_{gross})_{mean} \cong q_{mean} \frac{\Delta\theta}{\Delta T} \tag{5-4}$$

It would not cause too serious an error to regard this mean gross heat capacity as a true gross heat capacity at the mean temperature.

The perfect adiabatic calorimeter, however, is merely an imaginary device which never existed in the practical calorimetry. All actual calorimetries rely very much on the appropriate estimation of the heat leakage. If the heat leakage rate is known explicitly in terms of

energy per unit time, Equation (5-4) may be modified as follows:

$$(C_{gross})_{mean} = (q_{mean} + q_{corr.}) \frac{\Delta\Theta}{\Delta T} \qquad (5\text{-}5)$$

where q's are added algebraically. If the heat leakage rate is known only in the form of an equivalent temperature change $\Delta T_{corr.}$, that is, the change in temperature which would have taken place in the time interval $\Delta\Theta$ if no energy had been added electrically, Equation (5-4) may be modified as follows:

$$(C_{gross})_{mean} = \frac{q_{mean}\Delta\Theta}{(\Delta T - \Delta T_{corr.})} \qquad (5\text{-}6)$$

where ΔT's are subtracted algebraically. Equation (5-6) has been employed for the calculation throughout this project. For further illustration, a sample calculation is included in Appendix C.

V-2 Calculation of Constant-Volume Heat Capacity

The gross heat capacity C_{gross} was a sum of the heat capacity of the contents of the calorimeter, plus the heat capacity of the calorimeter itself, plus the heat capacity of those parts of electrical leads and suspension strings which receive heat from the calorimeter. Thus the net heat capacity of the contents could not be calculated without knowing the heat capacity of the calorimeter, etc. The calibration of the heat capacity of the calorimeter, etc., is discussed in detail in the following chapter. The value of this calibration was then designated as $C_{calr.}$, which was a function of temperature. It is obvious that

$$C_{net} = C_{gross} - C_{calr.} \qquad (5\text{-}7)$$

and

$$C_v = \frac{C_{net}}{m} \tag{5-8}$$

where m is the total mass of loading. Equations (5-7) and (5-8) were used for the calculation throughout this research.

The C_v was then plotted against the temperature, and a smoothed isomettic was drawn through these points. For the low densities, however, C_v was not calculated for each run but the gross heat capacity was first smoothed in the C_{gross} vs. T plot; then C_v was calculated at every 10°C interval based on the smoothed gross heat-capacity data. There should be no difference whether the smoothing process was carried out for the C_{gross} or for C_v, as far as the final results were concerned. However, if C_v was smoothed, we could show the actual fluctuation of C_v clearly on the same plot. The fluctuation of C_v was greatly magnified at low densities, and the smoothing process was extremely difficult due to the jamming of points with the adjacent isometrics.

Once several isometrics were determined at a suitable interval, data were cross-plotted in C_v vs. density with temperature as a parameter. Each isotherm was then extrapolated to the zero density to give C_v^* (ideal gas constant-volume heat capacity).

V-3 Estimation of the Accuracy

Taking the logarithm of both sides of Equation (5-6), and then its differentials, we have

$$\frac{d(C_{gross})_{mean}}{(C_{gross})_{mean}} = \frac{dq_{mean}}{q_{mean}} + \frac{d\Delta\theta}{\Delta\theta} - \frac{d(\Delta T-\Delta T_{corr.})}{(\Delta T-\Delta T_{corr.})} \tag{5-9}$$

If the uncertainty of the quantities involved in the right-hand side of Equation (5-9) can be estimated reasonably, the possible error of C_{gross} may be estimated accordingly.

The first term dq/q can be estimated as follows:

$$q_{mean} = \frac{\sum_{i=1}^{n} q_i}{n} - \frac{\left(\frac{\sum_{i=1}^{n} E_i}{n}\right)^2}{R} \qquad (5\text{-}10)$$

and

$$q_i = I_i E_i \qquad (5\text{-}11)$$

where I is current, E is voltage, R is resistance of the voltage measuring circuit, and q_i is instantaneous heat input rate. Equation (5-11) may be modified to

$$\frac{dq_i}{q_i} = \frac{dI_i}{I_i} + \frac{dE_i}{E_i} \qquad (5\text{-}12)$$

where dI/I could reach 0.0004 and dE/E approximately 0.0006. Hence, dq/q could be as much as 0.0010. This value refers to the maximum instrumental error only. In fact, the presence of the motor in series with the thermometer-heater increased the uncertainty of the mean power considerably since its counter EMF was not too steady and fluctuated erratically over a relatively small range. The balancing resistor did serve to minimize the steadily varying mean power but was not able to damp out this type of erratical fluctuation. The average of two or three readings was taken as q_{mean} which never varied from any instantaneous power by more than 0.3%. The last term of Equation (5-10) represents the power consumed in the voltage measuring circuit, which never exceeded 5% of the apparent power. So if the

same uncertainty were assumed, this term corresponds only to less than 0.01% in the over-all accuracy estimation. Based on the above consideration, the value of q_{mean} was probably reliable to about 2 parts per thousand.

The elapsed time, $\Delta\theta$, was measured by an electric timer which could be read to 1/1000 of one minute without any trouble. Since the heating period was usually 20 to 30 minutes, the elapsed time measurement was probably reliable to one part per ten thousand. Of course, the accuracy of the frequency of the a-c source had an important bearing to the estimated accuracy. Nevertheless, over a period of 20 to 30 minutes an average frequency should be extremely close to 60 cps and the over-all error should be negligible.

The accuracy of temperature measurement was probably no better than 0.05°C. This refers to the absolute value of the temperature and not to the change of temperature, ΔT, which was the difference between two measured temperatures, T_1 and T_2. Since the thermometer calibration was internally consistent, any error in the absolute value of temperature reading would be systematic, and an accuracy of temperature difference was definitely better than temperature itself. The estimated accuracy of the temperature difference, independent of its size, was probably around one part per thousand. There was still another uncertainty involved in ΔT because T_2 was not directly measured, but was determined by extrapolating the reading back to the time at the end of the heating period, using the drift rate. Except for a few cases at the high temperature, the drift rate was less than 0.0120°C/min. Assuming the drift rate was known to $\pm$ 10%, the possible error in total drift over a

10-minute period should be less than 0.012°C. The average ΔT was 12°C, and thus the uncertainty caused by this extrapolation was less than one part of one thousand in ΔT. Hence, ΔT was probably reliable to plus or minus two parts per thousand.

The heat leakage correction, $\Delta T_{corr.}$, was usually less than 2% of ΔT, and never exceeded 2.5% of ΔT. Therefore, the last term in Equation (5-7) may be approximated by

$$\frac{d(\Delta T - \Delta T_{corr})}{\Delta T - \Delta T_{corr}} = \frac{d\Delta T}{\Delta T} - \frac{d\Delta T_{corr}}{\Delta T} \qquad (5\text{-}13)$$

Assuming the drift rates were accurate to $\pm$ 10%, $d\Delta T_{corr}/\Delta T$ would be about two parts per thousand.

For the worst possible case in which all these uncertainties combined to cause the observed C_{gross} to deviate in the same direction, the maximum possible error in C_{gross} would be about 0.6%. Actually, the errors were random in their nature, and experimentally observed deviation seldom exceeded 0.4% of C_{gross}; most of the data fluctuated within $\pm$ 0.3% of C_{gross}. The calibration curve, discussed in the next chapter, was essentially the smoothed curve based on the extensive experimental data. Therefore, its reliability should be higher than any single measurement. It would not be too much out of line to assume that the calibration of the calorimeter heat capacity was better than two parts in thousand. Again for an unfavorable condition in which the observed C_{gross} deviated 0.3% in one direction and the calibration curve deviated 0.2% in the opposite direction, the error of final C_v would be 2.8% for the lowest density and 0.8% for the highest density attempted. According to the

principle of statistics, the reliability of the isometrics obtained by smoothing the extensive experimental data should be much better than the above estimation. Considering the observed fluctuations, we are inclined to claim 1/2% accuracy for the high density and 1% accuracy for the lowest densities.

The volume of the calorimeter was determined by means of nitrogen gas (see Appendix A). Its probable error was estimated as about one part per thousand. The mass of the contents of the calorimeter was also known to at least one part per thousand. The volume varied over the course of a series of runs at one density, by up to 0.32%. The data were based on the volume which the calorimeter would take at the mean temperature and pressure of that particular series. The thermal and elastic expansion were taken into consideration to evaluate this mean volume; the correction never exceeded 0.5% of the original volume and the uncertainty involved in this correction should not be more than 0.02% of the original volume. Considering the above factors, the maximum probable error in density might be as much as 0.35%.

VI. CALIBRATION OF HEAT CAPACITY OF THE CALORIMETER

VI-1 General Discussion

The former method of calibration as employed in de Nevers'[12] work was as follows. The calorimeter was loaded with a small amount of gas whose heat capacity had been known. The gross heat capacity was then measured according to the normal procedures described in Section IV-3. The heat capacity of the contents was evaluated as the known ideal-gas heat capacity plus a correction for non-zero density used in the calibration; the latter value was estimated by means of the established equation of state. Apparently, the calibration by this method depends on the accuracy of published C_v^* data and also the second derivative of the PVT equation. Besides these uncertainties, the method presents another difficulty. In this type of calorimeter, there is a limitation in the range of operating densities. While the upper limit is determined by the mechanical strength, the lower limit is mainly determined by the rate of convectional heat transfer. The low density results in the less effective forced convection and consequently, the less uniform temperature distribution during the heating period. This excessively uneven temperature distribution renders the reliability of the gross heat capacity data very doubtful. Thus, reasonably high density is required for accuracy of the gross heat capacity, but this increase of density, in turn, magnifies the uncertainty of correction term. Therefore, the ultimate result is by no means improved.

VI-2 Calibration by Extrapolation

A new method was devised to overcome these difficulties. The basic idea was to take the gross heat capacity at reasonable densities, and then to extrapolate isotherms to the zero mass on the gross heat capacity vs. mass plot. This extrapolation method is feasible only when linear or approximately linear extrapolation is possible at the range of low densities. If the isotherms are curved, the reliability of extrapolation is definitely insufficient for the critical requirements. Mathematically,

$$C_{gross} = C_{calr.} + mC_v^* + m(C_v - C_v^*) \qquad (6\text{-}1)$$

If the correction term $(C_v - C_v^*)$ is negligible, Equation (6-1) reduces to

$$C_{gross} = C_{calr.} + mC_v^* \qquad (6\text{-}2)$$

Equation (6-2), then, is a linear equation of mass m. The $C_{calr.}$ can be obtained as C_{gross} at m = 0. Now the problem is to find one actual gas whose C_v differes very slightly from its C_v^* in the projected operating range. In the P vs. T plot, the greater curvature of isometrics is generally observed below the critical temperature. For temperatures far above the critical, the isometrics are almost straight or $(d^2P/dT^2)_V \cong 0$. Consequently, $C_v - C_v^* \cong 0$ at this range. Similar conclusions can be reached if we examine several C_v vs. T plots. Regardless of the compounds under consideration, the general tendency of all isometrics is to converge as the temperature increases. This relation can also be predicted from the analysis of the equation of state. For instance, using the Martin-Hou equation, we have

$$C_v - C_v^* = -T\left(\frac{k}{T_c}\right)^2 e^{-k\frac{T}{T_c}}\left\{\frac{C_2}{(V-b)} + \frac{C_3}{2(V-b)^2} + \frac{C_5}{4(V-b)^4}\right\} \qquad (6\text{-}3)$$

or

$$C_v - C_v^* = g(V)\, T\, e^{-k\frac{T}{T_c}} \qquad (6\text{-}4)$$

The temperature function decreases roughly exponentially and $C_v - C_v^*$ becomes very small at temperatures far above the critical temperature. Thus we may conclude that the suitable gas for calibration is a gas whose critical temperature is well below the room temperature. Most of the so-called permanent gases probably suffice for this condition. However, the convenience of loading and weighing must also be taken into consideration.

VI-3 Results of Calibration

Tetrafluoromethane was chosen for the calibration purpose for two reasons: (1) Tetrafluoromethane was one of the common refrigerants under study, so the extensive gross heat capacity data can be used for both purposes. (2) Tetrafluoromethane satisfies the requirement discussed in the preceding section.

For the convenience of actual plotting, we may plot C_{gross}-mA vs. m instead of C_{gross} vs. m where A is an arbitrary constant. If A is equal or close to C_v^*, we may have an approximately horizontal isotherm. It is obvious that this procedure is merely mathematical in nature and does not even slightly change physical significance. For tetrafluoromethane, statistical C_v^* calculated by Chari[9] was used in place of constant A. The data are summarized in Table 6-1, and the results are presented in Figure 6-1, at 10°C intervals. The intercept of each isotherm is then cross plotted in Figure 6-3. A few isotherms for chlorodifluoromethane are shown in Figure 6-2 to show the consistency

TABLE 6-1

GROSS HEAT CAPACITY DATA OF TETRAFLUOROMETHANE USED IN THE CALIBRATION OF HEAT CAPACITY OF THE CALORIMETER

T	C^*_v(statis)	C_{gross}	mC^*_v	$C_{gross}-mC^*_v$	C_{gross}	mC^*_v	$C_{gross}-mC^*_v$	C_{gross}	mC^*_v	$C_{gross}-mC^*_v$	C_{gross}	mC^*_v	$C_{gross}-mC^*_v$
°C	cal/gm°C	cal/°C	cal/°C	cal/°C	cal/°C	cal/°C	cal/°C	cal/°C	cal/°C	cal/°C	cal/°C	cal/°C	cal/°C
		m = 160.70 gm.			m = 257.44 gm.			m = 334.72 gm.			m = 410.69 gm.		
30	0.1466	131.60	23.56	108.04	145.82	37.74	108.08	157.10	49.07	108.03	168.30	60.21	108.09
40	0.1498	133.00	24.07	108.93	147.49	38.56	108.93	159.07	50.14	108.93	170.48	61.52	108.96
50	0.1530	134.53	24.59	109.94	149.30	39.39	109.91	161.08	51.21	109.87	172.80	62.84	109.96
60	0.1560	135.92	25.07	110.85	151.09	40.16	110.93	103.07	52.22	110.85	175.00	64.07	110.93
70	0.1591	137.31	25.57	111.74	152.75	40.96	111.79	165.07	53.25	111.82	177.20	65.34	111.86
80	0.1621	138.71	26.05	112.66	154.50	41.73	112.77	167.06	54.26	112.80	179.35	66.57	112.78
90	0.1651	140.10	26.53	113.57	156.10	42.50	113.60	168.90	55.26	113.64	118.52	67.80	113.72
100	0.1680	141.46	27.00	114.46	157.70	43.25	114.45	170.73	56.23	114.50	183.61	69.00	114.61
110	0.1708	142.80	27.45	115.35	159.30	43.97	115.33	172.59	57.17	115.42	183.62	70.15	115.47
120	0.1736	144.06	27.90	116.16	160.90	44.69	116.21	174.35	58.11	116.24	187.60	71.30	116.30
130	0.1763	145.29	28.33	116.96	162.38	45.39	116.99	176.10	59.01	117.09			
140	0.1789	146.40	28.75	117.65	163.80	46.06	117.74	177.70	59.88	117.82			
150	0.1815	147.52	29.17	118.35	165.20	46.73	118.47	179.40	60.75	118.65			
160	0.1840	148.63	29.57	119.06	166.59	47.37	119.22	180.93	61.59	119.34			
170	0.1865	149.71	29.97	119.74	167.93	48.01	119.92	182.45	62.43	120.02			
180	0.1888	150.80	30.34	120.46	169.25	48.60	120.65	183.97	63.20	120.77			
190	0.1912	151.95	30.73	121.22	170.50	49.22	121.28	185.38	64.00	121.38			
200	0.1935	152.98	31.10	121.88	171.70	49.81	121.89	186.80	64.77	122.03			

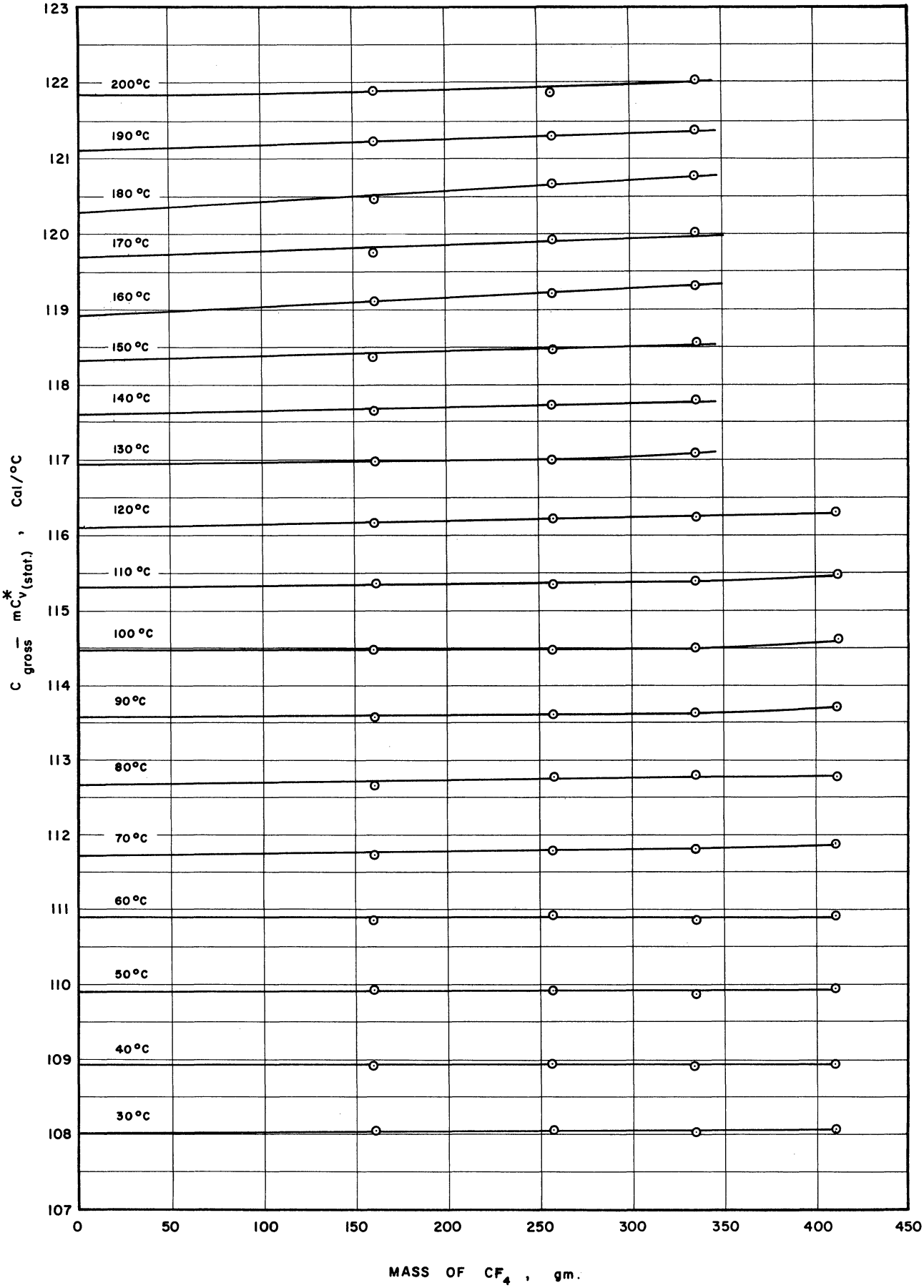

Figure 6-1. Calibration of the Calorimeter Heat Capacity by the Extrapolation Method Using Tetrafluoromethane.

TABLE 6-2

GROSS HEAT CAPACITY DATA OF CHLORODIFLUOROMETHANE USED IN THE CALIBRATION OF HEAT CAPACITY OF THE CALORIMETER

T	$C^*_{v(statis.)}$	C_{gross}	mC^*_v	$C_{gross}-mC^*_v$	C_{gross}	mC^*_v	$C_{gross}-mC^*_v$	C_{gross}	mC^*_v	$C_{gross}-mC^*_v$
°C	cal/gm°C	cal/°C	cal/°C	cal/°C	cal/°C	cal/°C	cal/°C	cal/°C	cal/°C	cal/°C
		m = 166.96 gm.			m = 254.10 gm.			m = 346.08 gm.		
90	0.1539	140.22	25.70	114.52	154.68	39.11	115.57	170.70	53.26	117.44
100	0.1564	141.37	26.11	115.26	155.83	39.74	116.09	171.80	54.13	117.67
110	0.1590	142.47	26.55	115.92	157.08	40.40	116.68	172.96	55.03	117.93
120	0.1614	143.63	26.95	116.68	158.30	41.01	117.29	174.21	55.86	118.35
130	0.1636	144.75	27.31	117.44	159.50	41.57	117.93	175.46	56.62	118.84
140	0.1659	145.88	27.70	118.18	160.84	42.16	118.68	176.75	57.41	119.34
150	0.1681	146.99	28.07	118.92	162.12	42.71	119.41	178.12	58.18	119.94
160	0.1704	148.10	28.45	119.65	163.42	43.30	120.12	179.62	58.97	120.65
170	0.1726	149.15	28.82	120.33	164.71	43.86	120.85	181.11	59.73	121.38
180	0.1749	150.21	29.20	121.01	166.03	44.44	121.59	182.68	60.53	122.15
190	0.1771	151.30	29.57	121.73	167.27	45.00	122.27	184.19	61.29	122.90
200	0.1791	152.38	29.90	122.38	168.53	45.51	123.02			

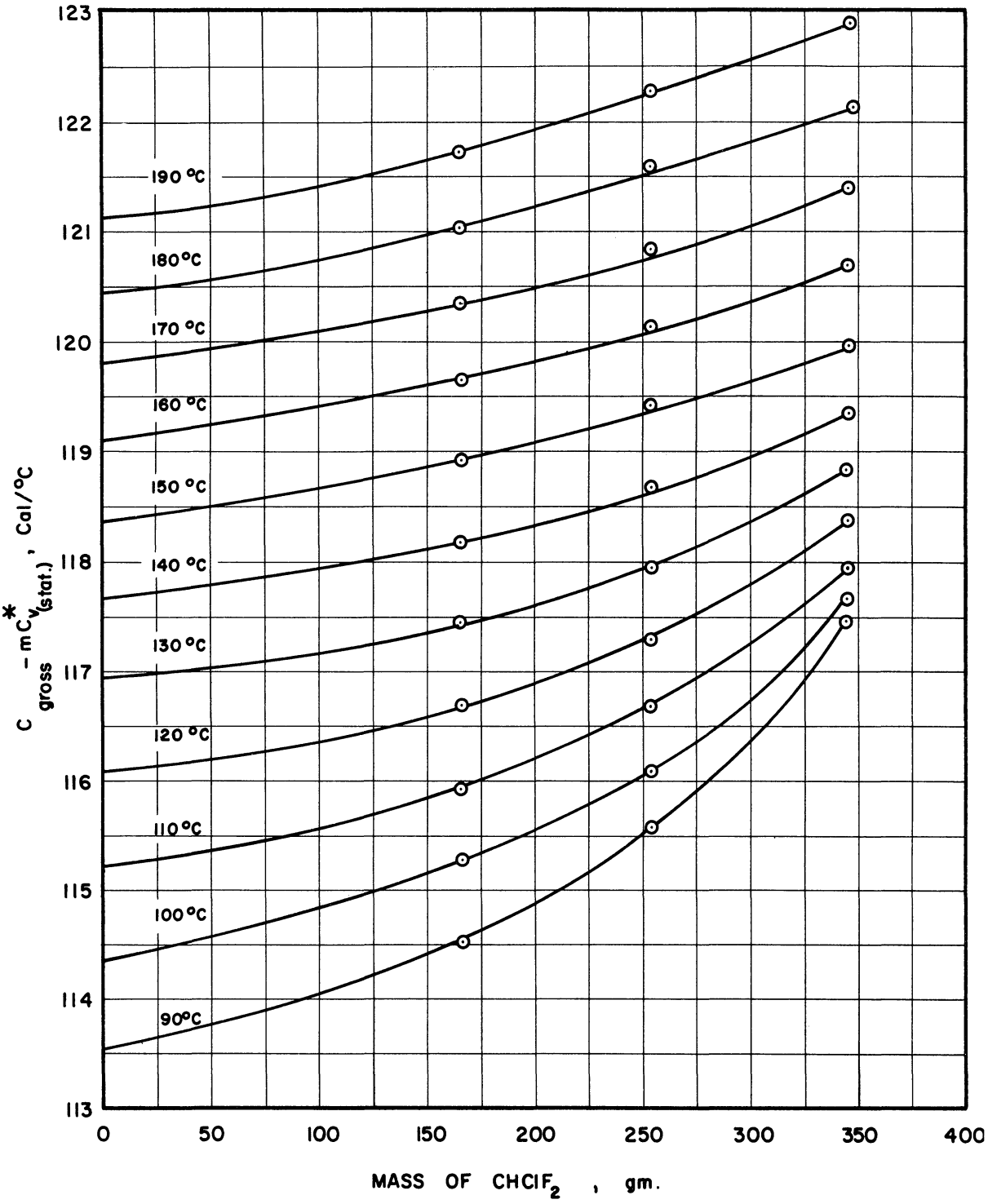

Figure 6-2. Calibration of the Calorimeter Heat Capacity by the Extrapolation Method Using Chlorodifluoromethane.

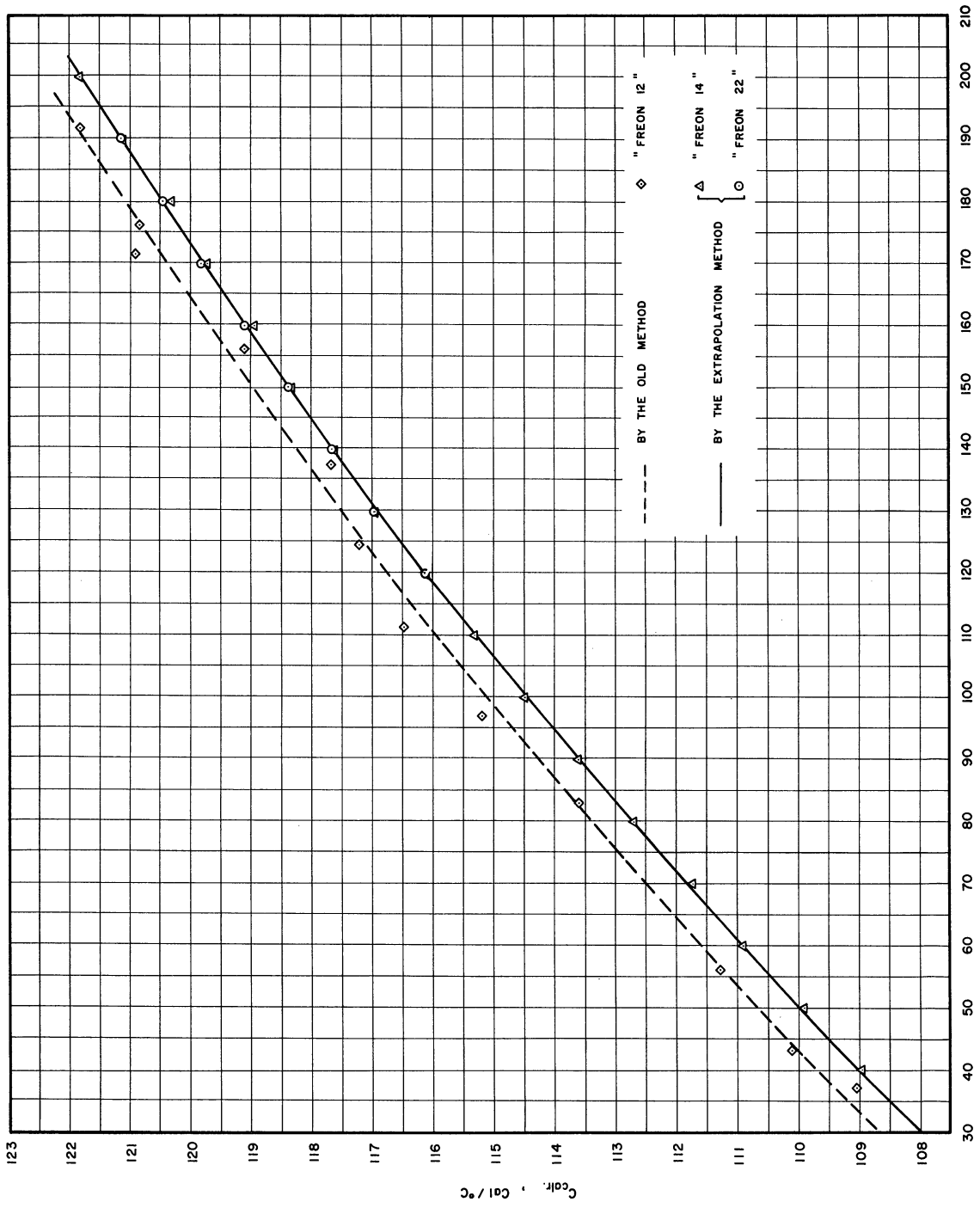

Figure 6-3. Heat Capacity of the Calorimeter.

of results. (For data see Table 6-2.) It should be noted that the critical temperature of chlorodifluoromethane is 96.01°C and the extrapolation is not very reliable for low temperatures.

VI-4 Comparison with the Former Method

Before the extensive data for tetrafluoromethane were collected, all tentative calculations of C_v were based on calibration by the former method as described in Section VI-1. Dichlorodifluoromethane was chosen for this purpose. C_v^* was based on Masi's data[32] and the correction was based on the Martin-Hou equation of state.[34] The experimental data are summarized in Table 6-3 and the final results are plotted in Figure 6-3. On the average, the results are about 0.5% higher than those based on the extrapolation method. This would naturally lead to the speculation that all data published by de Nevers and Martin[13] might be in considerable error. This was not the case, however, since C_v data were only collected over a considerably high density range in which the heat capacity of the contents was generally larger than that of the calorimeter. Thus this 0.5% discrepancy can cause only less than 0.5% error in their final results. In the present study, however, the situation is entirely different, since the density range is quite low; in this range at the worst, the heat capacity of the contents is only about 1/5 of the heat capacity of the calorimeter. This means that 1/2% discrepancy in the calibration may result in a 2.5% error in the final C_v data. Thus it was obvious that accuracy of calibration was a requisite to the success of the project. Besides the very good agreement between the experimental C_v^* and the statistical C_v^* for tetrafluoromethane, the

TABLE 6-3

CALIBRATION OF CALORIMETER HEAT CAPACITY BY THE OLD METHOD USING DICHLORODIFLUOROMETHANE

Run No.	T_{mean}	C_v^*	$C_v - C_v^*$	C_v	mC_v	C_{gross}	$C_{calr.}$
	°C	cal/gm°C	cal/gm°C	cal/gm°C	cal/°C	cal/°C	cal/°C
	m = 55.03 gm. Dichlorodifluoromethane						
A23	37.37	0.1303	.00344	0.1337	7.36	116.40	109.04
A11	43.36	0.1316	.00322	0.1348	7.42	117.52	110.10
A12	56.10	0.1344	.00279	0.1372	7.55	118.81	111.26
A13	83.20	0.1397	.00206	0.1418	7.80	121.34	113.54
A14	97.07	0.1423	.00176	0.1441	7.93	123.10	115.17
A15	111.45	0.1449	.00149	0.1464	8.06	124.51	116.45
A16	124.53	0.1473	.00128	0.1486	8.18	125.38	117.20
A17	137.50	0.1495	.00110	0.1506	8.29	125.94	117.65
A18	156.26	0.1523	.00088	0.1532	8.43	127.52	119.09
A19	171.55	0.1544	.00073	0.1551	8.54	129.44	120.90
A21	176.06	0.1550	.00069	0.1557	8.57	129.39	120.82
A22	191.83	0.1570	.00057	0.1576	8.67	130.49	121.82

dichlorodifluoromethane was again chosen for checking purposes. Experimental C_v was then compared with Masi's C_v^* data[32] plus the correction based on the Martin-Hou equation of state.[34] The result is plotted in Figure 7-1. The agreement is within 0.3%.

VII. EXPERIMENTAL RESULTS

VII-1 Constant Volume Heat Capacity of Dichlorodifluoromethane

No attempt was made to collect extensive C_v data for dichlorodifluoromethane since Masi[32] has published very reliable C_p^* (or C_v^*) data. A few experiments with this compound, however, were made to provide an appropriate check for the accuracy of C_v data taken on other compounds for which no experimental data are available. This also provided considerable confidence in the new method of calibrating the heat capacity of the calorimeter, as discussed in the preceding chapter.

A series of runs were taken all at one medium density, 0.05695 gm/cc or 10.2% of the critical density. The results are shown in Table 7-1, where the mean temperature, T_{mean}, is an arithmetic mean of the initial and final temperatures of the temperature range over which heat was added. The gross heat capacity, C_{gross}, is the mean gross heat capacity over the same temperature range, but is regarded as the true C_{gross}, at the mean temperature. The heat capacity of the calorimeter, etc., designated as $C_{calr.}$ is the calibrated value at the mean temperature. The net heat capacity, C_{net}, is the difference between C_{gross} and $C_{calr.}$ Constant-volume heat capacity, C_v, is obtained by dividing C_{net} by the total mass of contents.

To minimize the uncertainty involved in the correction term $(C_v-C_v^*)$ based on the Martin-Hou[34] equation of state, and thus to have a better comparison of the experimental data with Masi's published

TABLE 7-1

CONSTANT-VOLUME HEAT CAPACITY OF DICHLORODIFLUOROMETHANE (CF_2Cl_2)

Run No.	T_{mean} °C	C_{gross} cal/°C	$C_{calr.}$ cal/°C	C_{net} cal/°C	C_v cal/gm°C
	Dichlorodifluoromethane Loading No. 2 251.74 gm.		0.05695 gm/cc.		
E-1	122.25	155.03	116.80	38.23	0.1519
E-2	133.70	155.60	117.18	38.42	0.1526
E-3	144.56	156.90	117.95	38.95	0.1547
E-4	156.62	158.34	118.85	39.49	0.1569
E-5	162.13	158.62	119.22	39.40	0.1565
E-6	173.57	159.79	120.05	39.74	0.1579
E-7	184.90	160.79	120.80	39.99	0.1589

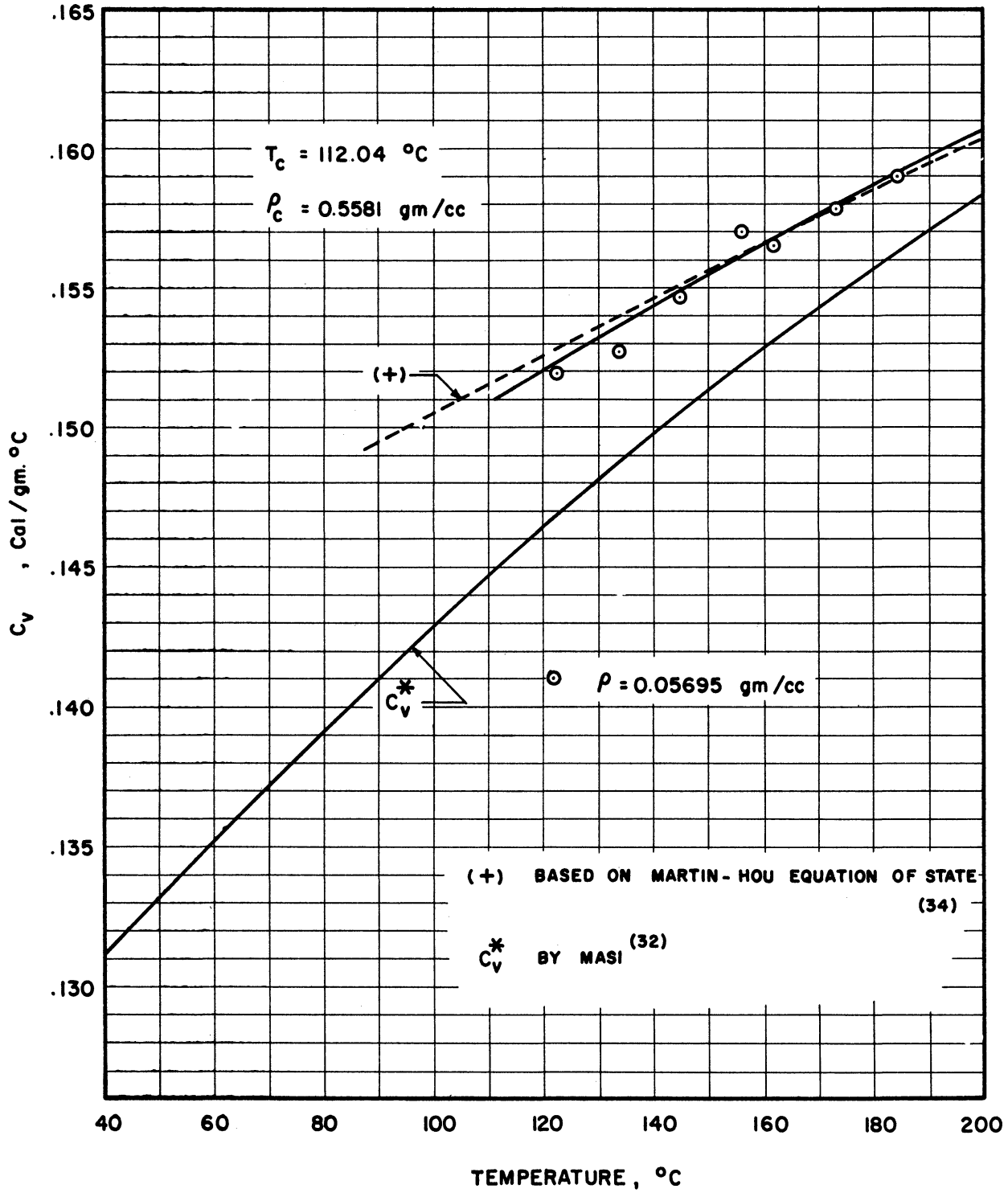

Figure 7-1. Constant-Volume Heat Capacity of Dichlorodifluoromethane (CCl_2F_2).

data, the temperature was confined to a range above the critical temperature, 233.6°F. The experimental results are plotted on a C_V vs. T plane in Figure 7-1. A smooth curve has been drawn through seven data points. The worst scatter of the data points from this isometric is 0.67 percent, and most of the data points deviate from this curve by less than 0.2 percent. The C_V calculated from Masi's C_V^* data plus the correction based on the Martin-Hou equation of state is also shown in Figure 7-1. Comparison of these two curves leads to the conclusion that agreement is within 0.3 percent. Allowing some possible error in the correction term $(C_V - C_V^*)$, say 10 percent, the discrepancy still would not exceed 1 percent since the maximum correction is only 4 percent of C_V.

VII-2. Constant-Volume Heat Capacity of Tetrafluoromethane

Due to the simple and symmetrical molecular structure of tetrafluoromethane, the spectroscopic data, or more specifically the assignment of the fundamental frequencies, are in close agreement among various authors. Therefore the statistically calculated values of C_V^* should be more reliable than those of other compounds studied, whose fundamental frequencies were chosen rather arbitrarily. For this reason, comparison of experimental C_V^* of this compound with the statistical C_V^* was of great interest.

The experimental results for tetrafluoromethane are shown in Table 7-2. They are presented in similar form as in Table 7-1, except

TABLE 7-2

CONSTANT-VOLUME HEAT CAPACITY OF TETRAFLUOROMETHANE (CF_4)

T	C_{gross}	$C_{calr.}$	C_{net}	C_v
°C	cal/°C	cal/°C	cal/°C	cal/gm°C
	Tetrafluoromethane Loading No. 1			
	160.70 gm.		0.03638 gm/cc.	
30	131.60	108.00	23.60	0.1469
40	133.00	108.95	24.05	0.1497
50	134.53	109.92	24.61	0.1531
60	135.92	110.90	25.02	0.1557
70	137.31	111.86	25.45	0.1584
80	138.71	112.75	25.96	0.1615
90	140.10	113.63	26.47	0.1647
100	141.06	114.46	27.00	0.1680
110	142.80	115.30	27.50	0.1711
120	144.06	116.11	27.95	0.1739
130	145.29	116.90	28.39	0.1767
140	146.40	117.64	28.76	0.1790
150	147.52	118.38	29.14	0.1813
160	148.63	119.10	29.53	0.1838
170	149.71	119.80	29.91	0.1861
180	150.80	120.47	30.33	0.1887
190	151.81	121.13	30.68	0.1909
200	152.80	121.78	31.02	0.1932

TABLE 7-2 (cont'd)

CONSTANT-VOLUME HEAT CAPACITY OF TETRAFLUOROMETHANE (CF_4)

T	C_{gross}	$C_{calr.}$	C_{net}	C_v
°C	cal/°C	cal/°C	cal/°C	cal/gm°C
	Tetrafluoromethane Loading No. 2			
	257.44 gm.		0.05822 gm/cc.	
30	145.82	108.00	37.82	0.1469
40	147.49	108.95	38.54	0.1497
50	149.30	109.92	39.38	0.1530
60	151.09	110.90	40.19	0.1561
70	152.75	111.86	40.89	0.1588
80	154.50	112.75	41.75	0.1622
90	156.10	113.63	42.47	0.1650
100	157.70	114.46	43.24	0.1680
110	159.30	115.30	44.00	0.1709
120	160.90	116.11	44.79	0.1740
130	162.38	116.90	45.48	0.1767
140	163.80	117.64	46.16	0.1793
150	165.20	118.38	46.82	0.1819
160	166.59	119.10	47.49	0.1845
170	167.93	119.80	48.13	0.1870
180	169.25	120.47	48.78	0.1895
190	170.50	121.13	49.37	0.1918
200	171.70	121.78	49.92	0.1939
	Tetrafluoromethane Loading No. 3			
	334.72 gm.		0.07563 gm/cc.	
30	157.10	108.00	49.10	0.1467
40	159.07	108.95	50.12	0.1497
50	161.08	109.92	51.16	0.1528
60	163.07	110.90	52.17	0.1559
70	165.07	111.86	53.21	0.1590
80	167.06	112.75	54.31	0.1623
90	168.90	113.63	55.27	0.1651
100	170.73	114.46	56.27	0.1681
110	172.59	115.30	57.29	0.1712
120	174.35	116.11	58.24	0.1740
130	176.10	116.90	59.20	0.1769
140	177.70	117.64	60.06	0.1794

TABLE 7-2 (cont'd)

CONSTANT-VOLUME HEAT CAPACITY OF TETRAFLUOROMETHANE (CF_4)

T	C_{gross}	$C_{calr.}$	C_{net}	C_v
°C	cal/°C	cal/°C	cal/°C	cal/gm°C
	Tetrafluoromethane Loading No. 3 (Cont'd) 334.72 gm.		0.07563 gm/cc.	
150	179.40	118.38	61.02	0.1823
160	180.93	11 .10	61.83	0.1847
170	182.45	119.80	62.65	0.1871
180	183.97	120.47	63.50	0.1897
190	185.38	121.13	64.25	0.1920
200	186.80	121.78	65.02	0.1942
	Tetrafluoromethane Loading No. 4 410.69 gm.		0.09290 gm/cc.	
30	168.30	108.00	60.30	0.1468
40	170.48	108.95	61.53	0.1498
50	172.80	109.92	62.88	0.1531
60	175.00	110.90	64.10	0.1561
70	177.20	111.86	65.34	0.1591
80	179.35	112.75	66.60	0.1622
90	181.52	113.63	67.89	0.1653
100	183.61	114.46	69.15	0.1684
110	185.62	115.30	70.32	0.1712
120	187.60	116.11	71.49	0.1741

that C_{gross} is read from the smoothed gross heat-capacity curve (see Appendix D, Figures D-1 and D-2) and C_v is calculated at every 10°C interval. Four densities were used ranging from 0.03638 gm/cc or 5.8% of the critical density to 0.09290 gm/cc or 14.9% of the critical density. The temperature range was from 30°C to 200°C for three low densities, but only up to 120°C for the highest density, to keep the pressure within 500 psi.

The results are plotted in Figure 7-2. The fluctuations of the gross heat capacity (see Appendix D) were generally less than 0.2% except in three runs at the lowest density in which the maximum fluctuation was 0.35%. Regardless of densities, all C_v data fluctuate along the statistically calculated C_v^* line by Chari.[9] The value of the correction term $C_v - C_v^*$ is practically negligible. The solid line in Figure 7-2 shows a lower limit of confidence for C_v and may be regarded as the experimental constant-volume heat capacity at the zero pressure. This observed line deviates from Chari's statistical calculation by only 0.2%. The dashed line in Figure 7-2 is based on Chari's correlation:

$$C_v^* = 3.00559282 \times 10^{-2} + 2.37043352 \times 10^{-4}T - 2.85660077 \times 10^{-8}T^2 - 2.95338806 \times 10^{-11}T^3 \qquad (7\text{-}1)$$

where

T is in °R and C_v^* is in Btu/lb°R.

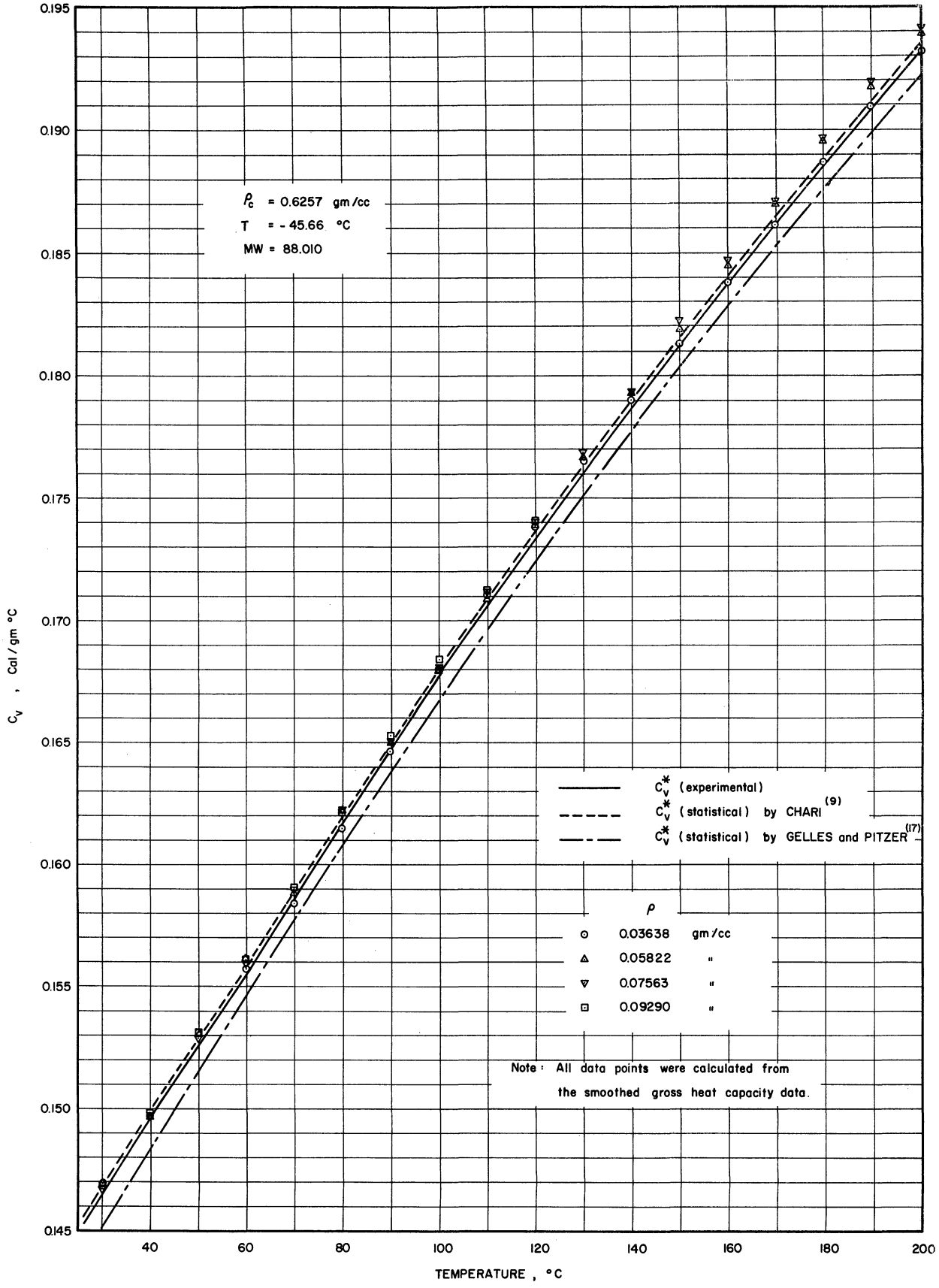

Figure 7-2. Constant-Volume Heat Capacity of Tetrafluoromethane (CF_4).

The statistical C_v^* by Gelles and Pitzer[17] is 0.4~0.6% less than the experiment values. This is also shown in Figure 7-2 for comparison.

VII-3. Constant-Volume Heat Capacity of Chlorodifluoromethane

The experimental results for chlorodifluoromethane are shown in Table 7-3. They are presented in the same form as in Tables 7-1 and 7-2. Data were taken for five densities, ranging from 0.0378 gm/cc up to 0.1239 gm/cc. These corresponded to 6.85 percent to 22.4% of critical density. The temperature range was from the saturation temperature (approximate) to 200°C for two low densities, and up to 190°C, 150°C, and 110°C, respectively, for three high densities to limit the pressure within 525 psi. For three low densities, as in the case of tetrafluoromethane C_{gross} was read from the smoothed gross heat-capacity curves (see Appendix D, Figures D-3 and D-4.) For two high densities, C_v was calculated for each run of experiments.

The results are also plotted in Figure 7-3. A smooth curve has been drawn through data points for each density; the maximum deviation is about 0.8 percent, and, except for two runs, all are less than 0.3 percent. For three low densities, the deviation in the final plot is negligible because data have been smoothed at the gross heat capacity level. Fluctuations of C_{gross} from the smoothed gross heat capacity curve are less than 0.3 percent except two runs which are up to 0.35%.

TABLE 7-3

CONSTANT-VOLUME HEAT CAPACITY OF CHLORODIFLUOROMETHANE ($CHClF_2$)

Run No.	T	C_{gross}	$C_{calr.}$	C_{net}	C_v
	°C	cal/°C	cal/°C	cal/°C	cal/gm°C
	Chlorodifluoromethane Loading No. 1				
	166.96 gm.		0.0378 gm/cc.		
	50	135.58	109.92	25.66	0.1537
	60	136.70	110.90	25.80	0.1545
	70	137.85	111.86	25.99	0.1557
	80	139.00	112.75	26.25	0.1572
	90	140.15	113.63	26.52	0.1588
	100	141.30	114.46	26.84	0.1608
	110	142.47	115.30	27.17	0.1627
	120	143.63	116.11	27.52	0.1648
	130	144.75	116.90	27.85	0.1668
	140	145.88	117.64	28.24	0.1691
	150	146.99	118.38	28.61	0.1714
	160	148.10	119.10	29.00	0.1737
	170	149.15	119.80	29.35	0.1758
	180	150.21	120.47	29.74	0.1781
	190	151.30	121.13	30.17	0.1807
	200	152.38	121.78	30.60	0.1833
	Chlorodifluoromethane Loading No. 2				
	254.10 gm.		0.0575 gm/cc.		
	50	149.70	109.92	39.78	0.1566
	60	150.90	110.90	40.00	0.1574
	70	152.22	111.86	40.36	0.1588
	80	153.40	112.75	40.65	0.1600
	90	154.62	113.63	40.99	0.1613
	100	155.83	114.46	41.37	0.1628
	110	157.08	115.30	41.78	0.1644
	120	158.30	116.11	42.19	0.1660
	130	159.59	116.90	42.69	0.1680
	140	160.84	117.64	43.20	0.1700
	150	162.12	118.38	43.74	0.1721
	160	163.42	119.10	44.32	0.1744
	170	164.71	119.80	44.91	0.1767
	180	166.03	120.47	45.56	0.1793
	190	167.27	121.13	46.14	0.1816
	200	168.53	121.78	46.75	0.1840

TABLE 7-3 (cont'd)

CONSTANT-VOLUME HEAT CAPACITY OF CHLORODIFLUOROMETHANE ($CHClF_2$)

Run No.	T	C_{gross}	$C_{calr.}$	C_{net}	C_v
	°C	cal/°C	cal/°C	cal/°C	cal/gm°C
	Chlorodifluoromethane Loading No. 3				
	346.08 gm.		0.0782 gm/cc.		
	60	167.85	110.90	56.95	0.1646
	70	168.70	111.86	56.84	0.1642
	80	169.67	112.75	56.92	0.1645
	90	170.70	113.60	57.07	0.1649
	100	171.80	114.46	57.34	0.1657
	110	172.96	115.30	57.66	0.1666
	120	174.26	116.11	58.15	0.1680
	130	175.60	116.90	58.70	0.1696
	140	176.95	117.64	59.31	0.1714
	150	178.35	118.38	59.97	0.1733
	160	179.80	119.10	60.70	0.1754
	170	181.22	119.80	61.42	0.1775
	180	182.68	120.47	62.21	0.1798
	190	184.19	121.13	63.06	0.1822
	Chlorodifluoromethane Loading No. 4				
	447.08 gm.		0.1011 gm/cc.		
A24	73.32	188.20	112.15	76.05	0.1701
A25	85.68	188.53	113.25	75.28	0.1684
A26	95.91	189.45	114.14	75.31	0.1684
A27	113.62	191.50	115.58	75.92	0.1698
A28	124.58	193.01	116.48	76.53	0.1712
A29	136.57	195.18	117.40	77.78	0.1740
A30	150.09	197.32	118.45	78.87	0.1764
	Chlorodifluoromethane Loading No. 5				
	548.22 gm.		0.1239 gm/cc.		
A31	75.63	208.33	112.36	95.97	0.1751
A32	87.85	209.08	113.44	95.64	0.1745
A33	100.19	208.72	114.46	94.26	0.1719
A34	110.19	210.78	115.29	95.49	0.1742
A35	84.56	208.32	113.15	95.17	0.1736

It is estimated that a single data point might deviate by as much as 2 percent if the gross heat capacity were not smoothed.

Figure 7-4 is a cross plot of Figure 7-3 into the C_v vs. density plane. The isotherms in Figure 7-4 are constructed by plotting the values of smooth isometrics in Figure 7-3, where those isometrics intersect the lines of constant temperature. None of the points in Figure 7-4 scatters from the smoothed curve by more than 0.3 percent. This indicates good internal consistency of the experimental data. Each isotherm is extrapolated to zero density to obtain ideal gas heat capacity, C_v^*, as a function of temperature. The values obtained by such extrapolation are then cross-plotted as C_v^* vs. temperature on Figure 7-3. The statistical C_v^* calculated by Martin et al.[26] is also shown in Figure 7-3 for comparison. The experimental values are higher than the calculated values by 0.8 percent on average. The statistical C_v^* calculated by Weissman, Meister, and Cleveland[45] is almost the same as that calculated by Gelles and Pitzer.[17] This is also shown in Figure 7-3 for comparison. Their values are lower than the experimental values by as much as 3.9 percent at 200°C and 4.5 percent at 80°C.

Figure 7-5 is analogous to Figure 7-4, except that each isotherm is translated downward by the amount of C_v^* corresponding to each temperature so that all isotherms pass the origin, yielding C_v-C_v^* vs. density plot with temperature as a parameter. Figure 7-6 is analogous

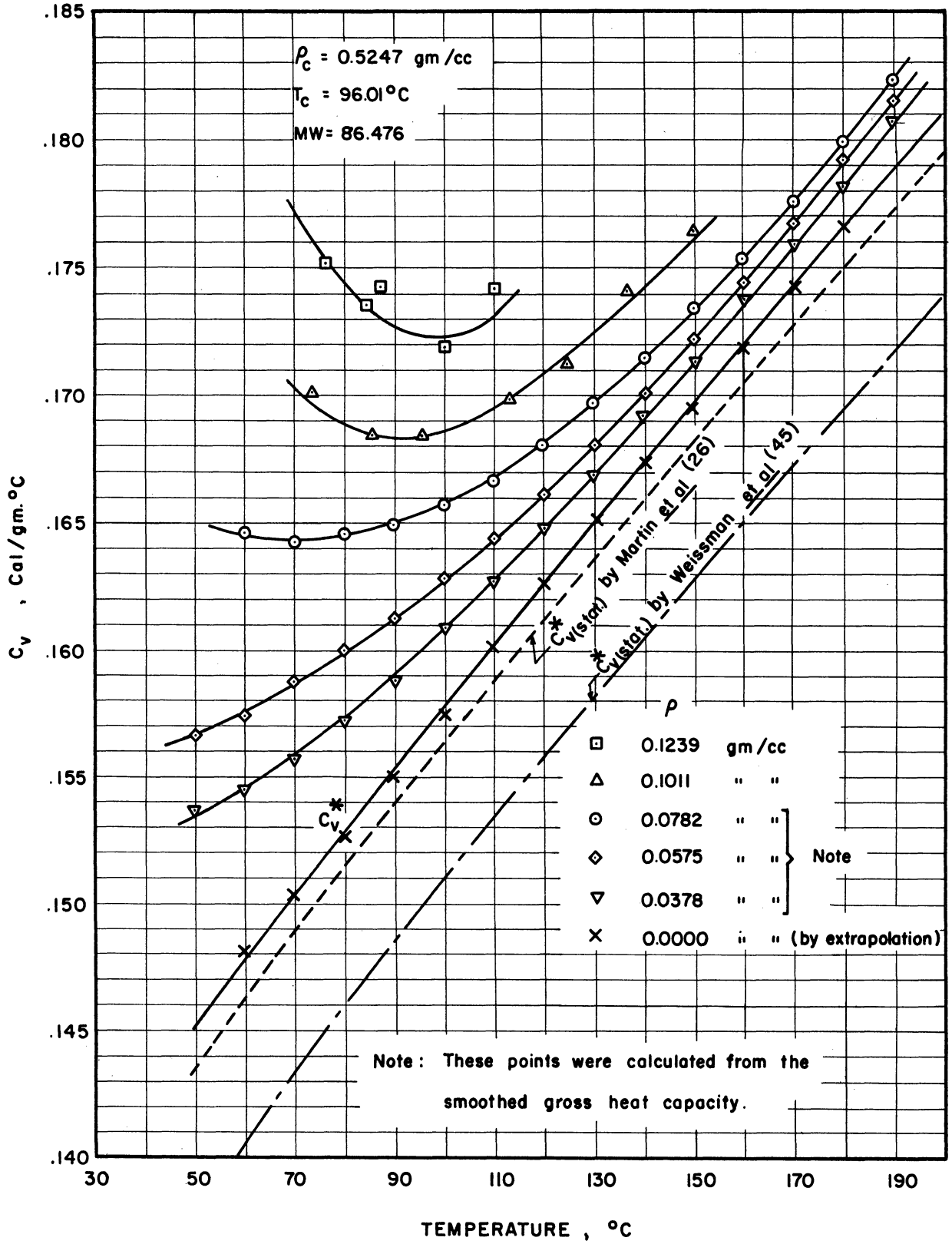

Figure 7-3. Constant-Volume Heat Capacity of Chlorodifluoromethane ($CHClF_2$).

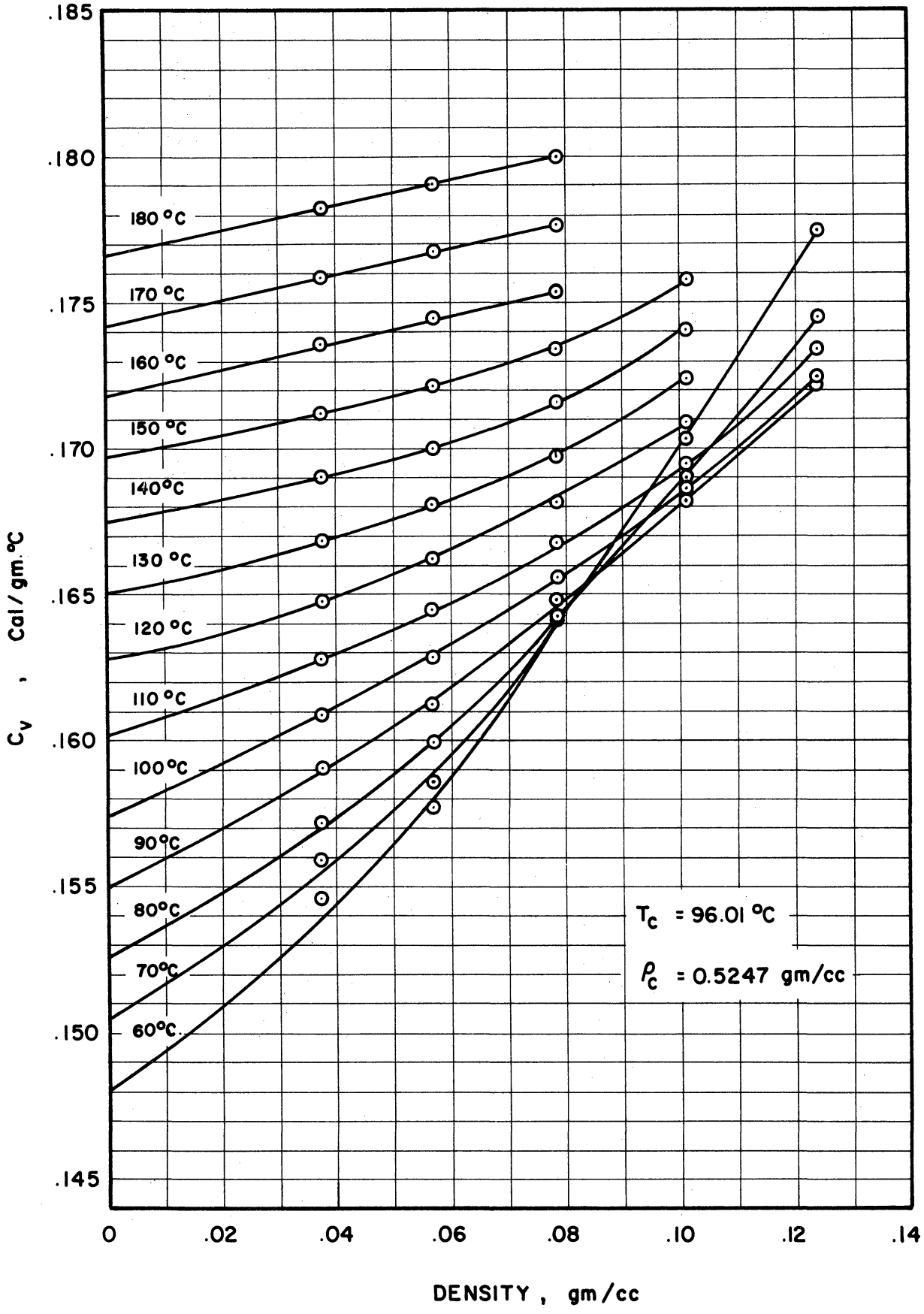

Figure 7-4. Constant-Volume Heat Capacity of Chlorodifluoromethane ($CHClF_2$). (This is a cross plot of Figure 7-3)

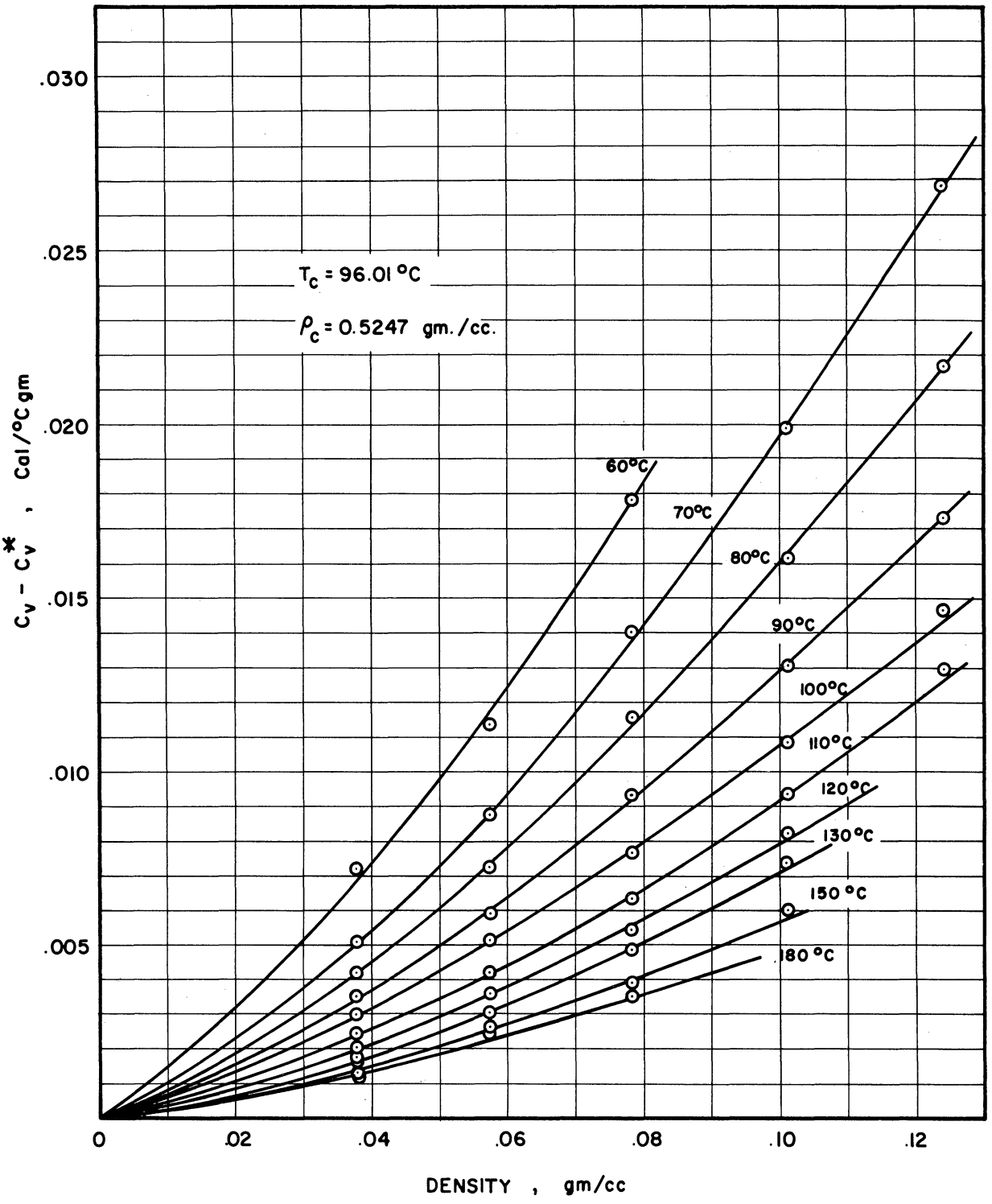

Figure 7-5. C_V-C_V* of Chlorodifluoromethane ($CHClF_2$) (This is a modified cross plot of Figure 7-3.)

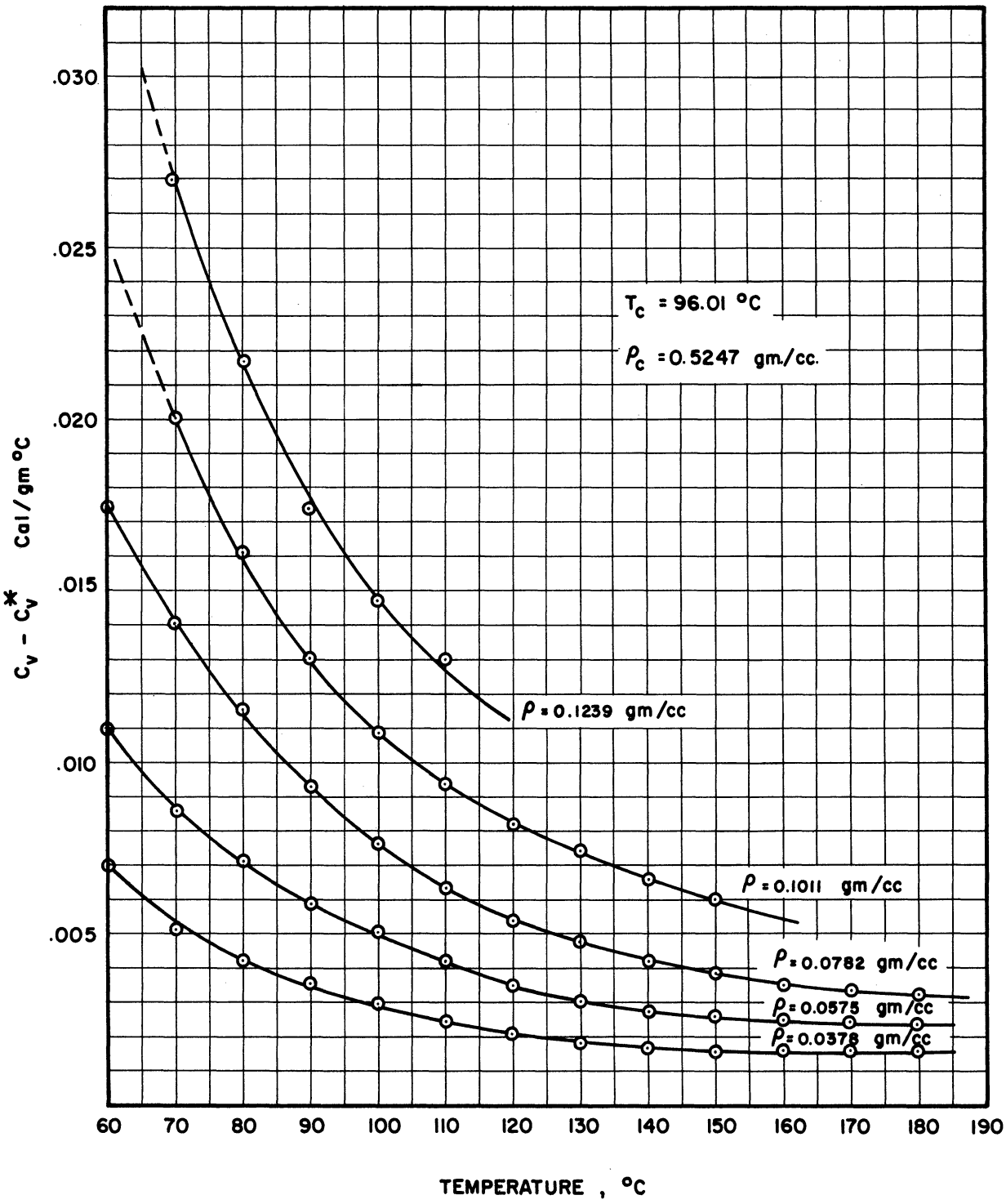

Figure 7-6. C_v-C_v* of Chlorodifluoromethane ($CHClF_2$). (This is a modified plot of Figure 7-3)

to Figure 7-3 but the isometrics are translated downward as in Figure 7-5, yielding a C_V-C_V* vs. temperature plot. These modified plots are very convenient for checking an equation of state since the PVT data influence only the correction term (C_V-C_V*)and not the absolute value of C_V, according to the following relation:

$$C_V - C_V^* = -\int_V^\infty T\left(\frac{d^2P}{dT^2}\right)_V dV \qquad (1\text{-}3)$$

VII-4. Constant-Volume Heat Capacity of Dichlorotetrafluoroethane

The experimental heat-capacity results for dichlorotetrafluoroethane are shown in Table 7-4. They are presented in the same way as in the case of chlorodifluoromethane. Data were collected for four densities, ranging from 0.0375 gm/cc up to 0.1357 gm/cc. These densities corresponded to 6.45 ~~percent~~ up to 23.4 ~~percent~~ of the critical density. For all densities, the temperature range was from the saturation temperature to 200°C. The estimated pressure was less than 500 psi for all runs. For low densities, the final C_V data were calculated based on the smoothed gross heat-capacity curves as before (see Appendix D. Figure D-5). For two high densities, the final C_V data were calculated directly from the measured gross heat capacity.

These results are plotted in Figure 7-7 on a C_V vs. temperature plane. The gross heat capacity never deviated from a smoothed curve by more than 0.55 percent and most of the data scattered by less than 0.4 percent. The maximum scatter of the final C_V would have been as high as 2.5 percent if gross heat-capacity data were not smoothed. For two high densities, the maximum scatter of the final C_V data is 0.55 percent from the smoothed curve, and most of points deviate from the smoothed curve by less than 0.3%.

TABLE 7-4

CONSTANT-VOLUME HEAT CAPACITY OF DICHLOROTETRAFLUOROETHANE
($CClF_2$-$CClF_2$)

Run No.	T	C_{gross}	$C_{calr.}$	C_{net}	C_v
	°C	cal/°C	cal/°C	cal/°C	cal/gm°C
	Loading No. 1. 165.67 gm. 0.0375 gm/cc.				
	80	141.12	112.75	28.37	0.1712
	90	142.22	113.63	28.59	0.1726
	100	143.33	114.46	28.87	0.1743
	110	144.43	115.30	29.13	0.1758
	120	145.57	116.11	29.46	0.1778
	130	146.70	116.90	29.80	0.1799
	140	147.78	117.64	30.14	0.1819
	150	148.80	118.38	30.42	0.1836
	160	149.83	119.10	30.73	0.1855
	170	150.88	119.80	31.08	0.1876
	180	151.90	120.47	31.43	0.1877
	190	152.95	121.13	31.82	0.1921
	200	153.95	121.78	32.17	0.1942
	Loading No. 2. 291.05 gm. 0.0658 gm/cc.				
	90	164.50	113.63	50.87	0.1748
	100	165.77	114.46	51.31	0.1763
	110	167.02	115.30	51.72	0.1777
	120	168.31	116.11	52.20	0.1793
	130	169.58	116.90	52.68	0.1810
	140	170.88	117.64	53.24	0.1829
	150	172.20	118.38	53.82	0.1849
	160	173.47	119.10	54.37	0.1868
	170	174.72	119.80	54.92	0.1887
	180	176.00	120.47	55.53	0.1908
	190	177.30	121.13	56.17	0.1930
	200	178.66	121.78	56.82	0.1952

TABLE 7-4 (cont'd)

CONSTANT-VOLUME HEAT CAPACITY OF DICHLOROTETRAFLUOROETHANE
($CClF_2$-$CClF_2$)

Run No.	T	C_{gross}	$C_{calr.}$	C_{net}	C_v
	°C	cal/°C	cal/°C	cal/°C	cal/gm°C
Loading No. 3. 440.56 gm. 0.0997 gm/cc.					
B56	108.57	195.33	115.17	80.16	0.1819
B57	119.38	197.01	116.05	80.96	0.1838
B58	130.71	197.85	116.95	80.90	0.1836
B59	155.87	201.77	118.78	82.99	0.1884
B60	165.86	202.60	119.50	83.10	0.1886
B61	182.41	204.93	120.61	84.32	0.1914
B62	193.64	207.33	121.38	85.95	0.1951
B63	145.81	199.88	118.10	81.78	0.1856
B64	174.65	204.16	120.08	84.08	0.1908
Loading No. 4. 600.17 gm. 0.1357 gm/cc.					
B27	115.29	228.16	115.73	112.43	0.1873
B28	124.87	229.26	116.50	112.76	0.1879
B29	134.84	230.18	117.26	112.92	0.1881
B30	145.77	230.92	118.09	112.83	0.1880
B31	155.98	232.01	118.80	113.21	0.1886
B32	166.10	233.65	119.51	114.14	0.1902
B33	177.41	236.22	120.27	115.95	0.1932
B34	186.34	237.99	120.87	117.12	0.1951
B35	195.77	239.77	121.52	118.25	0.1970

Figure 7-8 is a cross plot of Figure 7-7, and is similar to Figure 7-4. The maximum scatter of the cross-plotted data on the C_v vs. density plane is 0.2 percent. Each isotherm is extrapolated to zero density to determine the ideal gas heat capacity which is then cross-plotted on Figure 7-7. The statistical C_v^* calculated by Martin[25] is also shown in Figure 7-7 for comparison. The dashed line in Figure 7-7 is based on his equation:

$$C_v^* = 0.0175 + 3.49 \times 10^{-4} T - 1.67 \times 10^{-7} T^2 \qquad (7\text{-}2)$$

where T is in °R, C_v^* in Btu/lb.°R. The values of C_v^* calculated from this equation are generally higher than the experimental values in a range of from 100 to 200°C. The maximum difference is about 3.4 percent at 100°C. The statistical C_v^* of isomeric dichlorotetrafluoroethane (CF_3CFCl_2) was calculated by Smith, Alpert, Saunders, Brown, and Moran.[42] Their value of C_v^* for CF_3CFCl_2 is 0.1702 cal/gm°C at 400°K, which compares with an experimental value of 0.1767 for $CClF_2CClF_2$ at 400°K.

Figure 7-9 is analogous to Figure 7-8, showing $C_v - C_v^*$ as a function of density with temperature as a parameter. It is to be noted that the isotherms of temperature higher than the critical temperature are practically straight, and linear extrapolation has been made insofar as possible. In Figures 7-8 and 7-9, isotherms have been drawn at 10°C intervals from 110°C to 200°C. Figure 7-10 is analogous to Figure 7-7, showing $C_v - C_v^*$ as a function of temperature with density as a parameter.

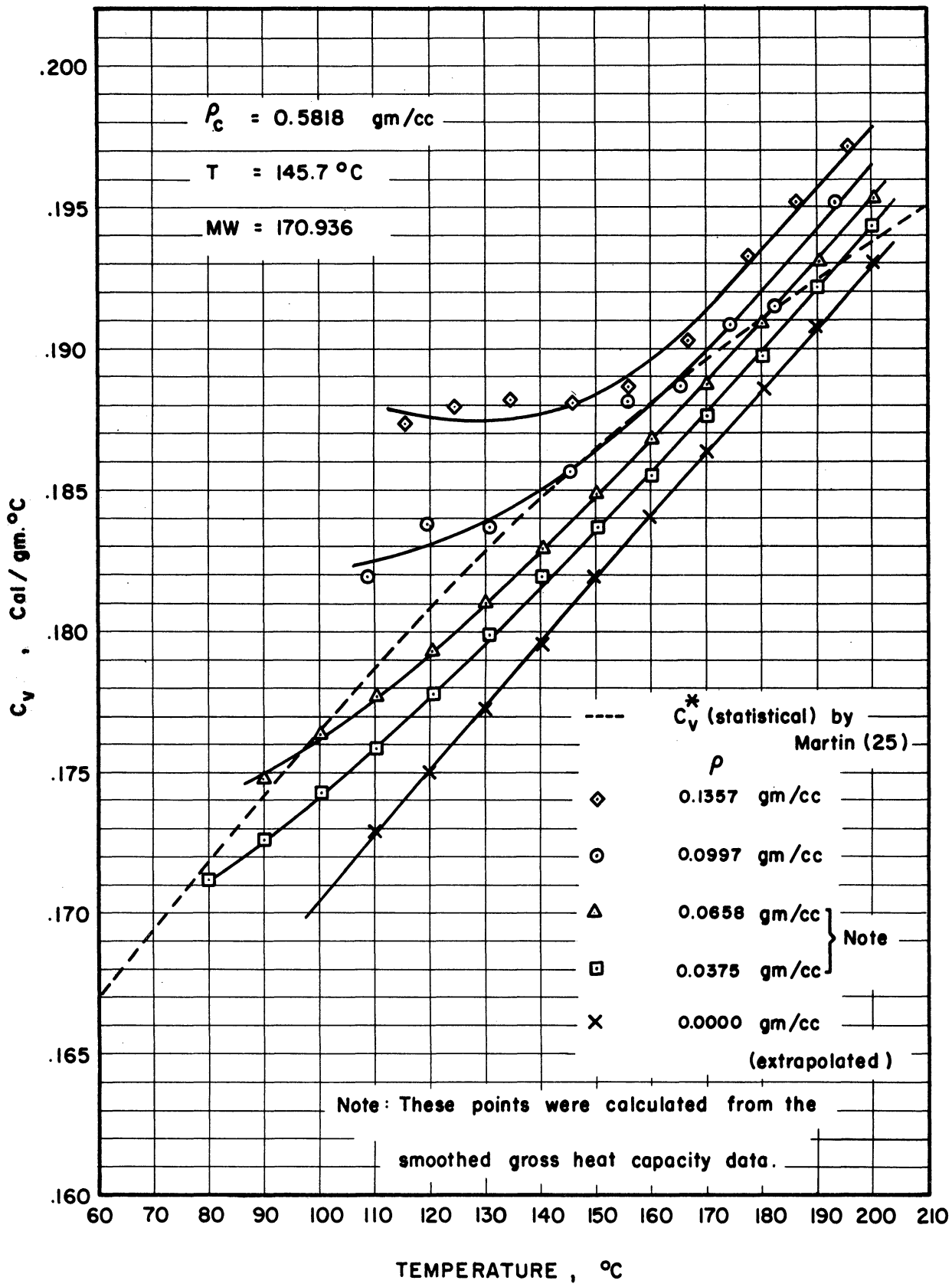

Figure 7-7. Constant-Volume Heat Capacity of Dichlorotetrafluoroethane ($CClF_2CClF_2$)

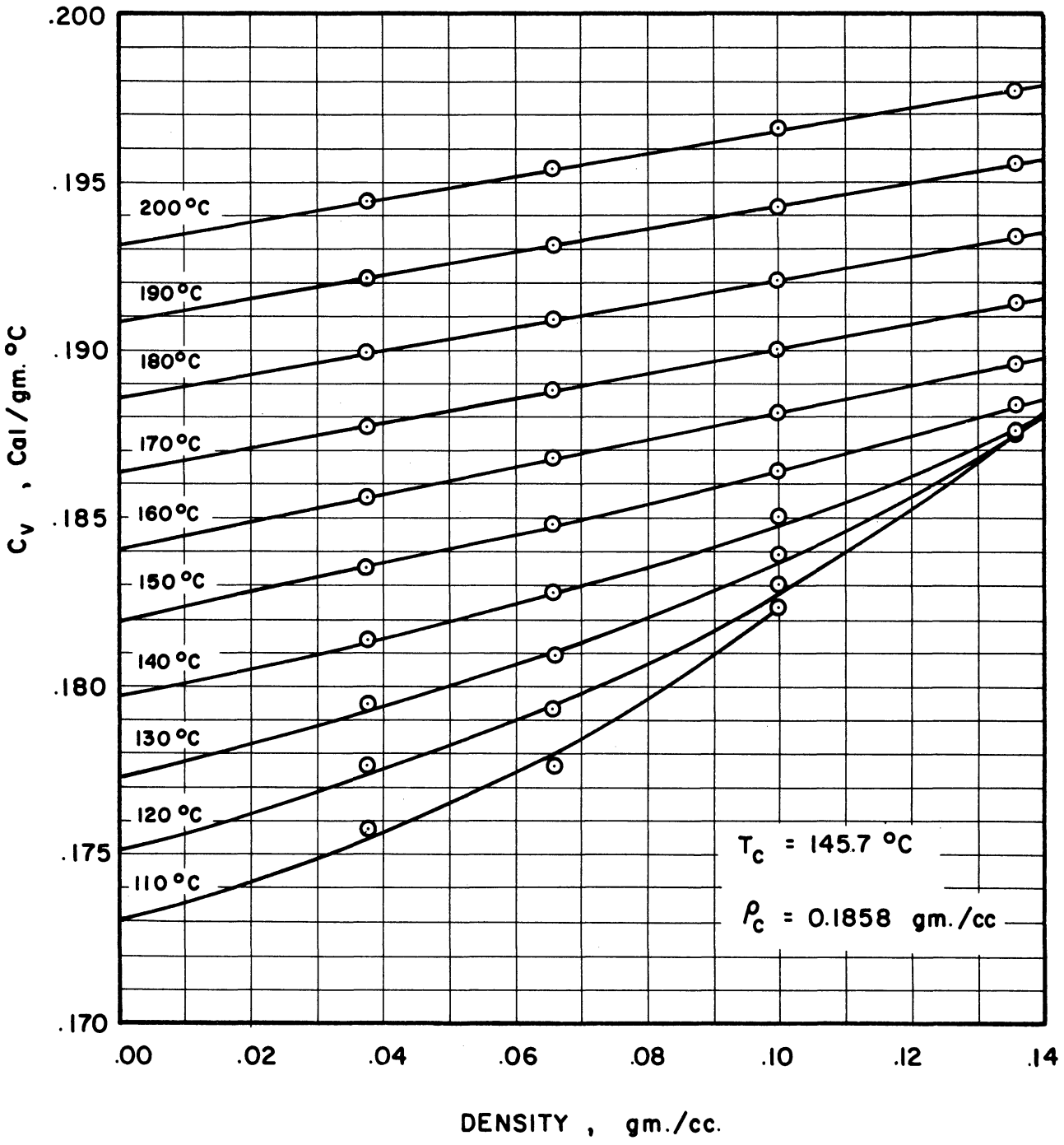

Figure 7-8. Constant-Volume Heat Capacity of Dichlorotetrafluoroethane ($CClF_2CClF_2$)
(This is a cross plot of Figure 7-7.)

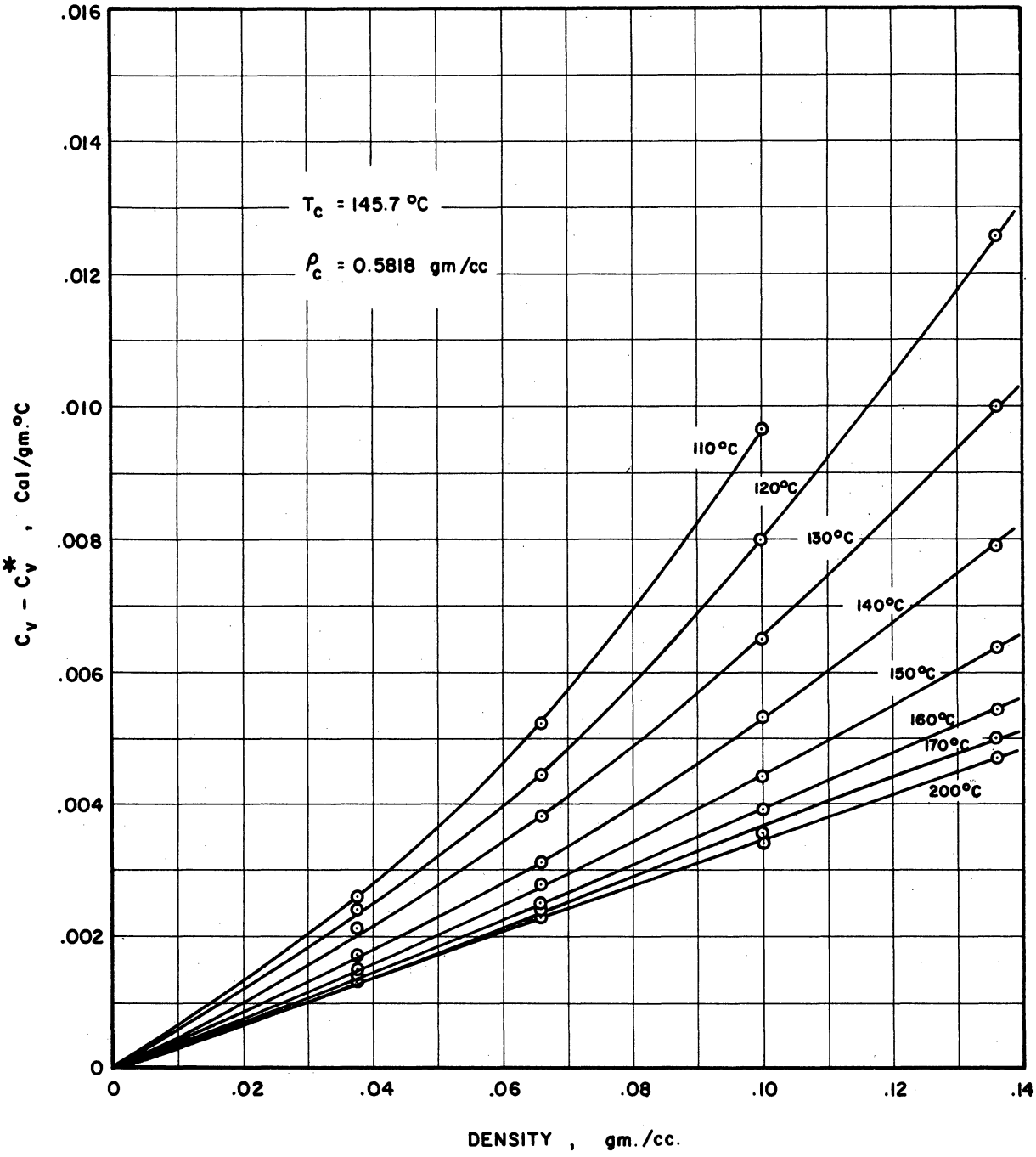

Figure 7-9. C_V-C_V* of Dichlorotetrafluoroethane ($CClF_2CClF_2$)
(This is a modified cross plot of Figure 7-7)

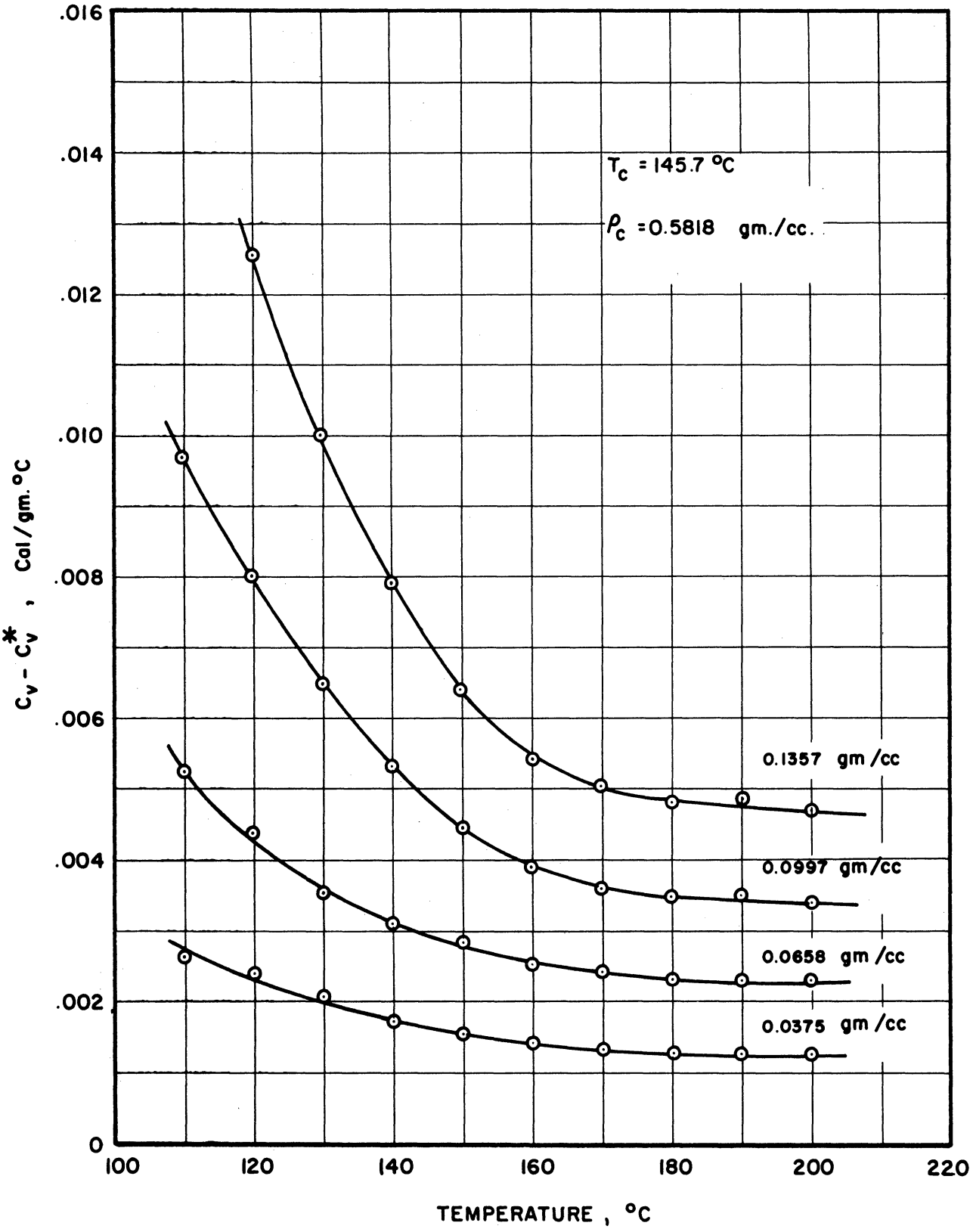

Figure 7-10. C_V-C_V* of Dichlorotetrafluoroethane. ($CClF_2CClF_2$)
(This is a modified plot of Figure 7-7)

VII-5 Constant-Volume Heat Capacity of Chloropentafluoroethane

The experimental heat-capacity results for chloropentafluoroethane are shown in Table 7-5. They are presented in the same form as the results for the other compounds studied in this research. Data were collected for five densities ranging from 0.0427 gm/cc up to 0.2219 gm/cc. These corresponded to 7.16% to 37.2% of the critical density. The temperature range for three low densities was from the saturation temperature up to 200°C, and for two high densities it was from the saturation temperature up to temperatures at which the calculated pressure of the gas was between 500 and 525 psi. For three low densities, C_v was calculated from the smoothed gross heat-capacity data (see Appendix D, Figures D-6 and D-7). For two high densities, C_v was calculated directly from the observed gross heat-capacity data.

The results are plotted in Figure 7-11 on the C_v vs. temperature plane with density as a parameter. The maximum scatter of the gross heat-capacity data is 0.3%, but most of the data deviate by less than 0.2%. If the C_v were calculated directly from the individual experimental gross heat capacity without smoothing, the maximum deviation in the final C_v would have been 1.3%. As a result of smoothing C_{gross}, the scatter of C_v in Figure 7-11 is practically negligible for three low densities. For two high densities, however, the maximum scatter of C_v is 0.19%.

Figure 7-12 is a cross plot of Figure 7-11, which is similar to Figure 7-4. The maximum scatter of the cross-plotted data is 0.2%. Each isotherm has been extrapolated to zero density to determine the ideal-gas heat capacity C_v^*. The C_v^* thus determined is then cross-plotted as C_v^* vs. temperature in Figure 7-11. The statistical C_v^* of

TABLE 7-5

CONSTANT-VOLUME HEAT CAPACITY OF CHLOROPENTAFLUOROETHANE ($CClF_3$-CF_3)

Run No.	T	C_{gross}	$C_{calr.}$	C_{net}	C_v
	°C	cal/°C	cal/°C	cal/°C	cal/gm°C
	Loading No. 1. 188.86 gm. 0.0427 gm/cc.				
	50	141.88	109.92	31.96	0.1692
	60	143.31	110.90	32.41	0.1716
	70	144.78	111.86	32.92	0.1743
	80	146.21	112.75	33.46	0.1772
	90	147.60	113.63	33.97	0.1799
	100	149.01	114.46	34.55	0.1829
	110	150.30	115.30	35.00	0.1853
	120	151.58	116.11	35.47	0.1878
	130	152.85	116.90	35.95	0.1904
	140	154.04	117.64	36.40	0.1927
	150	155.25	118.38	36.87	0.1952
	160	156.41	119.10	37.31	0.1976
	170	157.58	119.80	37.78	0.2000
	180	158.70	120.47	38.23	0.2024
	190	159.80	121.13	38.67	0.2048
	200	160.88	121.78	39.10	0.2070
	Loading No. 2. 393.11 gm. 0.0889 gm/cc.				
	50	177.55	109.92	67.63	0.1720
	60	179.42	110.90	68.52	0.1743
	70	181.25	111.86	69.39	0.1765
	80	183.15	112.75	70.40	0.1791
	90	185.00	113.63	71.37	0.1816
	100	186.81	114.46	72.35	0.1840
	110	188.60	115.30	73.30	0.1865
	120	190.37	116.11	74.26	0.1889
	130	192.04	116.90	75.14	0.1911
	140	193.70	117.64	76.06	0.1935
	150	195.45	118.38	77.07	0.1961
	160	197.10	119.10	78.00	0.1984
	170	198.71	119.80	78.91	0.2007
	180	200.32	120.47	79.85	0.2031
	190	202.00	121.13	80.87	0.2057

TABLE 7-5 (Cont'd)

CONSTANT-VOLUME HEAT CAPACITY OF CHLOROPENTAFLUOROETHANE ($CClF_3$-CF_3)

Run No.	T	C_{gross}	$C_{calr.}$	C_{net}	C_v
	°C	cal/°C	cal/°C	cal/°C	cal/gm°C
	Loading No. 3. 592.52 gm. 0.1340 gm/cc.				
	60	217.89	110.90	106.90	0.1804
	70	219.50	111.86	107.64	0.1817
	80	221.25	112.75	108.50	0.1831
	90	223.05	113.63	109.42	0.1847
	100	224.85	114.46	110.39	0.1863
	110	226.82	115.30	111.52	0.1882
	120	228.80	116.11	112.69	0.1902
	130	230.80	116.90	113.90	0.1922
	140	232.85	117.64	115.21	0.1944
	150	235.00	118.38	116.62	0.1968
	160	237.12	119.10	118.02	0.1992
	170	239.30	119.80	119.50	0.2017
	180	241.52	120.47	121.05	0.2043
	190	243.55	121.13	122.42	0.2066
	Loading No. 4. 791.79 gm. 0.1791 gm/cc.				
C14	65.26	259.10	111.40	147.70	0.1865
C15	75.65	260.00	112.36	147.64	0.1865
C16	86.30	261.59	113.31	148.28	0.1873
C17	96.91	263.26	114.21	149.05	0.1883
C18	108.01	266.11	115.12	150.99	0.1907
C19	117.46	267.90	115.89	152.01	0.1920
C20	129.01	270.04	116.83	153.21	0.1935
C21	136.90	271.67	117.42	154.25	0.1948
C22	145.33	274.24	118.06	156.18	0.1973
C23	154.27	276.56	118.69	157.87	0.1994
	Loading No. 5. 981.10 gm. 0.2219 gm/cc.				
C24	71.72	300.93	112.00	188.93	0.1926
C25	82.27	300.25	112.96	187.29	0.1909
C26	91.31	301.24	113.73	187.51	0.1911
C27	100.28	302.66	114.48	188.18	0.1918
C28	109.23	303.90	115.22	188.68	0.1923
C29	121.50	307.41	115.97	191.44	0.1951

chloropentafluoroethane was calculated by Martin, Long, and Service,[31] who correlated their results in the following equation.

$$C_v^* = 0.034157 + 3.17723 \times 10^{-4}T - 1.37593 \times 10^{-7}T^2 \qquad (7\text{-}3)$$

where T is in °R and C_v^* is in Btu/lb-°F. This equation is plotted in Figure 7-11 for comparison. The statistical C_v^* agrees reasonably well at high temperatures but predict high by as much as 3.2% at 70°C. The statistical C_v^* calculated by Smith et al.,[42] is also shown in Figure 7-11 for comparison. Their values are lower than the experimental values by 1.8% at 400°K and by 2.4% at 473°K, Martin et al.[30] also calculated the C_v^* from the measured value of the velocity of sound, which gave 24.40 Btu/lb mole-°F at 79.8°F. This compares with the observed values of 24.62 Btu/lb mole-°F at 79.8°F. However, the velocity of sound measurement was not considered very precise by Martin et al., and error in the calculated heat capacity could be as great as 6%.

Based on the experimental C_v^*, Figure 7-13 is constructed analogously to Figure 7-12, but showing $C_v - C_v^*$ as a function of density with temperature as a parameter. On Figures 7-12 and 7-13, isotherms are drawn at 10°C intervals from 60 up to 200°C. Figure 7-14 is a modified plot of Figure 7-11 and also a cross plot of Figure 7-13, showing $C_v - C_v^*$ as a function of temperature with density as a parameter.

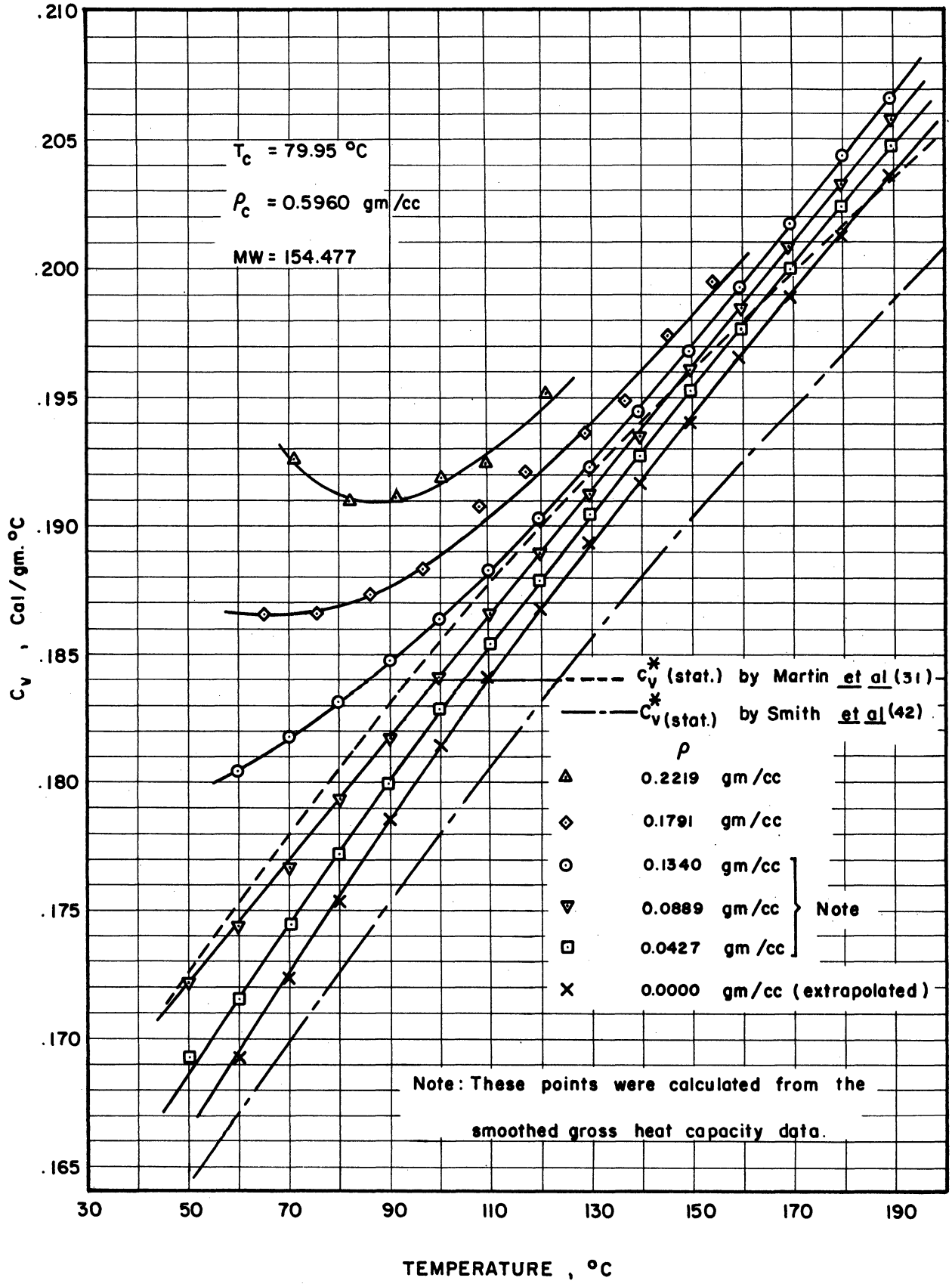

Figure 7-11. Constant-Volume Heat Capacity of Chloropentrafluoroethane ($CClF_2CF_3$)

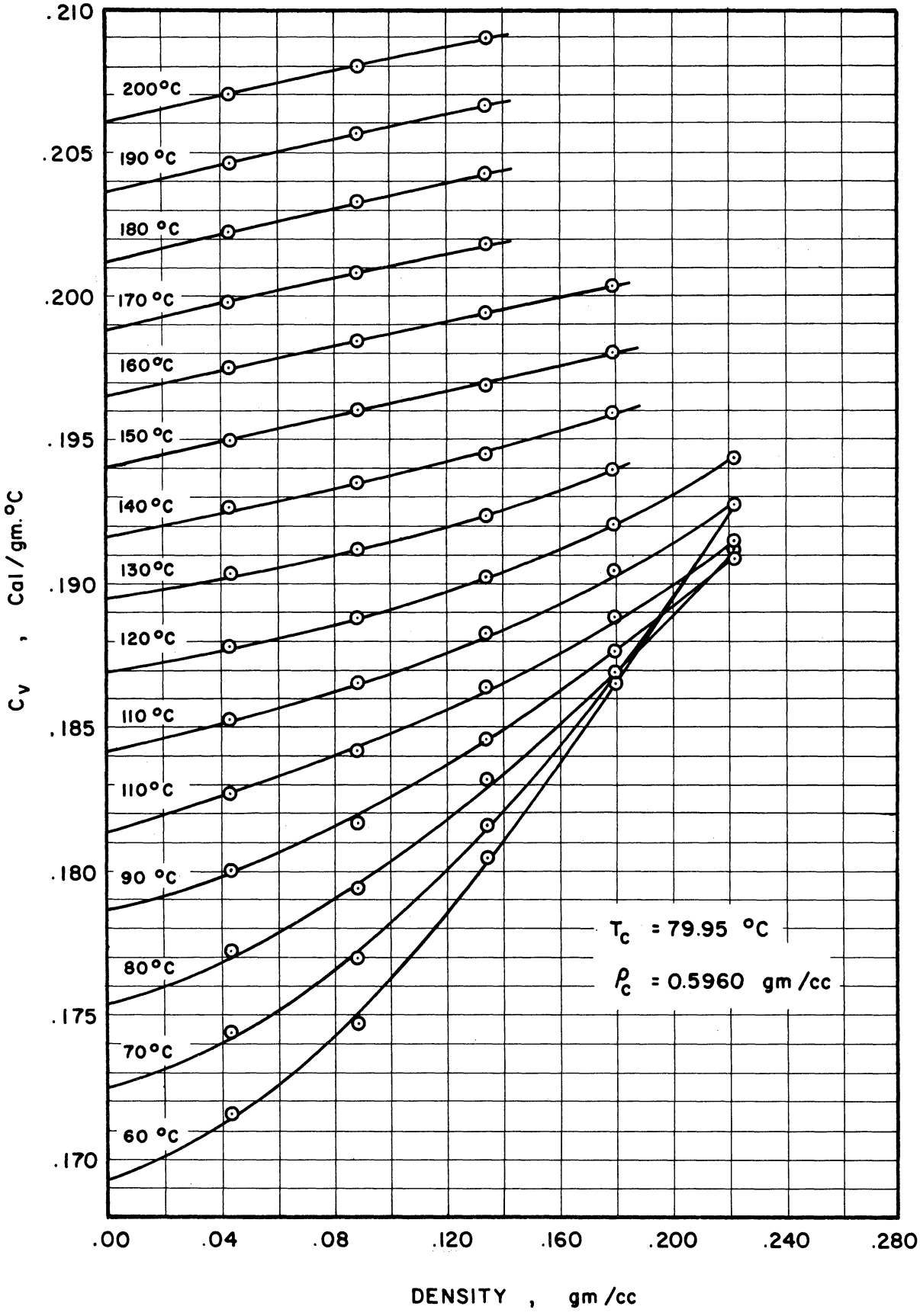

Figure 7-12. Constant-Volume Heat Capacity of Chloropentafluoroethane ($CClF_2CF_3$)
(This is a cross plot of Figure 7-11.)

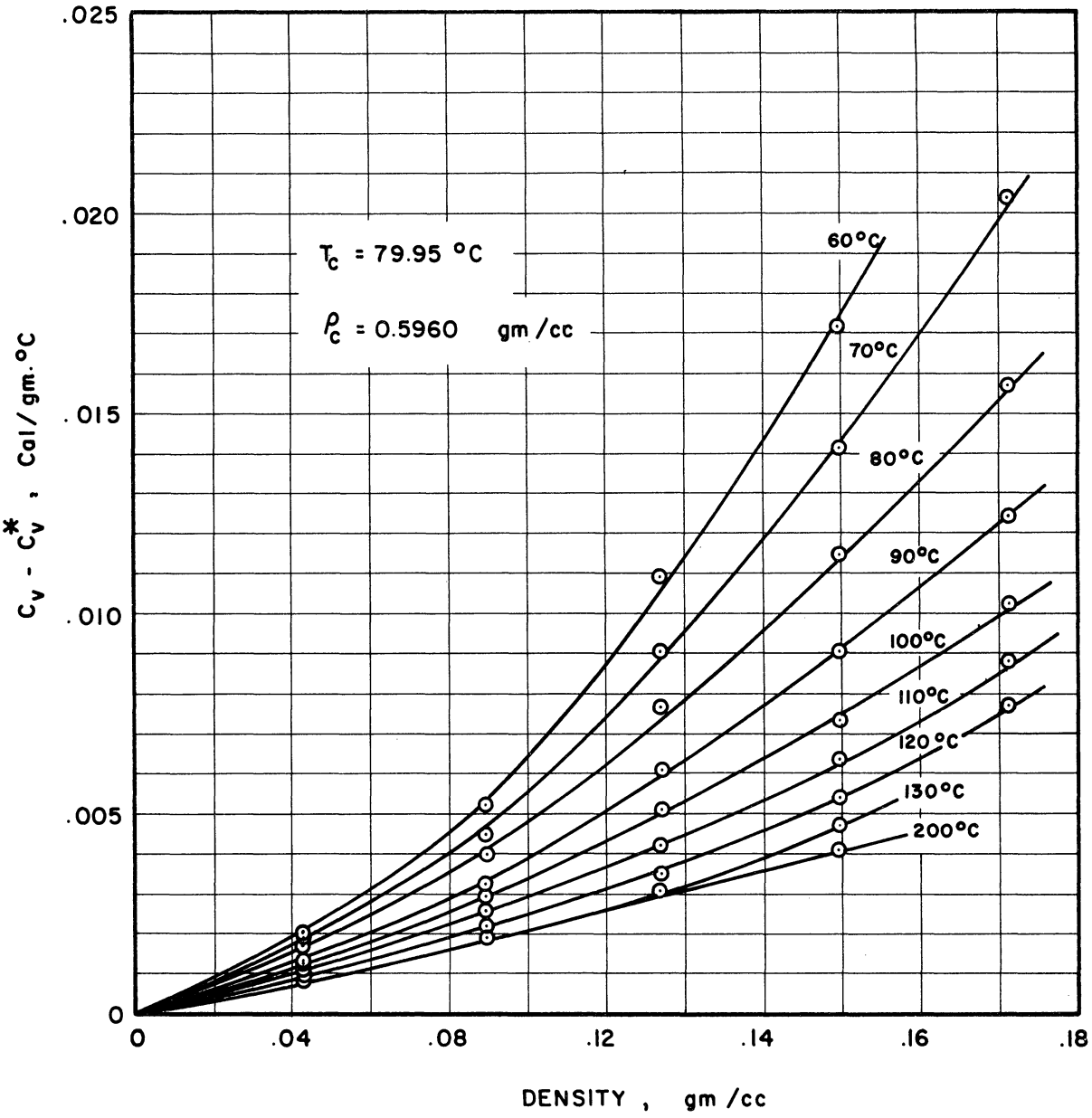

Figure 7-13. C_V-C_V* of Chloropentafluoroethane ($CClF_2CF_3$)
(This is a modified cross plot of Figure 7-11)

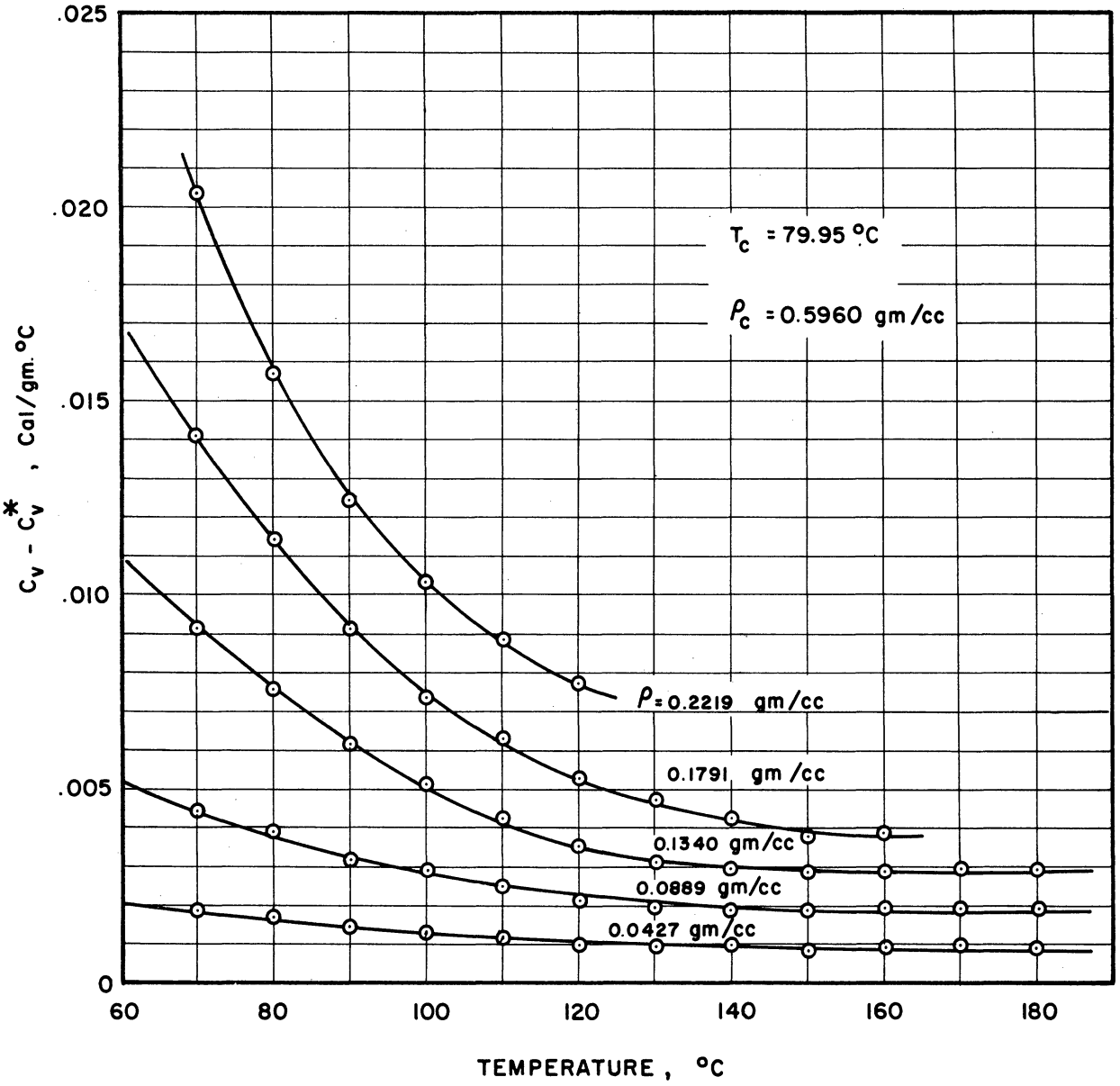

Figure 7-14. C_v-C_v* of Chloropentafluoroethane ($CClF_2CF_3$)
(This is a modified plot of Figure 7-11.)

VIII. DISCUSSIONS OF EXPERIMENTAL RESULTS

VIII-1 Characteristics of C_V as a Function of Temperature and Density

In general, C_V increases with increasing density and also increases with increasing temperature at high temperatures. In the vicinity of or below the critical temperature, however, C_V may increase with decreasing temperature if the density is considerably high. Figures 7-3, 7-7, and 7-11 all indicate this tendency. On the other hand, the values of $C_V - C_V^*$ for any isometric always decrease with increasing temperature and approach zero as the temperature increases. Judging from the case of tetrafluoromethane, it seems reasonable to assume that $C_V - C_V^*$ is practically negligible at the reduced temperatures $T/T_c = 1.3$ or higher. This fact has been utilized in the calibration of heat capacity of the calorimeter (see Section VI-2). Mathematically, it means

$$C_V - C_V^* = -\int_V^\infty T\left(\frac{d^2P}{dT^2}\right)_V dV \cong 0 \quad \text{or} \quad \left(\frac{d^2P}{dT^2}\right)_V \cong 0 \qquad (8\text{-}1)$$

Martin and Hou[27] also pointed out (based on the state data)

$$\left(\frac{d^2P}{dT^2}\right)_V = 0 \qquad \text{for high temperatures.} \qquad (1\text{-}8)$$

In other words, the isometrics on the P vs. T plot are practically straight at those temperatures where T/T_c is 1.3 or higher.

On the C_V vs. density plots, the experimental C_V data show that, within the density range studied (less than 37% of the critical density), all low-temperature isotherms curve upward slightly but increase so rapidly that they intersect with the high-temperature isotherms at considerably low density. de Nevers[12] has advanced a tentative conclusion

on the tendency of this upward curvature of the isotherms at a low-density range. The present research has fully confirmed his conclusion. The upward curvature reduces its intensity gradually with increasing temperature and becomes practically zero at the low density range for isotherms more than 50°C removed from the critical temperature. In the case of dichlorotetrafluoroethane, the isotherm is practically straight only 10°C removed from the critical temperature. Thus it is apparent that temperature not only influences the relative position of isotherms but also affects their characteristics.

In the C_v-C_v^* vs. temperature plots, all isometrics are monotonically decreasing functions of temperature with different upward curvatures. The maximum curvature does not occur at the same temperature for different densities.

From the above discussion, it is not difficult to see that, in a pure mathematical sense, C_v-C_v^* cannot be correlated in the following form:

$$C_v - C_v^* = f(T)g(\rho) \qquad (8\text{-}2)$$

since Equation (8-2) indicates that the general shape of isotherms is solely determined by density alone, while that of the isometrics is determined by temperature alone. The more complicated form is probably required to express the experimental data correctly. Nevertheless, a form as represented by Equation (8-2) is usually preferred for its simplicity. While the empirical correlation of the experimental C_v data may be used in the calculation of thermodynamic properties, there is another interesting application in connection with the development of an equation of state, based on the exact thermodynamic relation:

$$\left(\frac{dC_v}{dV}\right)_T = -\rho^2\left(\frac{dC_v}{d\rho}\right)_T = T\left(\frac{d^2P}{dT^2}\right)_V \qquad (8\text{-}3)$$

Supposing $C_v - C_v^*$ is correlated in the certain form with 1 or 2% maximum error, the differentiation once with respect to density (or volume) and subsequent integration twice with respect to temperature would probably shed light on a better form of an equation of state. Although the development of the PVT equation is beyond the scope of the present project, the mathematical procedures are illustrated using a simple example as follows.

Supposing $C_v - C_v^*$ is correlated as follows:

$$C_v - C_v^* = -\frac{1}{T^n}\left\{\frac{C_2}{(V-b)} + \frac{C_3}{2(V-b)^2} + \frac{C_4}{3(V-b)^3} + \frac{C_5}{4(V-b)^4}\right\} \qquad (8\text{-}4)$$

where C_1, C_2 ----, b, and n are all arbitrary constants, we have

$$\left(\frac{dC_v}{dV}\right)_T = \frac{1}{T^n}\left\{\frac{C_2}{(V-b)^2} + \frac{C_3}{(V-b)^3} + \frac{C_4}{(V-b)^4} + \frac{C_5}{(V-b)^5}\right\} \qquad (8\text{-}5)$$

Using Equation (8-3), we obtain

$$\left(\frac{d^2P}{dT^2}\right)_V = \frac{1}{T^{n+1}}\left\{\frac{C_2}{(V-b)^2} + \frac{C_3}{(V-b)^3} + \frac{C_4}{(V-b)^4} + \frac{C_5}{(V-b)^5}\right\} = \frac{Y(V)}{T^{n+1}} \qquad (8\text{-}6)$$

where

$$Y(V) = \frac{C_2}{(V-b)^2} + \frac{C_3}{(V-b)^3} + \frac{C_4}{(V-b)^4} + \frac{C_5}{(V-b)^5} \qquad (8\text{-}7)$$

Integrating once with respect to T, we have

$$\left(\frac{dP}{dT}\right)_V = -\frac{Y(V)}{nT^n} + B_{(V)} \qquad (8\text{-}8)$$

where $B_{(V)}$ is a function of V or ρ alone. The second integration with respect to T yields:

$$P = \frac{Y_{(V)}}{n(n-1)T^{n-1}} + B_{(V)}T + A_{(V)} \qquad (8\text{-}9)$$

where $A_{(V)}$ is an integration constant. It is obvious that the forms of $B_{(V)}$ and $A_{(V)}$ cannot be determined simply by correlating C_v data, but the so-called curvature term can be determined.

VIII-2 Statistical and Experimental C_v^*

For tetrafluoromethane, the agreement between the experimental and statistical C_v^* is very good on the basis of probable experimental error. This should not be interpreted, however, as a casual coincidence since the independent facts are available to support the results. First, the C_v of dichlorodifluoromethane measured in the same calorimeter agrees well with Masi's[32] C_v^* corrected by the Martin-Hou equation to the same density. Secondly, the tetrafluoromethane molecule is simple and symmetrical, and the set of fundamental frequencies is well established with only a slight differences existing among various authors. These small differences in frequencies do not make appreciable differences in heat capacity. Chari's calculation was based on a set of fundamental frequencies determined by Goubeau *et al.*,[19] plus an anharmonic contribution based on the semi-empirical method presented by McCullough *et al.*,[33] using assumptions employed by Albright *et al.*,[1]. In Gelles and Pitzer's[17] calculation, no anharmonic contribution was added. This is why their C_v^* is about 0.5 to 0.8% less than that obtained by Chari. The observed C_v^* lies between Chari's and Gelles and Pitzer's values, but is closer to Chari's values. The difference between the observed values and those given by Chari is actually within the experimental precision of this work.

For chlorodifluoromethane, a set of fundamental frequencies is not definitely established. The most questionable point is the selection of one of the fundamental frequencies. Martin et al.[26] selected 831 cm^{-1} as a fundamental, while Weissman, Meister, and Cleveland[45] chose 1178 cm^{-1} for this same fundamental. Weissman et al. maintained that 831 cm^{-1} is due to the presence of dichlorofluoromethane ($CHCl_2F$). It is interesting that, according to Smith et al.,[43] the Raman spectra of dichlorofluoromethane indicates no absorption band at 831 while chlorodifluoromethane has a fairly strong band at 831. The same authors also indicated that Raman spectra of both compounds showed no marked band at 1178. In fact, even in the infrared spectrum a band at 1178 is merely a medium absorption band comparable to many such bands which are not selected as fundamentals. Besides this, the infrared spectra of $CHCl_2F$ given by Weissman et al. indicates a band at 831 only as a shoulder of a strong band at 804. The $CHClF_2$ sample used by the present author has a purity of 99.9+% by gas chromatography according to the specification of the supplier, the "Freon" Products Laboratory of E. I. du Pont de Nemours and Company. The infrared spectra of the sample shows a band at 830 cm^{-1}, but the mass spectrograph indicates only a negligible amount of $CHCl_2F$ if any. Whether 831 is a fundamental is a controversial point, but in the light of the experimental C_v^* obtained in this study, it seems reasonable to conclude that the selection of 831 is more reasonable than the selection of 1178 as given by Weissman et al. Table 8-1 shows the list of fundamental frequencies selected by those authors.

For dichlorotetrafluoroethane, the statistical C_v^* calculated by Martin[25] was based on the spectroscopic data of Glockler and Sage[18]

and of Smith, Nielsen, Berryman, Claasen, and Hudson.[43] The choice of fundamental frequencies was rather arbitrary and the existence of free internal rotation was assumed. The calculated values are generally higher than the experimental C_v^* and the slope of the calculated C_v^* curve is not as steep as the experimental one. This clearly indicates that too many low frequencies have been selected as fundamentals. Also, the assumption of free internal rotation may be in error.

For chloropentafluoroethane, the statistical C_v^* calculated by Martin, Long, and Service[30] was based on the infrared spectral data of Barcelo[4] and the Raman spectral data. A potential barrier of 1750 cal/gm mole was also used by them to calculate the contribution by the hindered internal rotation. The values of their calculation are generally higher than the experimental C_v^* of this work and the slope of the C_v^* curve is less than the observed one. This indicates that one or two low wave-number fundamentals should be replaced by the higher frequency fundamentals. On the other hand, C_v^* calculated by Smith et al.[42] are generally lower than the experimental data. This indicates that their selection of fundamental frequencies cover too many high frequencies. The fundamental frequencies selected by both Martin et al. and Smith et al. are listed in Table 8-2 for comparison.

VIII-3 Comparison of the Experimental Data with the Equation of State

As mentioned in Section I-4, the experimental C_v data may be employed to check the equation of state. Most of the modern equations of state represent the C_v-C_v^* as a function of temperature and density which are separable mathematically, i.e.,

$$C_v - C_v^* = f(T)g(\rho) \qquad (8\text{-}10)$$

Table 8-1. Fundamental Frequencies of Chlorodifluoromethane (cm^{-1})

Pitzer and Gelles[38]	Cleveland, Weissman, Meister[45]	Martin et al.[26]
365	369	369
422	421	415
595	596	596
809	808	799
--	--	831
1116	1116	1099
1178	1178	--
1131	1312	1310
1347	1345	1350
3023	3025	3035

Table 8-2. Fundamental Frequencies of Chloropentafluoroethane (Wave number, cm^{-1})

Values Used by Martin et al.[30]	Values used by Smith et al.[42]
75	171? (tortion)
189	186
264	218
316	315
333	331
367	366
448	442
560	454
596	560
648	596
704	648
762	762
984	982
1128	1133
1180	1185
1230	1241 (2)*
1348	1350

* statistical weight

It is obvious that on the C_V-C_V* vs. density plane we get a family of similar isotherms, any one of which may be constructed by simply multiplying the ordinates of any other isotherms with a certain factor which is solely determined by the temperature function f(T). Therefore, the comparison of the experimental data with those predicted by the equation of state must be somehow concentrated on the characteristics rather than on their absolute values. Similarly, on the C_V-C_V* vs. temperature plane, we have a family of isometrics, any one of which can be constructed simply by multiplying the ordinates of any other isometrics by a factor, which in turn is determined solely by the density function g (ρ). So, in the course of comparison, the absolute values of C_V-C_V* are not of much interest but the characteristics of these isometrics must be carefully examined.

The Martin-Hou equation has been developed for all compounds studied except chloropentafluoroethane.[8, 25, 26, 34] Comparisons of experimental data with those predicted by the Martin-Hou equation in the C_V-C_V* vs. density plane are presented in Figure 8-1 for chlorodifluoromethane, and in Figure 8-2 for dichlorotetrafluoroethane. In both Figure 8-1 and Figure 8-2, the isotherms predicted by the Martin-Hou equation show a slightly downward curvature while the experimental isotherms indicate a slightly upward curvature. de Nevers and Martin[13] also drew a similar conclusion for perfluorocyclobutane and propylene in the low-density range. Predicted C_V-C_V* values are greater than experimental values in the case of chlorodifluoromethane, but are much less in the case of dichlorotetrafluoroethane. In the case of chlorodifluoromethane, the difference between the experimental and predicted values of C_V-C_V*

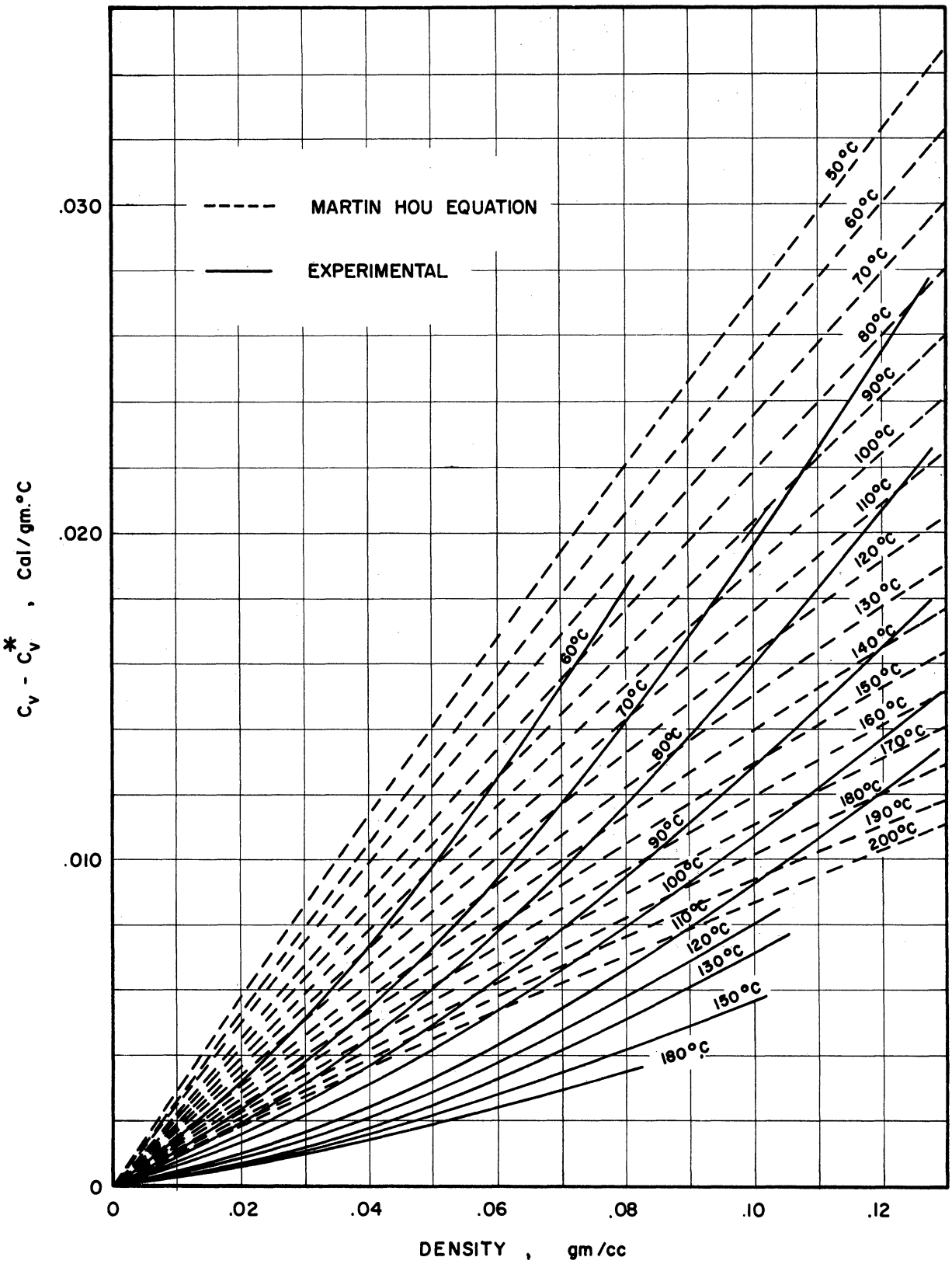

Figure 8-1. Comparison of Experimental C_v-C_v* of Chlorodifluoromethane with Those Predicted by the Martin-Hou Equation.

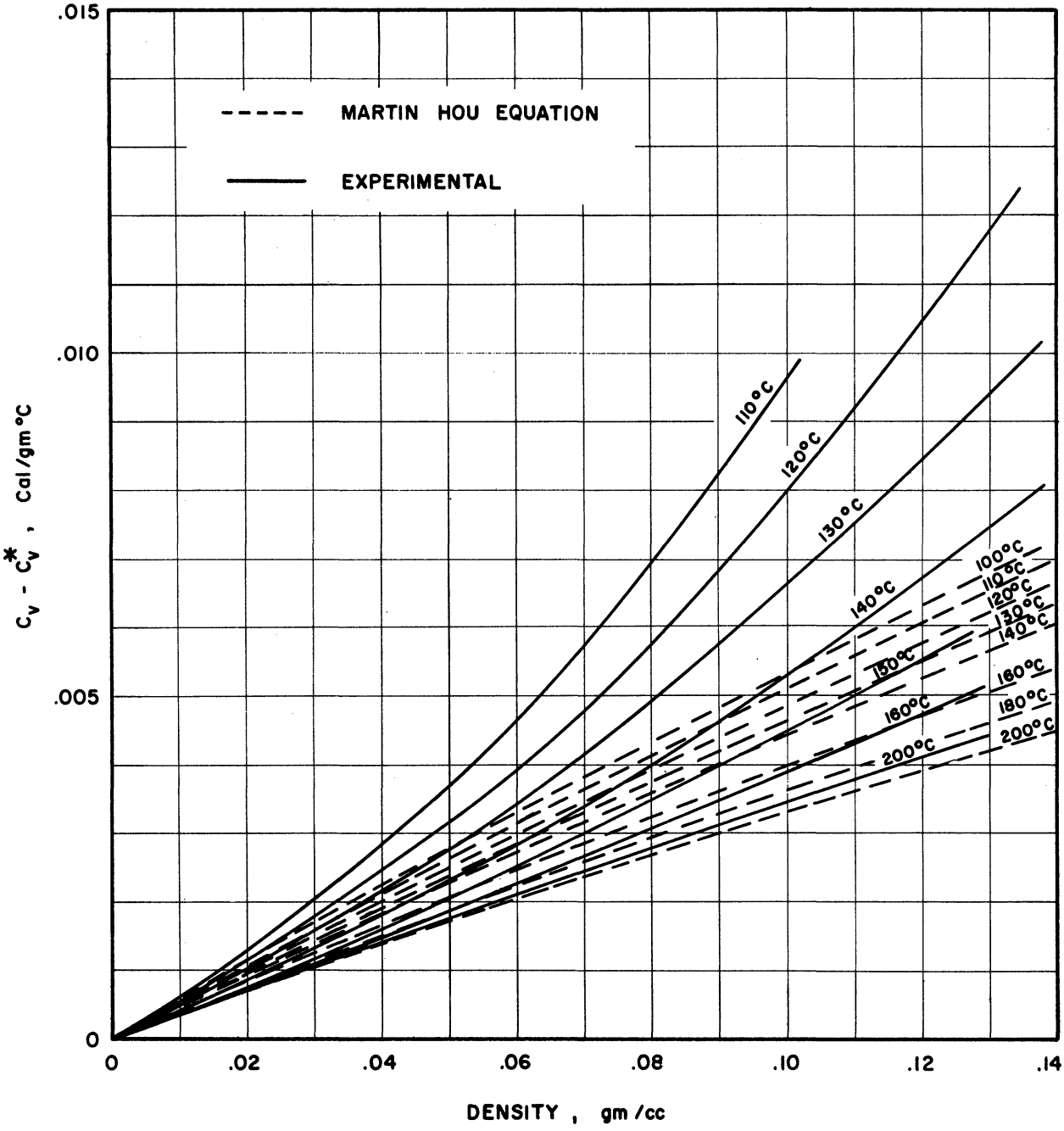

Figure 8-2. Comparison of Experimental C_v-C_v^* of Dichlorotetrafluoroethane with that Predicted by Martin-Hou Equation. (Comparison of Density Function)

reaches 0.0070 cal/gm°C, which corresponds to about 5% in experimental C_v. We can see, however, a tendency for both experimental and predicted values to get close at some higher density. In the case of dichlorotetrafluoroethane, the discrepancy between experimental and predicted values reaches as much as 0.0060 cal/gm°C, which corresponds to about 3.5% of the experimental C_v within the experimental range. There is no tendency, however, for both the experimental and predicted values to get closer at any higher density. In view of the fairly good agreement at high temperatures (above 160°C), but poor agreement at temperatures below the critical temperature, it is reasonable to suspect that the temperature function predicts too low for the low temperatures.

The adequacy of the temperature function is best examined on the C_v-C_v^* vs. temperature plot. Comparisons of the experimental C_v-C_v^* with those predicted by the Martin-Hou equation on the C_v-C_v^* vs. temperature plane are presented in Figure 8-3 for chlorodifluoromethane, and in Figure 8-4 for dichlorotetrafluoroethane. In these figures, both experimental and predicted values of C_v-C_v^* are monotonically decreasing functions of temperature. But the rates of decrease are quite different; the experimental data decrease rapidly at the range below the critical temperature and quickly approach the asymptotical values at 160°C for chlorodifluoromethane and at 190°C for dichlorotetrafluoroethane, while predicted values decrease rather slowly and do not approach the asymptotical values within the experimental range. In general, the experimental temperature functions have a greater curvature than what can be predicted by the Martin-Hou equation, i.e.,

$$f(T) = Te^{-k\frac{T}{T_c}} \qquad (8\text{-}11)$$

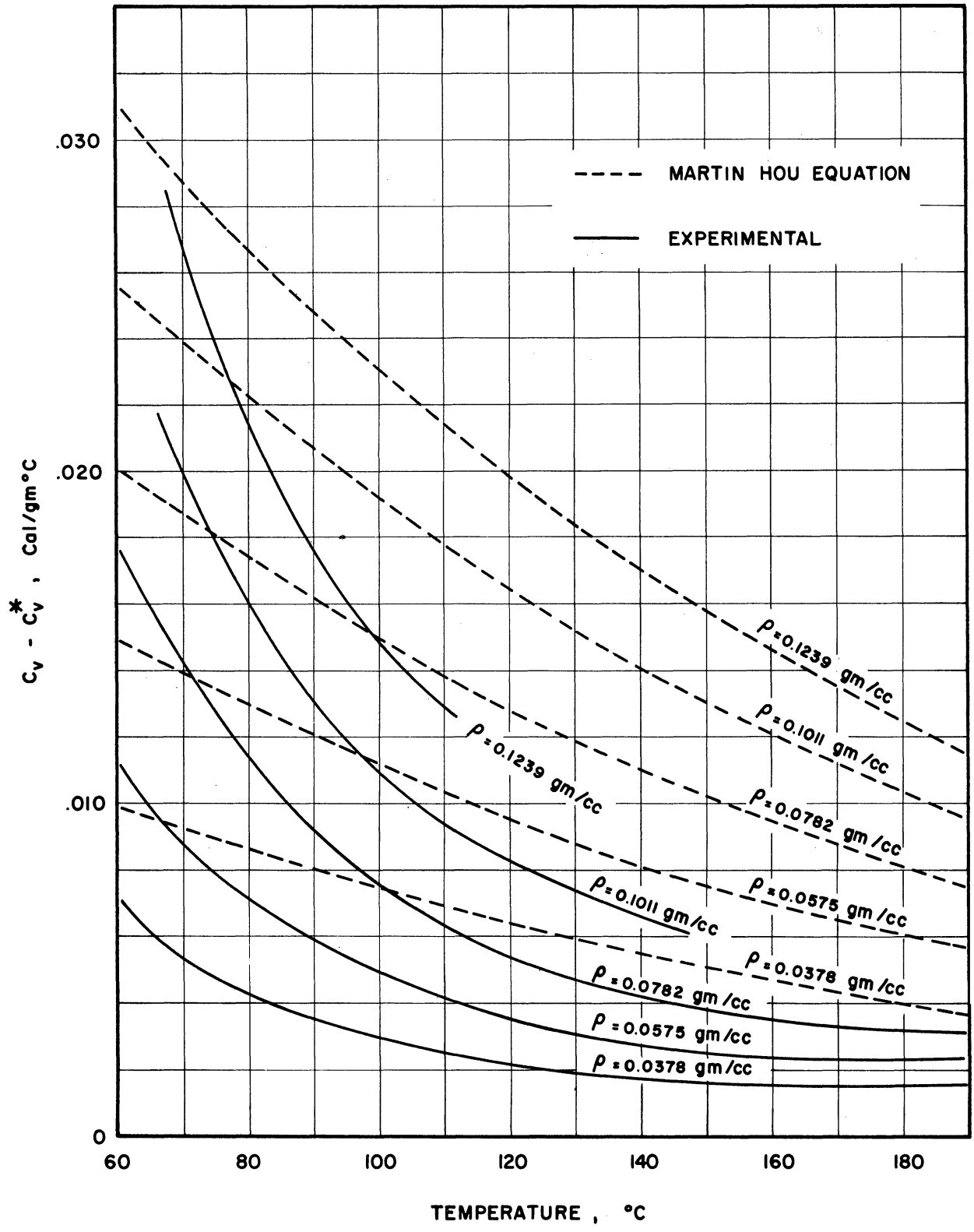

Figure 8-3. Comparison of Experimental C_V-C_V* of Chlorodifluoromethane with Those Predicted by Martin-Hou Equation (Comparison of a Temperature Function).

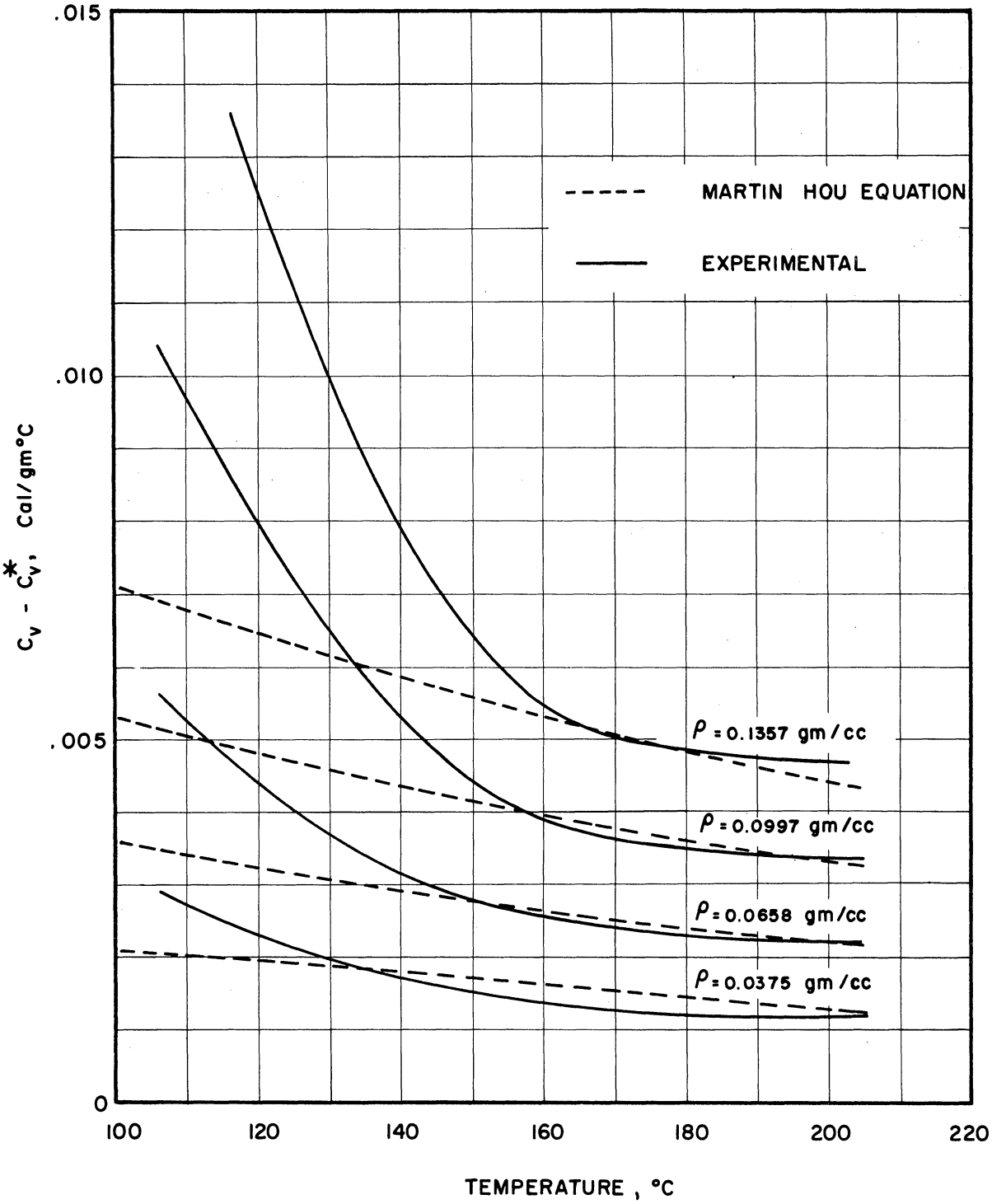

Figure 8-4. Comparison of Experimental C_v-C_v^* of Dichlorotetrafluoroethane with Those Predicted by the Martin-Hou Equation. (Comparison of a Temperature Function.)

The maximum curvature of the experimental isometrics occurs at temperatures around the critical temperature depending on the density. This fact would suggest that the temperature function, independent of density, is not capable of representing the data in the strict sense. And parallel to the argument presented in Section VIII-1, the experimental data would probably require a somewhat complicated functional relation, such as

$$C_V - C_V^* = f(T)\, g(\rho)\, h(T, \rho) \qquad (8\text{-}12)$$

In the case of dichlorotetrafluoroethane, the experimental data agree with the predicted values quite well above the critical temperature for all densities. Thus it is reasonable to say that the temperature function causes the main discrepancy at the lower temperatures.

No Martin-Hou equation has been developed for chloropentafluoroethane, but Martin *et al.*[30] have correlated the data in the following form.

$$P = A + BT - C/T^3 \qquad (8\text{-}13)$$

The complete equation with its constants is included in Appendix F. The heat capacity predicted by Equation (8-13) has the following form.

$$C_V - C_V^* = \frac{g(\rho)}{T^4} \qquad (8\text{-}14)$$

The density function in Equation (8-14) is quite similar to that predicted by the Martin-Hou equation but is in much simpler form. There is not much to expect from this simple density function but the temperature function is different from that derived from the Martin-Hou equation. For this reason, the experimental data are compared with those predicted by Equation (8-13) on the $C_V - C_V^*$ vs. temperature plane. The actual values of $C_V - C_V^*$ predicted by Equation (8-13) are all less than

any experimental isometrics due to the excessively low values of the density function. Two of these predicted isometrics are shown in Figure 8-5 by dotted lines. For the convenience of comparison (with emphasis on the curvature of the isometrics), arbitrary values are assigned to the density function so as to make the predicted C_v-C_v* coincide with the experimental values at 100°C. Figure 8-5 shows that the curvature of a temperature function is still not enough to represent the experimental data but seems a little better than those derived from the Martin-Hou equation for chlorodifluoromethane and dichlorotetrafluoroethane. Of course, it should be noted that a curvature predicted by the Martin-Hou equation is very much dependent on the value of k. The value of k is 3.75 for chlorodifluoromethane and 3.00 for dichlorotetrafluoroethane. Figure 8-6 shows the effects of values of k on a curvature of isometrics, in which C_v-C_v* is plotted vs. reduced temperature. An arbitrary value is assigned to a density function to raise the curves to a level which is convenient to compare one another. In general, the curvature of isometrics increases with increasing value of k, and it would probably require k = 7.0 or more for the satisfactory representation of the experimental data.

Tetrafluoromethane presents another interesting case for test of the equation of state, in which C_v-C_v* is practically zero for all temperatures and densities studied. The Martin-Hou equation which is correlated by Bhada[8] is used. The maximum value of C_v-C_v* should occur at the lowest temperature and highest density in the entire experimental range. The value of C_v-C_v* at 30°C and 0.0928 gm/cc is 0.0002 cal/gm°C, which is practically negligible. It is clear, then, that the Martin-Hou equation predicts the right curvature of isometrics in the P vs. T plot at the temperature range which is $1.3T_c$ or higher.

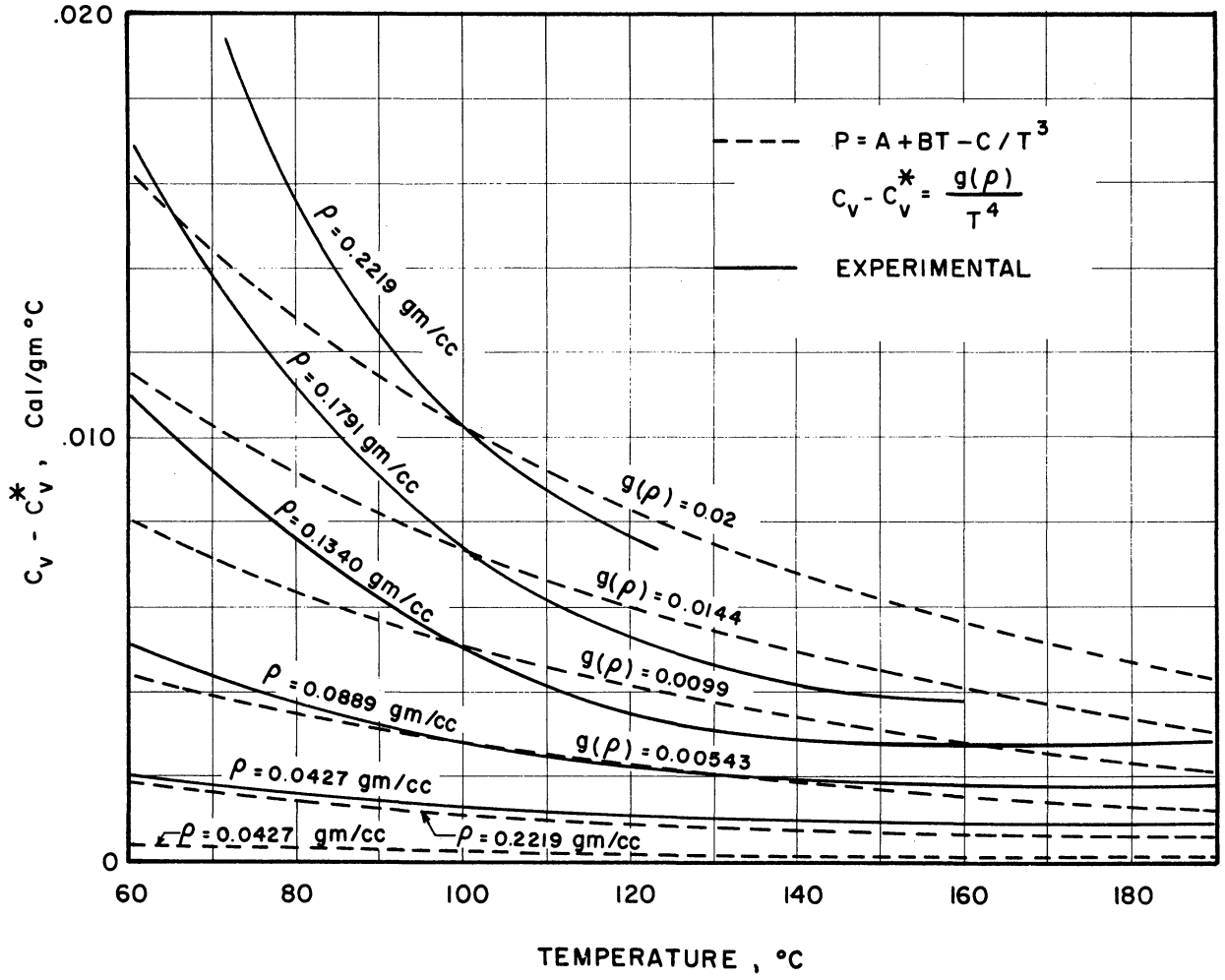

Figure 8-5. Comparison of Experimental C_V-C_V* of Chloropentafluoroethane with Those Predicted by $P = A + BT - C/T^3$ Type of Equation of State.

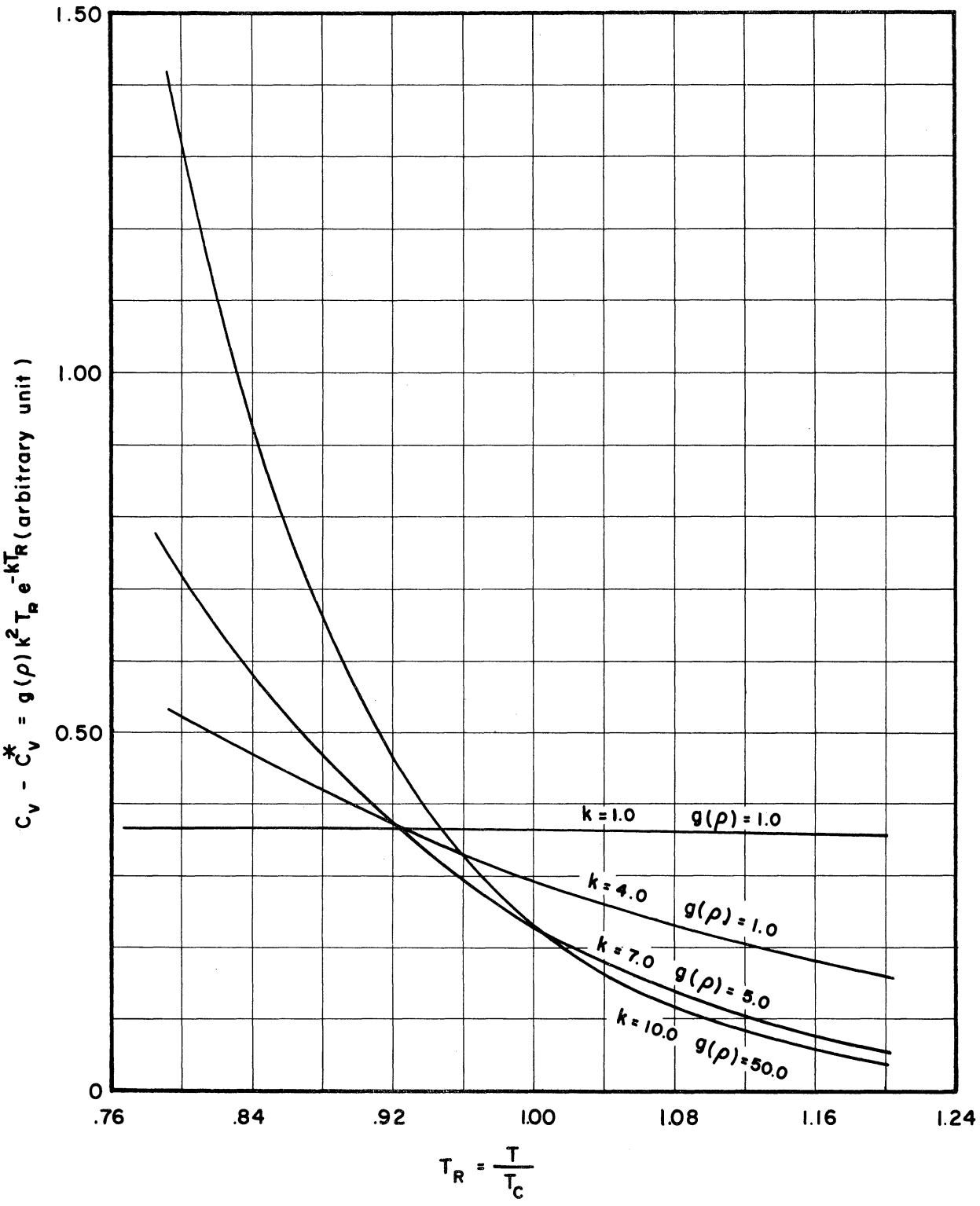

Figure 8-6. Effect of k in the Martin-Hou Equation upon the Curvature of a Temperature Function.

VIII-4 The Law of Corresponding State and C_v Data

If two gases obey the law of corresponding state, they must have the same $C_v-C_v^*$ (expressed in molar basis) at the same reduced temperature and reduced density. This may be derived as follows. The law of corresponding state maintains that the compressibility factor defined as

$$z = \frac{PV}{RT} = \frac{P}{RT\rho} \tag{8-15}$$

is a function of reduced temperature and reduced pressure (or reduced density) and independent of the kind of gases. According to Equation (8-15), we have

$$\left(\frac{dP}{dT}\right)_\rho = R\rho\left[T\frac{dz}{dT} + z\right] \tag{8-16}$$

$$\left(\frac{d^2P}{dT^2}\right)_\rho = R\rho\left[T\left(\frac{d^2z}{dT^2}\right)_\rho + \frac{2}{\rho}\left(\frac{dz}{dT}\right)_\rho\right] \tag{8-17}$$

Substituting this into Equation (1-3), we have

$$C_v-C_v^* = -RT\int_0^\rho \left[\frac{T}{\rho}\left(\frac{d^2z}{dT^2}\right)_\rho + \frac{2}{\rho}\left(\frac{dz}{dT}\right)_\rho\right]d\rho \tag{8-18}$$

Substituting $T = T_RT_c$ and $\rho = \rho_R\rho_c$, we obtain

$$C_v-C_v^* = -RT_R\int_0^{\rho_R} \left[\frac{T_R}{\rho_R}\left(\frac{d^2z}{dT_R^2}\right)_\rho + \frac{2}{\rho_R}\left(\frac{dz}{dT_R}\right)_\rho\right]d\rho_R \tag{8-19}$$

de Nevers and Martin[13] studied the experimental $C_v-C_v^*$ for propylene and perfluorocyclobutane and concluded that, although the law of corresponding state is sufficiently accurate to make approximate generalization of PVT data, it is not sufficiently accurate to generalize $C_v-C_v^*$ data. Since two compounds studied by them are quite different in their molecular structure, the present author wonders whether

the law may be applicable even for C_V-C_V* if two gases are somewhat similar in their molecular structures. In Figure 8-7, values of C_V-C_V* are compared on the reduced basis. For chlorodifluoromethane, dichlorotetrafluoroethane, chloropentafluoroethane, and propylene, the agreement is not too bad. The worst difference is about 30 percent and mostly they agree within 10 percent. Since C_V-C_V* is only about 5 percent of C_V itself, the difference of 10 to 30 percent in C_V-C_V* may be regarded as an experimental error. Obviously, perfluorocyclobutane must be excluded from this generalization for it has a cyclic structure instead of chain structure. It seems reasonable to conclude that for gases of similar molecular structure, the law of corresponding state is applicable to C_V-C_V* as well as to the PVT relations.

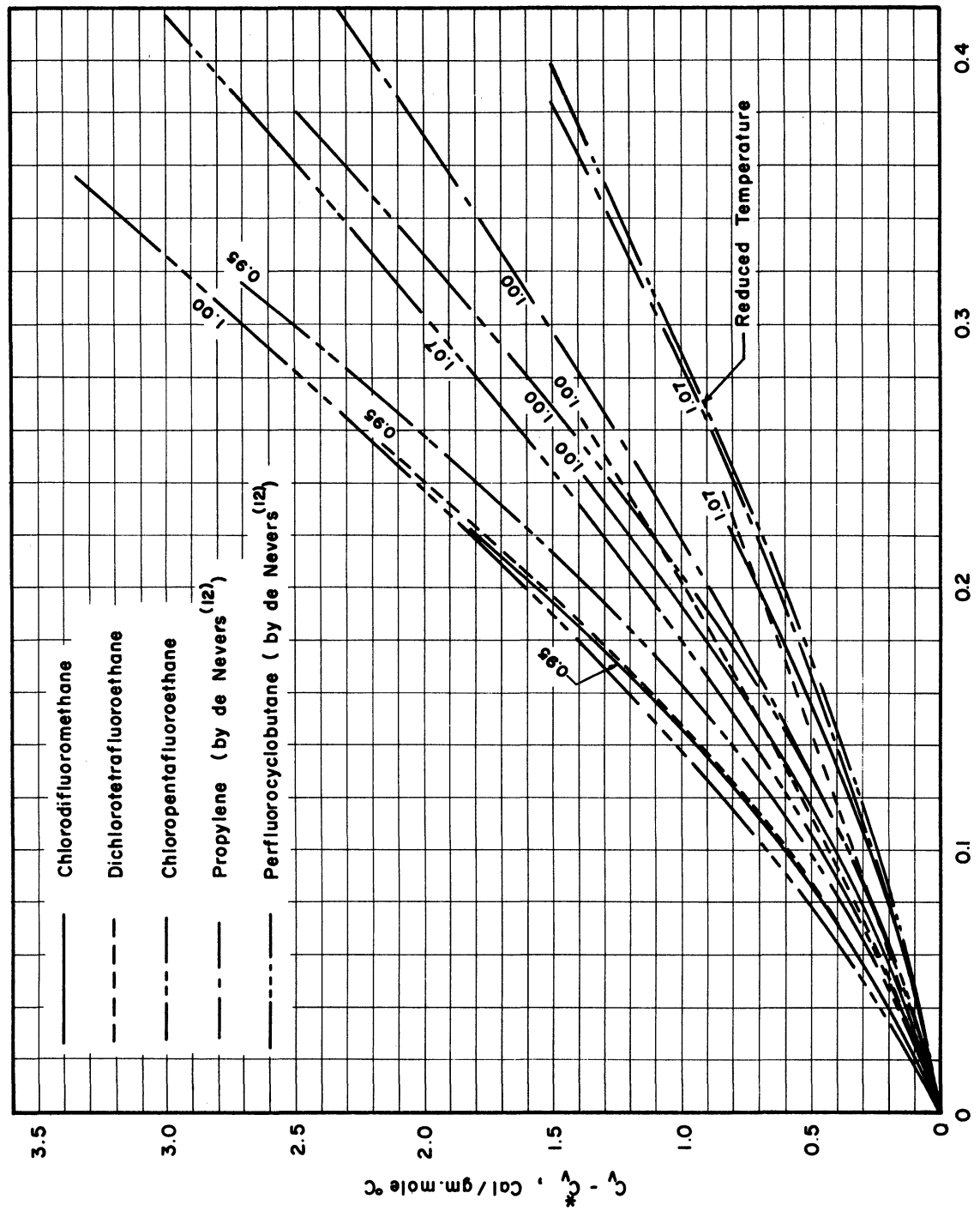

Figure 8-7. C_v-C_v^* As a Function of Reduced Temperature and Reduced Density.

IX. CONCLUSIONS

1. It has been shown that the thin-wall large-volume calorimeter originated by de Nevers[12] can be improved to produce constant-volume heat-capacity data at low densities. It is possible to determine the ideal-gas heat capacity, C_v^*, by extrapolating such data to zero density. The highest working temperature was successfully raised from 150°C to 200°C.

2. Comparison of the experimentally determined ideal-gas heat capacities, C_v^*, with those statistically calculated has revealed the following:

a. For tetrafluoromethane, the values calculated by Chari[9] and his C_v^* equation in cubic form agree with the experimental C_v^* within 0.2 percent. Those calculated by Gelles and Pitzer[17] are lower than the observed values by 0.6 percent on the average.

b. For chlorodifluoromethane, the values calculated by Martin et al.[26] are lower than the experimental data by 0.8 percent on the average. It can be expected to have better agreement if an anharmonic contribution is added to their calculations. The values calculated by Weissman et al.,[45] however, are lower than the experimental values by 4.0 percent at 400°K.

c. For dichlorotetrafluoroethane, the values calculated by Martin[25] and his C_v^* equation in quadratic form agree well with the experimental data at 200°C, but are higher than experimental values by as much as 3.4 percent at 100°C.

d. For chloropentafluoroethane, the values of C_v^* calculated by Martin et al.[31] agree with the experimental data at 190°C but are higher by as much as 3.3% at 60°C. The values calculated by Smith et al.[42] are lower than the observed values by 1.8% at 400°K and 2.4% at 473°K.

3. The experimental data show the following characteristics within the range of experiment, 30-200°C and 100-500 psi:

a. For tetrafluoromethane, $C_v - C_v^*$ is practically negligible.

b. On the $C_v - C_v^*$ vs. density plot (except CF_4), all isotherms curve upward slightly.

c. On the $C_v - C_v^*$ vs. temperature plot (except CF_4), all isometrics are monotonically decreasing functions with an upward curvature and approach the asymptotical values at temperatures about 50°C higher than the critical temperature. The maximum curvature occurs at the temperatures around the critical temperature depending on the density.

4. The Martin-Hou equation predicts the downward curvature of the isotherms at the low densities on the $C_v - C_v^*$ vs. density plot, which does not represent the experimental data correctly.

5. The temperature function derived from the Martin-Hou equation, which has a form of $T\exp(-kT/T_c)$, cannot represent the experimental isometrics on the $C_v - C_v^*$ vs. temperature plane with a sufficient curvature if the value of k is less than 7.0. An equation which has a form $P = A + BT - C/T^3$ does not represent the experimental isometrics satisfactorily.

6. The Martin-Hou equation predicts the negligible $C_V - C_V^*$ at temperatures far above the critical, which is in good agreement with experimental results of tetrafluoromethane.

7. The law of corresponding state is applicable to $C_V - C_V^*$ if the gases are similar in their molecular structure.

8. The extrapolation method as developed in this research for calibrating the alorimeter heat capacity is a reliable method.

APPENDIX A

DETERMINATION OF THE CALORIMETER VOLUME

A-1 Advantages of Using Nitrogen Gas as a Calibration Medium

In the previous investigation done by Noel de Nevers,[12] the volume of the calorimeter was determined by the weight of distilled water which filled up the calorimeter. Although the principles involved were quite simple, a technical difficulty arose in the course of feeding and removing water from the calorimeter. Tiny bubbles could be formed inside the calorimeter in spite of precautions, and the water which got into the motor was rather difficult to remove.

To avoid these difficulties, compressed pure nitrogen (bone dry) was employed in place of water. Nitrogen gas was preferred because it was available in high purity and its compressibility factors were known to the sufficient accuracy.

A-2 Basic Principle

Let P_1 and P_2 be two different pressures in which the following quantities are measured.

W_1, W_2 --------- Gross weights of the calorimeter plus gas

z_1, z_2 --------- Compressibility factors PV/RT

T_1, T_2 --------- Temperatures

w ---------- Net weight of the calorimeter

V ---------- Volume of the calorimeter

M ---------- Molecular weight of nitrogen

If we assume that the volume of the calorimeter remains practically constant in the vicinity of room temperature and at the moderate range of

pressures (3-10 atm), we have

$$\frac{P_1 V}{z_1 R T_1} = \frac{W_1 - w}{M} \tag{A-1}$$

$$\frac{P_2 V}{z_2 R T_2} = \frac{W_2 - w}{M} \tag{A-2}$$

(A-1) - (A-2), we get

$$\left(\frac{P_2}{z_1 T_1} - \frac{P_2}{z_2 T_2}\right) \frac{V}{R} = \frac{W_1 - W_2}{M} \tag{A-3}$$

Hence

$$V = \frac{(W_1 - W_2)R}{M} \Big/ \left(\frac{P_1}{z_1 T_1} - \frac{P_2}{z_2 T_2}\right) \tag{A-4}$$

Now if $P_2 \to 0$, Equation (A-4) reduces to

$$V = \frac{(W_1 - W_2)R}{M} \Big/ \frac{P_1}{z_1 T_1} = \frac{(W_1 - W_2)\, z_1 R T_1}{M P_1} \tag{A-5}$$

Either Equation (A-4) or (A-5) may be used for calculation; z_1 and z_2 can be obtained from the National Bureau of Standards' Circular 564, Nov., 1955.

A-3 Measuring Apparatus

The measuring apparatus is shown diagramatically in Figure A-1. The nitrogen used was the bone-dry grade by Matheson Co. The pressure gauge was by Heise Co. (0-500#). The vacuum pump was of the Hyvac 2 type.

A-4 Procedures

(a) To avoid evacuation of the pressure gauge, the gauge was purged with pure nitrogen several times. The procedure consisted of filling the gauge with compressed nitrogen and the subsequent release of it into the atmosphere. The valve V_3 is always closed except the external line was filled with nitrogen.

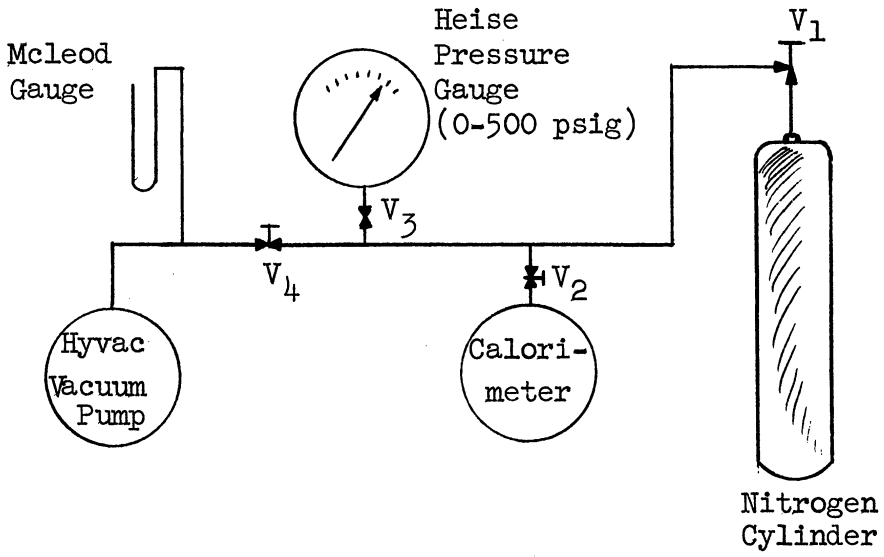

Figure A-1 Schematic Diagram of Determining the Calorimeter Volume.

(b) After evaculation of the calorimeter (with V_3 and V_1 closed), V_2 was closed and a calorimeter was disconnected for weighing.

(c) Before feeding the calorimeter with pure nitrogen, the line was first evacuated. Then, with V_4 closed, the calorimeter was filled with an appropriate amount of nitrogen. When equilibrium was reached, the temperature and pressure were measured and then the calorimeter was closed and disconnected from the system for weighing.

(d) The same procedures were repeated several times for the different pressures.

A-5 Results

Run No.	Temp. °K	abs.Pres.atm.	z	gross wt,gm.	Volume
1		0.000013		998.72	
2	299.96	12.1279*	0.99823	1059.74	4412 cc
3	299.75	11.4345	0.99826	1056.24	4408
4	299.98	10.7066	0.99833	1052.63	4415
5	298.75	9.4685	0.99836	1046.47	4405
6	299.05	8.0263	0.99861	1039.16	4407

Average Volume 4409 cc

* The accuracy of pressure measurements was estimated at no better than 0.05%. The extra digits, however, were retained on the conversion.

APPENDIX B

CALIBRATION OF RESISTANCE THERMOMETER

The standard resistance thermometer is usually certified on the International Temperature Scale, of which the fixed and reproducible equilibrium temperatures are the ice point, steam point, sulfur point, etc., and the specified interpolation formula is as follows: For the range 0 to 630°C,

$$t = \frac{R_t - R_o}{\alpha R_o} + \delta\left(\frac{t}{100} - 1\right)\frac{t}{100} \qquad \text{(B-1)}$$

devised by Callendar and commonly used in this country. Equation (B-1) may be put in the equivalent international formula,

$$R_t = R_o(1 + At + Bt^2) \qquad \text{(B-2)}$$

where R_t is the resistance of the thermometer at temperature t and R_o is the resistance at 0°C.

One of the international requirements for a standard thermometer is that α, or $R_{100}-R_0/100R_0$, must be greater than 0.00391. It was found, unfortunately, that the resistance thermometer as described in Section III-2 generally does not satisfy this requirement. For this reason, it was decided to calibrate the thermometer not only at three fixed points but also at several temperatures in the range of interest, and two constants evaluated by a least-square fitting.

Because of lack of the available facility, the sulfur point was omitted. The resistance was measured at the ice point a few times with a 24-hour annealing period between two successive measurements to make sure the resistance was stable. The resistance at temperatures other than the

ice point was measured by immersing the thermometer into an agitated oil bath whose temperature was in turn measured by the Leeds and Northrup resistance thermometer No. 1227385, for which an NBS calibration dated June 25, 1958, was available. The temperatures were recorded to 0.001°C although their reliability was definitely less than this. Due to the small capacity of the oil bath and the manual control of the heating element, the temperature fluctuation was estimated to be of the order of 0.01°C per minute, and the possible temperature difference between two points in the oil bath might have reached 0.2°C.

The ice point, being a fixed point, was not subject to the above difficulties and was considered more reliable than any other measurements. Hence, R_o = 23.8257 ohms was used directly in Equation (B-2) and the constants A and B were evaluated by fitting the following data:

Leeds & Northrup No. 1227385, ohms	Temperature, °C	Thermometer Calibrated, ohms
25.5205	0.000	23.8257
28.1293	25.749	26.1166
34.7968	92.466	32.1214
35.5888	100.481	32.8688
40.6941	152.618	37.4662
45.1152	198.454	41.4626

The values obtained for two constants were: $A = 3.80518 \times 10^{-3}$; $B = -3.6997 \times 10^{-7}$. The maximum scatter of the data from the calibrated curve was about 0.15% in resistance which corresponded to about 0.3°C. Most of the data fitted within 0.15°C.

APPENDIX C

SAMPLE CALCULATIONS

C-1 Volume of the Calorimeter

The volume of the calorimeter at the room temperature, 27°C, and 130 psia was calibrated according to the method described in Appendix A. In the process of experiments, this volume changed gradually due to the thermal and elastic expansion. These changes were estimated as follows:

$$d(\ln V) = \left(\frac{d\ln V}{dT}\right)_p dT + \left(\frac{d\ln V}{dp}\right)_T dp \qquad (C\text{-}1)$$

or

$$\frac{dV}{V} = \left(\frac{dV}{VdT}\right)_p dT + \left(\frac{dV}{Vdp}\right)_T dp \qquad (C\text{-}2)$$

where (dV/VdT) was a volumetric coefficient of thermal expansion and approximately three times the linear coefficient of thermal expansion. The value of the linear expansion was 5.0×10^{-6} per degree C for the type of steel used according to the ASM Metal Handbook.[3] $(dV/Vdp)_T$ was a coefficient of elastic expansion and related to Young's modulus as follows:

$$\left(\frac{dV}{Vdp}\right)_T \cong 3\left(\frac{dr}{rdp}\right)_T = \frac{(3)(0.25)(\text{diameter})}{(\text{wall thickness})(\text{Young's Modulus})} \qquad (C\text{-}3)$$

For 8-inch diameter, 0.031-inch wall thickness, and 30×10^6 psi for Young's modulus, we obtained

$$\left(\frac{dV}{Vdp}\right)_T = 0.667 \times 10^{-5} \text{ per psi} \qquad (C\text{-}4)$$

Hence

$$\frac{dV}{V} = 1.5 \times 10^{-5}\, dT + 0.667 \times 10^{-5}\, dp \qquad (C\text{-}5)$$

As an example, for chloropentafluoroethane loading No. 5, the temperature range was 71.7-121.5°C and the pressure range was 335-500 psi. Hence the average temperature was 97°C and the average pressure, 418 psi. The mean volume for this particular loading was then estimated at this average condition, using Equation (C-5).

$$\frac{dV}{V} = 1.5 \times 10^{-5} (97-27) + 0.667 \times 10^{-5} (418-130) = 0.00297$$

$$\therefore \quad V = 4409 \times 1.00297 = 4422 \text{ cc.}$$

Therefore the average density was

$$\rho = \frac{981.10}{4422} = 0.2219 \text{ gm/cc.}$$

C-2 Gross Heat Capacity

As an example, the calculation of Run No. C-24 is illustrated below. The primary data are as follows:

The heating period started at 2:23 and ended at 2:54.

The elapsed time, $\Delta\theta$, was 31.173 minutes.

The power was measured three times during the heating period, which read:

Voltage (volts)	Current (amp)
18.30	0.4165
18.38	0.4143
18.46	0.4123

The temperatures were measured before and after the heating period at the following times. The resistance shown was a sum of the normal and reverse readings which corresponded to exactly twice the true resistance of the thermometer.

	Time	Ohms
Before heating	2:07	59.5833
	2:12	59.5827
	2:17	59.5815
	2:22	59.5805
After heating	3:04	61.5482
	3:09	61.5468
	3:14	61.5454
	3:19	61.5435

From the above primary data, the gross heat capacity was calculated. The thermometer resistance at the start of the heating period, R_1, was just one-half the total reading at 2:22 (1 min. difference was neglected), i.e., 29.7900 ohms including the bridge zero correction. The change of total resistance before heating period was -0.0009 ohms in 5 minutes which corresponded to the drift of -0.0009 ohms in true resistance in ten minutes. This value in resistance was equivalent to -0.0010°C/min. and designated as $drift_1$. Similarly, the drift rate after heating period was estimated. The average drift was -0.0015 ohms in ten minutes in the true resistance which was equivalent to -0.0017°C/min. at this temperature. This was $drift_2$. The resistance at the end of the heating period was determined by extrapolating the resistance at 3:04 back to 2:54 using the value of $drift_2$ (linear extrapolation). The value obtained was 30.7753 ohms including the bridge zero correction. This was R_2. R_1 and R_2 were then converted into temperatures using the calibration formula:

$$R = 23.8257 (1 + 0.00380518t - 3.6997 \times 10^{-7} t) \qquad (C\text{-}6)$$

where R is the resistance in ohms and t is the temperature in °C. (For calibration of the thermometer, see Appendix B.) The results were T_1 = 66.213°C and T_2 = 77.235°C. Hence, ΔT = 11.022°C.

The correction for heat leakage was estimated in terms of corresponding temperature change, using the drift rates, i.e.,

$$\Delta T_{corr.} = \left(\frac{drift_1 + drift_2}{2}\right)\Delta\theta = \frac{-(.0010 + 0.0017)}{2}\ (31.173) = -0.042°C$$

By multiplying the voltage and current, the gross power inputs at various times were calculated, which yielded 7.622, 7.615, and 7.611 watts, respectively. The average was 7.616 watts. Some of this calculated gross power, however, was dissipated in the voltage measuring circuit, which was parallel with the thermometer-heater and motor (see Figure 3-9). The voltage-measuring circuit consisted of two standard resistors and one voltmeter whose total equivalent resistance was found to be 2015 $\pm$ 5 ohms. Hence, the power consumed in this circuit was

$$q = IE = \frac{E^2}{R} = \frac{E^2}{2015} \qquad (C\text{-}7)$$

For this particular run, the average voltage was 18.38 volts and, therefore, the power loss was 0.168 watts according to Equation (C-7). Their difference, 7.448 watts, was then the net power.

The gross heat capacity was then calculated by Equation (5-6) as follows:

$$C_{gross} = \frac{q_{mean}\,\Delta\theta}{(\Delta T - \Delta T_{corr.})} \qquad \frac{(7.448)(31.173)(14.3403)}{(11.022 + 0.042)} = 300.93\ cal/°C$$

where 14.3403 cal/watt-min. was a conversion factor.

The correction for the expansion work done by the gas on the calorimeter was neglected on the basis that for each 10°C interval the volume increase was only about 0.015% of the original volume and the correction would have been less than 0.02% of the total heat input.

C-3 Constant-Volume Heat Capacity of the Gas

The mean gross heat capacity as calculated in Section C-2 was then regarded as the true gross heat capacity at the mean temperature. For example, in Run No. C-24, T_1 was 66.213°C and T_2 77.235°C. Hence, their arithmatic mean was

$$T_{mean} = \frac{66.213 + 77.235}{2} = 71.72°C$$

At 71.72°C, the heat capacity of the calorimeter was read from Figure 6-3 to be 112.00 cal/°C. The difference between C_{gross} and $C_{calr.}$ was designated as C_{net}. Hence,

$$C_{net} = C_{gross} - C_{calr.} = 300.93 - 112.00 = 188.93 \text{ cal/°C}$$

and

$$C_v = \frac{C_{net}}{m} = \frac{187.07}{981.10} = 0.1926 \text{ cal/gm.°C}$$

where m is the mass of the gas loaded.

APPENDIX D

DETAILED GROSS HEAT-CAPACITY DATA

In Tables D-1 through D-5, the runs are numbered in chronological order (carrying the same number as the original data sheets). The letters, A, B, etc., indicate the compound loaded. (Exceptions are those runs for dichlorodifluoromethane originally intended for the calibration of calorimeter heat capacity, i.e., Run No. A-11 through No. A-23.) Those runs which did not suffice for the criteria of acceptable experimental conditions are discarded regardless of the magnitude of their deviation from the smoothed curve. In each table are listed the values of T_1, T_2, $-\text{drift}_1$, $-\text{drift}_2$, mean power, $\Delta\theta$, $(\Delta T - \Delta T_{corr.})$, C_{gross}, and T_{mean}. The loadings are numbered in the order of increasing density for each compound.

For those loadings whose final results were not calculated directly from the individual gross heat-capacity but were evaluated by the smoothed gross heat-capacity data, the gross heat-capacity data are plotted in Figures D-1 through D-7. A smooth curve has been drawn through those data points for each loading. Based on these smooth curves, the final constant-volume heat-capacity data were calculated.

TABLE D-1

GROSS HEAT CAPACITY WITH DICHLORODIFLUOROMETHANE LOADING

Run No.	T_1	T_2	$-drift_1$	$-drift_2$	Mean Power	$\Delta\theta$	$\Delta T - \Delta T_{corr.}$	C_{gross}	T_{mean}
	°C	°C	°C/min.	°C/min.	Watts	min.	°C	cal/°C	°C
Dichlorodifluoromethane Loading No. 1. 55.03 gm. Recovered 54.70 gm.									
A-11	37.051	49.665	.0000	.0011	3.847	26.904	12.629	117.52	43.36
A-12	49.658	62.541	.0011	.0022	3.824	28.012	12.929	118.81	56.10
A-13	75.927	90.465	.0045	.0050	4.772	25.996	14.661	121.34	83.20
A-14	90.348	103.797	.0050	.0056	4.795	24,309	13,578	123.10	97.07
A-15	104.803	118.093	.0067	.0074	4.703	24.858	13.465	124.51	111.45
A-16	117.909	131.142	.0074	.0088	4.682	25.090	13.436	125.38	124.53
A-17	130.886	144.112	.0088	.0102	4.654	25.412	13.467	125.94	137.50
A-18	148.465	164.051	.0113	.0125	4.640	30.567	15.950	127.52	156.26
A-19	163.760	179.330	.0125	.0137	4.622	31.205	15.979	129.44	171.55
A-21	168.768	183.347	.0103	.0114	4.389	30.656	14.912	129.39	176.06
A-22	185.328	199.336	.0137	.0149	5.775	24.192	15.354	130.49	191.83
A-23	32.484	42.250	-.0006	.0000	3.855	20.551	9.760	116.40	37.37
Dichlorodifluoromethane Loading No. 2. 251.74 gm. Recovered 251.01 gm.									
E-1	116.983	127.613	.0037	.0059	5.701	20.344	10.728	155.03	122.25
E-2	127.457	139.937	.0059	.0074	5.690	24.111	12.643	155.60	133.70
E-3	138.501	150.615	.0063	.0077	5.704	23.554	12.279	156.90	144.56
E-4	150.378	162.853	.0077	.0091	5.666	24.715	12.683	158.34	156.62
E-5	156.408	167.857	.0065	.0095	5.233	24.616	11.646	158.62	162.13
E-6	167.612	179.542	.0095	.0112	5.226	26.010	12.199	159.79	173.57
E-7	178.865	190.944	.0099	.0118	6.724	20.513	12.302	160.79	184.90

TABLE D-2

GROSS HEAT CAPACITY WITH TETRAFLUOROMETHANE LOADING

Run No.	T_1	T_2	-drift$_1$	-drift$_2$	Mean Power	$\Delta\theta$	$\Delta T - \Delta T_{corr.}$	C_{gross}	T_{mean}
	°C	°C	°C/min.	°C/min.	Watts	min.	°C	cal/°C	°C
Tetrafluoromethane Loading No. 3. 334.72 gm. Recovered 334.20 gm.									
D-10	29.080	41.638	.0000	.0011	7.281	19.009	12.568	157.92	35.36
D-11	40.832	53.695	.0006	.0017	7.239	19.930	12.886	160.55	47.26
D-12	53.648	67.044	.0017	.0028	7.234	21.157	13.444	163.25	60.35
D-13	66.624	78.794	.0025	.0034	7.205	19.643	12.228	165.98	72.71
D-14	86.961	97.812	.0037	.0045	5.980	21.573	10.939	169.12	92.39
D-15	97.678	108.901	.0045	.0056	6.015	22.510	11.337	171.27	103.29
D-16	109.362	120.422	.0056	.0062	5.989	22.631	11.194	173.64	114.89
D-17	120.279	131.651	.0062	.0074	5.974	23.645	11.533	175.64	125.97
D-18	131.467	142.920	.0074	.0087	5.969	24.089	11.647	177.04	137.19
D-19	148.993	159.435	.0068	.0079	5.437	24.547	10.622	180.18	154.21
D-20	159.211	170.357	.0079	.0097	5.435	26.628	11.380	182.36	164.78
D-21	169.555	180.542	.0100	.0112	5.119	28.137	11.285	183.02	175.05
D-22	180.969	192.211	.0112	.0129	7.314	20.273	11.486	185.13	186.59
Tetrafluoromethane Loading No. 1. 160.70 gm. Recovered 159.47 gm.									
D-23	27.866	41.399	.0007	.0009	6.322	19.722	13.535	132.09	34.63
D-24	41.347	53.579	.0009	.0025	6.309	18.219	12.262	134.42	47.46
D-25	53.501	66.812	.0025	.0038	6.297	20.087	13.374	135.63	60.16
D-26	78.246	92.127	.0025	.0038	6.221	21.743	13.949	139.06	85.19
D-27	92.031	106.056	.0038	.0051	6.213	22.352	14.124	140.99	99.04
D-28	113.629	128.423	.0045	.0057	6.141	24.423	14.919	144.17	121.03
D-29	128.261	140.208	.0057	.0076	5.408	22.770	12.098	145.97	134.23
D-30	140.566	150.960	.0069	.0084	4.574	23.612	10.575	146.46	145.76
D-31	152.998	164.615	.0069	.0084	5.110	23.879	11.800	148.29	158.81
D-33	175.259	186.534	.0099	.0114	5.117	23.684	11.527	150.77	180.90
D-34	186.074	197.530	.0110	.0126	5.101	24.380	11.744	151.86	191.80
D-35	30.212	43.600	.0010	.0009	6.376	19.406	13.387	132.53	36.91
D-36	60.872	73.672	.0012	.0027	6.335	19.334	12.838	136.81	67.27
D-37	102.615	115.710	.0041	.0052	5.709	23.061	13.202	143.01	109.16
D-38	146.322	158.505	.0074	.0084	5.455	23.388	12.368	147.92	152.41
D-39	165.702	177.421	.0085	.0104	5.417	23.056	11.937	150.04	171.56
Tetrafluoromethane Loading No. 2. 257.44 gm. Recovered 256.68 gm.									
D-41	25.449	39.259	.0000	.0016	6.752	20.833	13.827	145.88	32.35
D-42	39.215	52.046	.0016	.0031	6.758	19.729	12.877	148.48	45.63
D-43	52.180	64.387	.0017	.0025	6.762	19.029	12.247	150.67	58.28
D-44	64.326	76.525	.0025	.0034	6.778	19.258	12.256	152.73	70.43
D-45	76.420	88.926	.0034	.0044	6.710	20.242	12.585	154.76	82.67
D-46	102.198	113.764	.0035	.0045	5.816	22.243	11.655	159.18	107.98
D-47	113.911	125.873	.0049	.0058	5.886	23.050	12.085	160.98	119.89
D-48	125.726	137.487	.0058	.0069	5.886	22.991	11.907	162.99	131.61
D-49	136.840	149.039	.0073	.0081	5.872	24.118	12.385	163.98	142.94
D-51	166.315	177.065	.0088	.0101	5.436	23.628	10.973	167.86	171.69
D-52	176.129	187.266	.0097	.0109	5.401	24.895	11.393	169.24	181.70
D-53	188.500	199.308	.0103	.0124	6.811	19.338	11.027	171.29	193.90
Tetrafluoromethane Loading No. 4. 410.69 gm. Recovered 409.33 gm.									
D-54	32.197	44.612	.0004	.0011	7.152	20.588	12.430	169.88	38.40
D-55	44.585	57.202	.0011	.0018	7.224	21.139	12.648	173.14	50.89
D-56	57.121	69.887	.0018	.0025	7.214	21.736	12.813	175.49	63.50
D-57	69.819	82.829	.0025	.0034	7.225	22.552	13.077	178.68	76.32
D-58	81.734	93.698	.0030	.0039	6.718	22.614	12.042	180.92	87.72
D-59	98.411	109.615	.0025	.0034	6.281	23.040	11.272	184.10	104.01
D-60	109.601	120.689	.0036	.0042	6.318	23.056	11.178	186.88	115.14

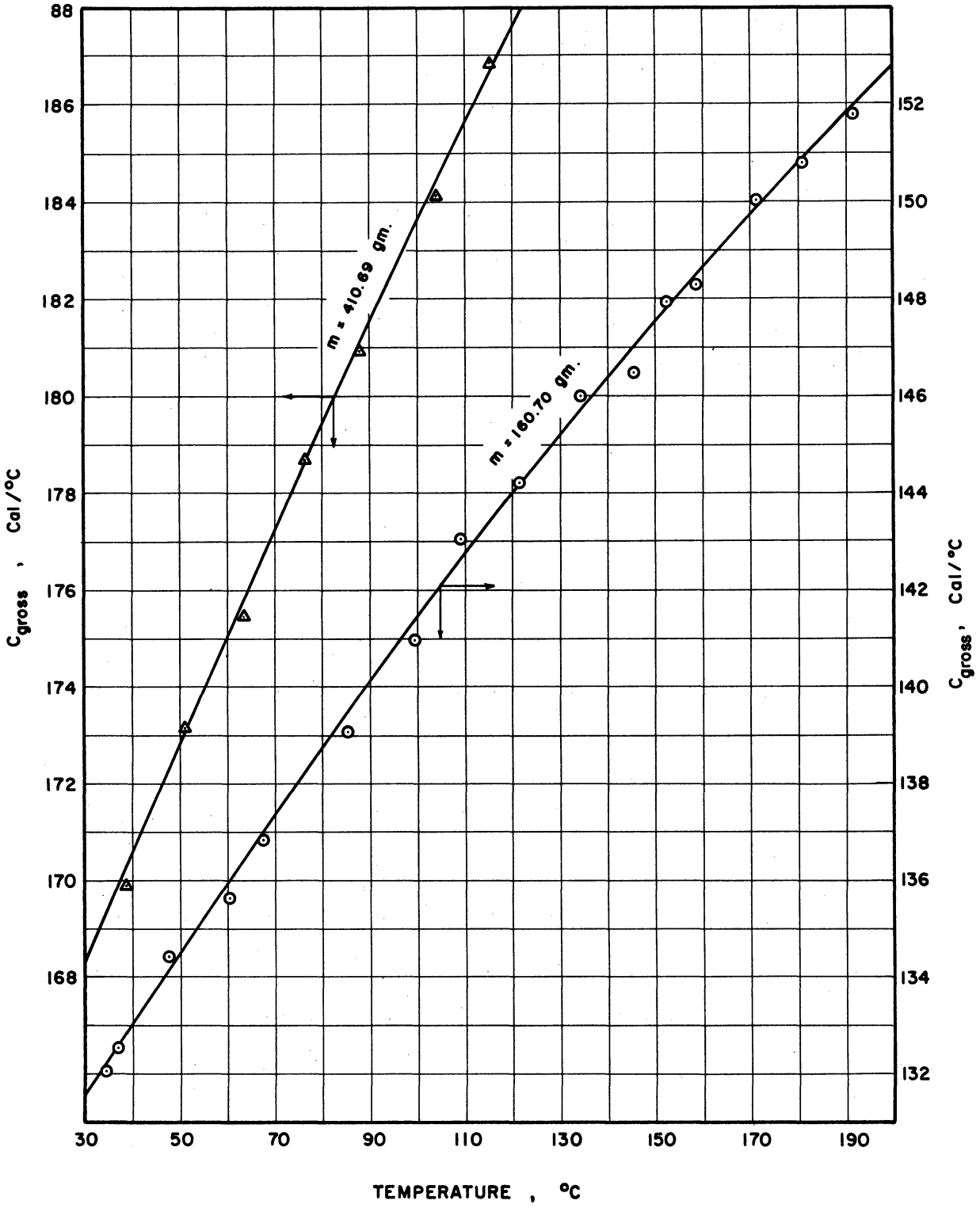

Figure D-1. Gross Heat Capacity with Tetrafluoromethane Loading.

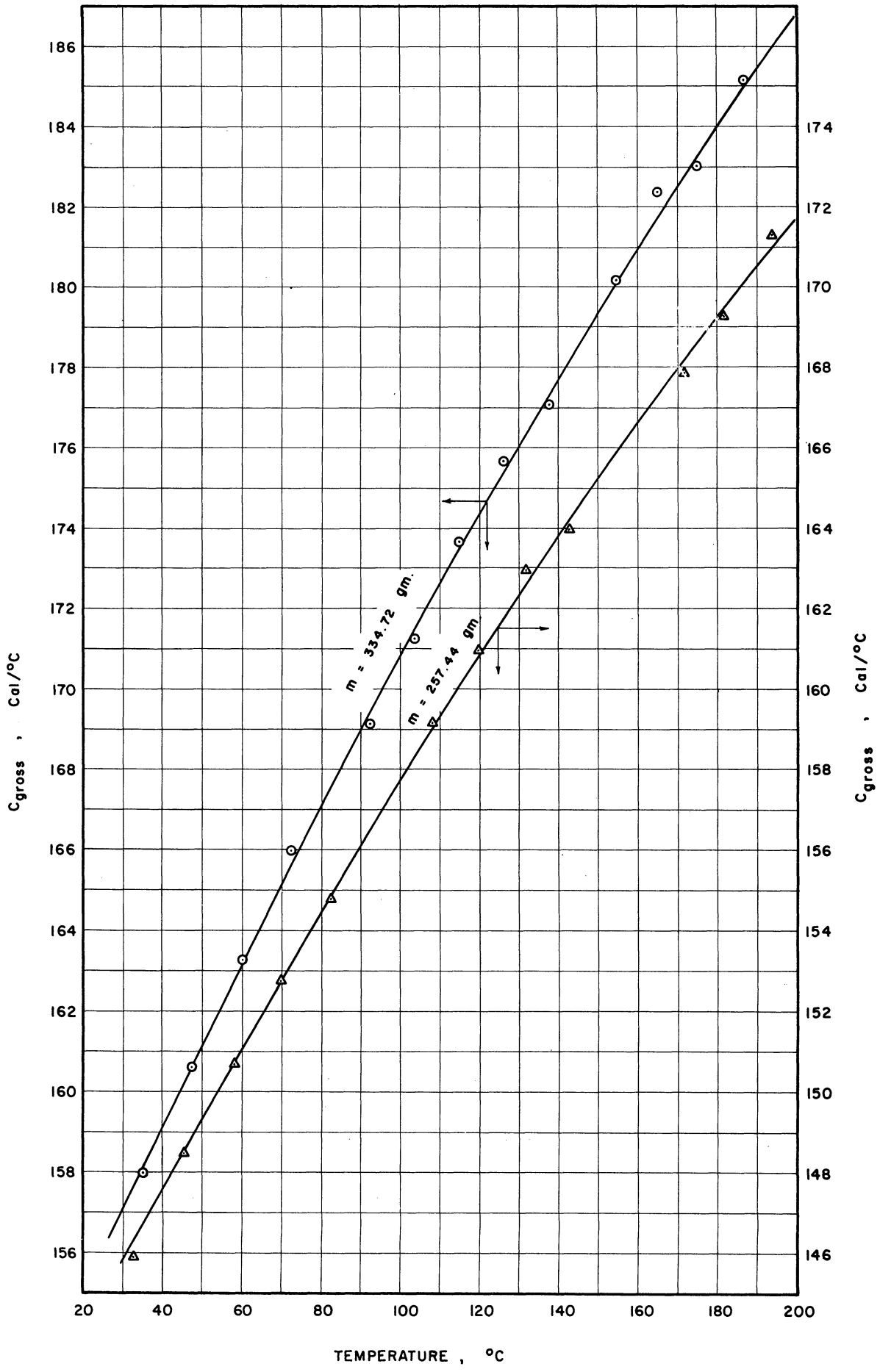

Figure D-2. Gross-Heat Capacity with Tetrafluoromethane Loading.

TABLE D-3

GROSS HEAT CAPACITY WITH CHLORODIFLUOROMETHANE LOADING

Run No.	T_1	T_2	-drift$_1$	-drift$_2$	Mean Power	$\Delta\theta$	$\Delta T - \Delta T_{corr.}$	C_{gross}	T_{mean}
	°C	°C	°C/min.	°C/min.	Watts	min.	°C	cal/°C	°C
			Chlorodifluoromethane Loading No. 3. 346.08 gm. Recovered 346.05 gm.						
A-2	69.567	79.147	.0021	.0026	4.498	25.263	9.639	169.05	74.36
A-3	88.198	100.462	.0024	.0037	6.005	24.531	12.339	171.21	94.33
A-4	100.370	112.300	.0037	.0046	5.973	24.246	12.031	172.62	106.34
A-5	123.358	135.493	.0045	.0061	6.080	24.644	12.266	175.18	129.43
A-6	135.340	147.819	.0061	.0065	6.057	25.838	12.641	177.54	141.58
A-7	147.665	159.910	.0060	.0068	6.037	25.628	12.409	178.80	153.79
A-8	167.286	181.972	.0051	.0065	6.974	26.941	14.842	181.54	174.63
			Chlordifluoromethane Loading No. 4. 447.08 gm. Recovered 446.81 gm.						
A-24	67.302	79.344	.0015	.0019	6.461	24.545	12.084	188.20	73.32
A-25	79.675	91.693	.0025	.0039	6.463	24.607	12.097	188.53	85.68
A-26	90.013	101.807	.0037	.0038	6.436	24.396	11.885	189.45	95.91
A-27	108.435	118.814	.0039	.0052	5.937	23.586	10.486	191.50	113.62
A-28	118.685	130.468	.0052	.0061	6.253	25.674	11.928	193.01	124.58
A-29	129.274	143.873	.0055	.0068	8.393	23.913	14.746	195.18	136.57
A-30	143.671	156.512	.0068	.0080	8.384	21.334	12.999	197.32	150.09
			Chorodifluoromethane Loading No. 5. 548.22 gm. Recovered 547.93 gm.						
A-31	69.543	81.707	.0018	.0029	6.981	25.437	12.224	208.33	75.63
A-32	81.634	94.060	.0029	.0037	6.964	26.195	12.512	209.08	87.85
A-33	93.962	106.408	.0037	.0046	6.922	26.402	12.556	208.72	100.19
A-34	104.134	117.296	.0042	.0050	8.474	23.014	13.268	210.78	110.72
A-35	79.691	89.434	.0022	.0022	6.689	21.262	9.790	208.32	84.56
			Chlorodifluoromethane Loading No. 2. 254.10 gm. Recovered 254.08 gm.						
A-36	41.969	55.276	.0011	.0019	4.774	29.176	13.351	149.61	48.62
A-37	103.258	116.202	.0024	.0034	6.060	23.440	13.012	156.55	109.73
A-38	115.851	126.884	.0045	.0056	5.788	21.314	11.141	158.80	121.37
A-39	126.681	139.021	.0056	.0068	5.752	24.286	12.491	160.37	132.85
A-40	138.839	150.761	.0068	.0079	5.721	23.754	12.097	161.10	144.80
A-41	167.224	179.202	.0074	.0103	5.263	26.669	12.214	164.79	173.21
A-42	178.940	192.441	.0103	.0108	5.266	30.541	13.823	166.85	185.69
A-43	60.477	75.686	.0009	.0020	6.623	24.337	15.235	151.72	68.08
A-44	90.556	105.449	.0031	.0043	6.604	24.553	14.984	155.19	98.00
A-47	99.761	111.681	.0028	.0036	6.152	21.242	11.988	156.32	105.72
			Chlorodifluoromethane Loading No. 1. 166.96 gm. Recovered 166.71 gm.						
A-49	52.993	66.388	.0014	.0020	6.192	20.664	13.430	136.62	59.69
A-50	66.341	79.472	.0020	.0031	6.170	20.639	13.184	138.51	72.90
A-51	83.367	96.006	.0041	.0050	6.165	20.140	12.731	139.86	89.69
A-52	95.921	109.472	.0050	.0060	6.128	21.978	13.672	141.27	102.70
A-53	109.349	121.956	.0060	.0074	6.120	20.787	12.746	143.14	115.65
A-54	121.422	134.050	.0056	.0068	5.500	23.370	12.773	144.31	127.73
A-57	157.773	169.183	.0091	.0102	5.462	22.105	11.623	148.96	163.48
A-58	168.906	179.512	.0102	.0120	5.374	21.100	10.840	150.00	174.21
A-60	136.561	148.461	.0056	.0068	5.210	23.563	12.046	146.14	142.51
A-62	161.991	173.857	.0097	.0108	5.198	24.113	12.113	148.39	167.92
A-63	173.585	185.170	.0108	.0125	5.191	23.940	11.865	150.20	179.38
A-64	184.860	196.345	.0125	.0125	5.181	23.950	11.784	150.99	190.60

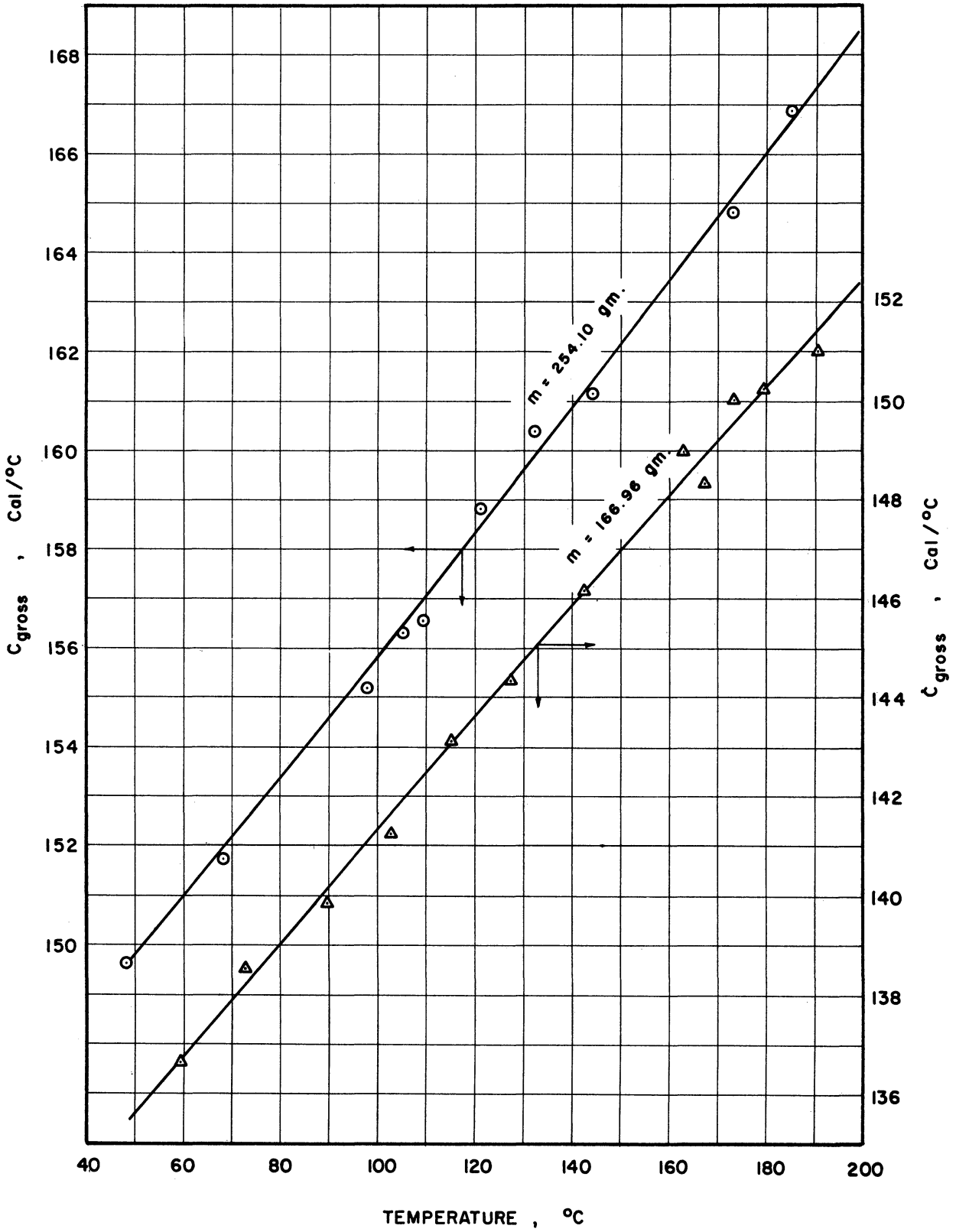

Figure D-3. Gross Heat Capacity with Chlorodifluoromethane Loading.

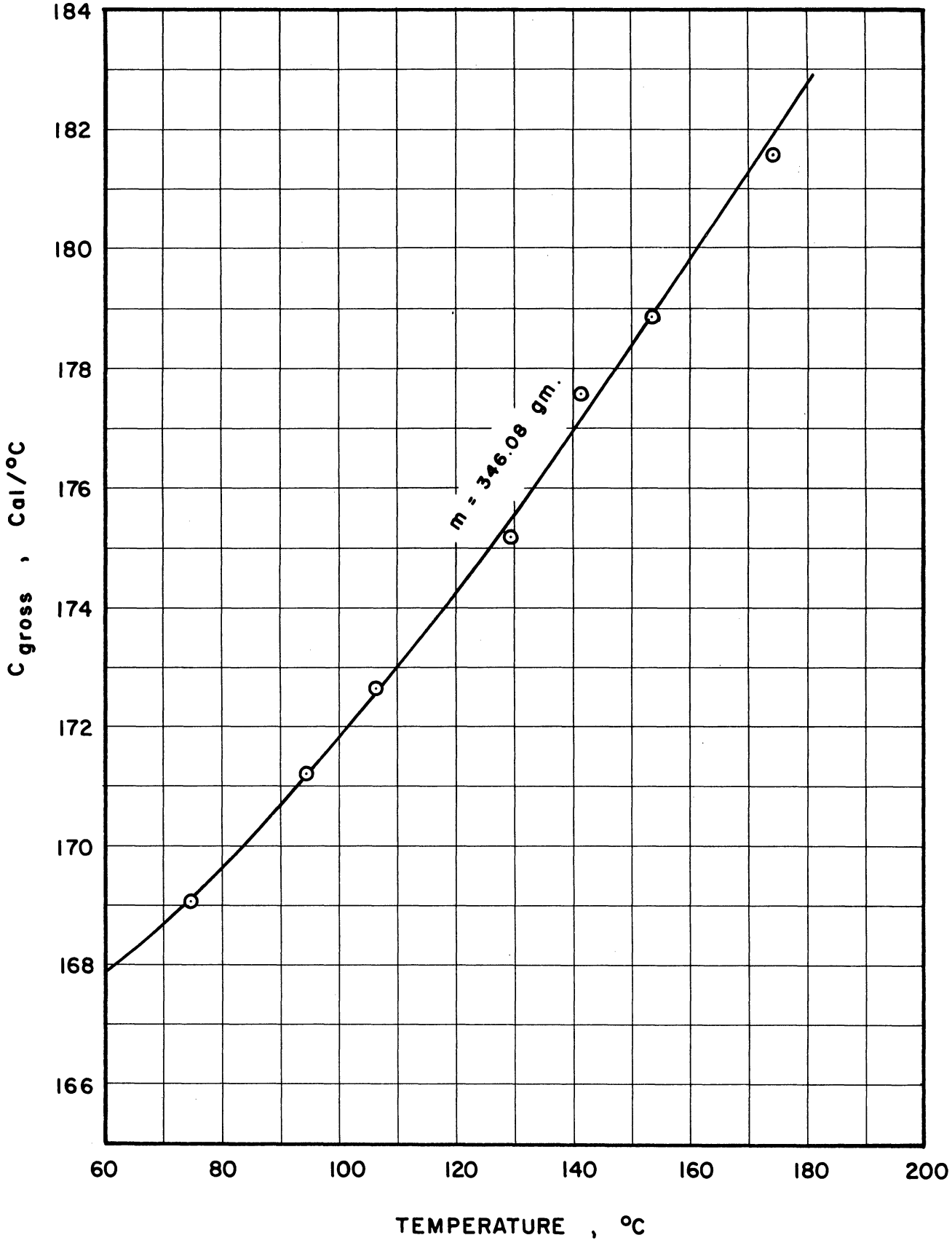

Figure D-4. Gross Heat Capacity with Chlorodifluoromethane Loading.

TABLE D-4

GROSS HEAT CAPACITY WITH DICHLOROTETRAFLUOROETHANE LOADING

Run No.	T_1	T_2	$-drift_1$	$-drift_2$	Mean Power	$\Delta\theta$	$\Delta T - \Delta T_{corr.}$	C_{gross}	T_{mean}
	°C	°C	°C/min.	°C/min.	Watts	min.	°C	cal/°C	°C
				Dichlorotetrafluoroethane Loading No. 2. 291.05 gm. Recovered 290.85 gm.					
B-9	82.558	96.182	.0023	.0029	6.154	25.508	13.690	164.43	89.37
B-10	95.170	107.304	.0030	.0036	6.160	22.906	12.210	165.72	101.24
B-11	107.215	119.427	.0036	.0045	6.158	23.414	12.307	168.00	113.32
B-12	119.312	131.600	.0045	.0054	6.147	23.838	12.406	169.38	125.46
B-13	131.477	142.899	.0054	.0063	6.132	22.501	11.554	171.26	137.19
B-15	147.233	159.120	.0057	.0065	6.243	23.123	12.028	172.12	153.18
B-16	158.989	169.948	.0065	.0074	5.769	23.303	11.121	173.36	164.47
B-17	167.581	178.805	.0068	.0071	5.753	23.239	11.392	175.54	173.19
B-19	187.007	197.556	.0091	.0103	5.596	23.873	10.781	177.69	192.28
B-20	115.685	129.163	.0021	.0029	6.869	23.191	13.536	168.76	122.42
B-21	128.419	140.824	.0044	.0051	6.388	23.150	12.515	169.44	134.62
B-22	140.712	152.954	.0051	.0057	6.324	23.465	12.369	172.04	146.83
B-23	152.898	165.793	.0057	.0066	6.355	24.738	13.047	172.79	159.35
B-24	164.188	175.741	.0057	.0068	5.983	23.758	11.701	174.20	169.96
B-25	175.580	186.914	.0068	.0080	5.784	24.426	11.515	175.94	181.25
B-26	186.712	197.394	.0080	.0092	5.775	23.340	10.883	177.61	192.05
				Dichlorotetrafluoroethane Loading No. 4. 600.17 gm. Recovered 599.97 gm.					
B-27	110.538	120.047	.0034	.0035	6.342	24.064	9.592	288.16	115.29
B-28	119.959	129.778	.0035	.0042	6.333	25.029	9.915	229.26	124.87
B-29	129.675	140.000	.00 2	.0051	6.296	26.639	10.449	230.18	134.84
B-30	140.568	150.971	.00 2	.0057	5.942	28.575	10.5 4	230.92	145.77
B-31	150.830	161.138	.0057	.0070	5.923	28.655	10.490	232.01	155.98
B-32	160.962	171.229	.0070	.0080	5.908	23.913	10.484	233.65	166.10
B-33	172.375	182.441	.0055	.0064	7.318	22.967	10.203	236.22	177.41
B-34	181.103	191.581	.0069	.0080	7.308	24.204	10.658	237.99	186.34
B-35	191.385	200.156	.0080	.0092	7.313	20.455	8.947	239.77	195.77
				Dichlorotetrafluoroethane Loading No. 1. 165.67 gm. Recovered 165.72 gm.					
B-36	71.605	81.927	.0013	.0028	4.307	23.683	10.371	141.04	76.77
B-37	81.854	92.257	.0028	.0039	4.286	24.163	10.484	141.65	87.06
B-38	91.293	105.157	.0036	.0054	5.879	23.672	13.971	142.85	98.23
B-39	105.021	117.371	.0054	.0064	5.861	21.457	12.477	144.54	111.20
B-40	117.210	129.056	.0064	.0078	5.841	20.936	11.995	146.20	123.13
B-41	125.977	139.488	.0064	.0074	5.457	25.756	13.689	147.24	132.73
B-42	139.312	151.275	.0074	.0091	5.439	23.231	12.155	149.07	145.29
B-43	151.086	163.584	.0091	.0114	5.435	24.527	12.749	149.94	157.34
B-45	186.063	193.227	.0135	.0165	6.501	22.163	13.496	153.10	186.65
B-47	91.354	104.631	.0015	.0026	5.948	22.314	13.323	142.85	97.99
B-48	137.588	149.872	.0066	.0075	5.454	23.570	12.450	148.06	143.73
B-53	158.677	170.771	.0108	.0120	5.383	24.005	12.368	149.83	164.72
B-54	170.414	182.56	.0120	.0131	5.370	25.006	12.756	150.96	176.64
B-55	186.620	198.392	.0131	.0149	5.304	24.406	12.114	153.24	192.51
				Dichlorotetrafluoroethane Loading No. 3. 440.56 gm. Recovered 440.40 gm.					
B-56	103.161	113.980	.0045	.0053	6.231	23.906	10.936	195.33	108.57
B-57	113.848	12 ..918	.0053	.0073	6.229	24.758	11.226	197.01	119.38
B-58	124.748	136.692	.0073	.0087	6.211	27.012	12.160	197.85	130.72
B-59	150.418	161.330	.0075	.0086	6.199	25.228	11.115	201.77	155.87
B-60	160.570	171.140	.0080	.0097	6.175	24.681	10.788	202.60	165.86
B-61	176.721	188.074	.0091	.0109	6.011	27.646	11.629	204.93	182.40
B-62	187.795	199.468	.0109	.0138	5.996	29.010	12.031	207.33	193.63
B-63	140.575	151.054	.0052	.0066	5.940	24.934	10.626	199.88	145.81
B-64	169.435	179.873	.0092	.0103	5.682	26.807	10.699	204.16	174.65

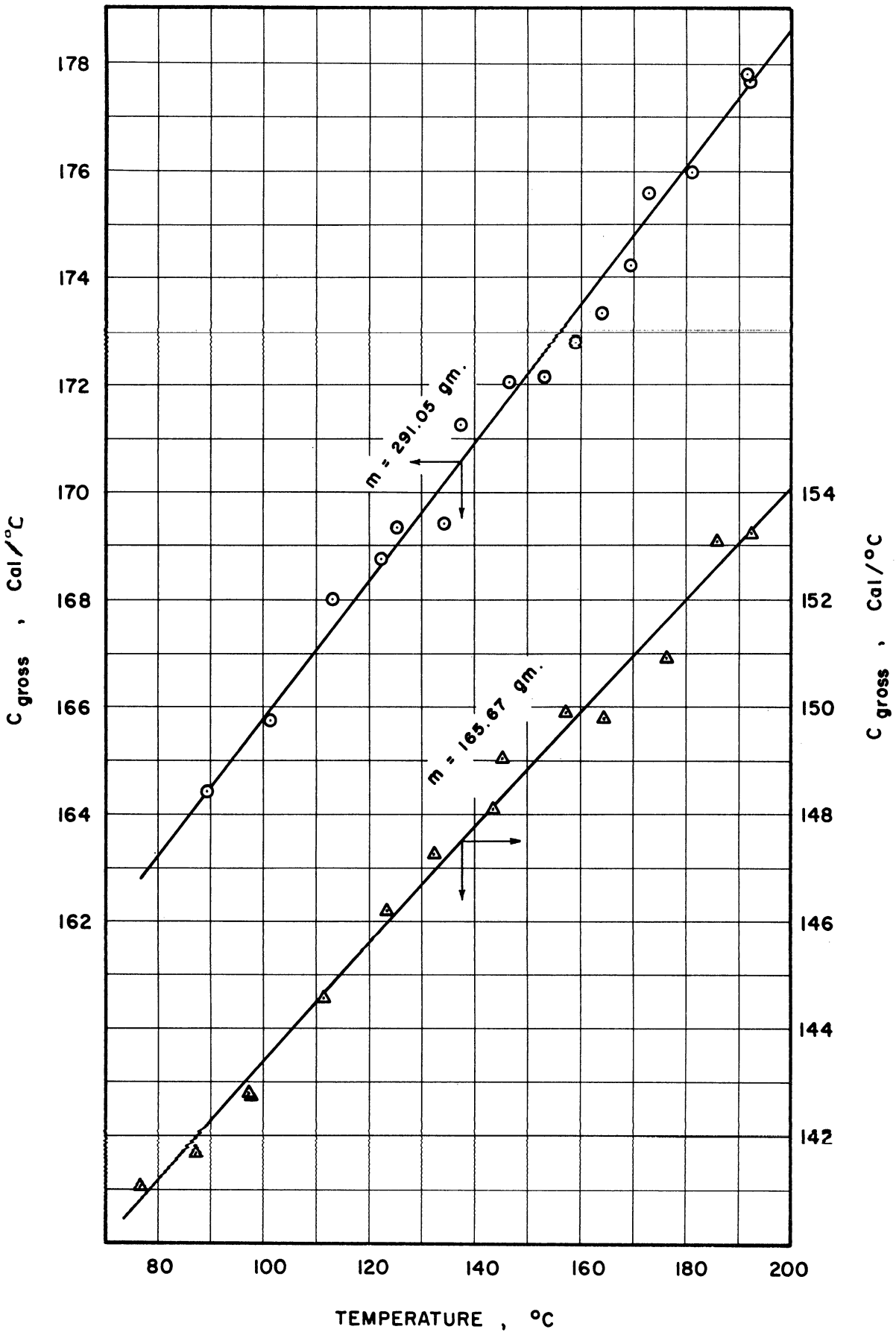

Figure D-5. Gross Heat Capacity with Dichlorotetrafluoroethane Loading.

TABLE D-5

GROSS HEAT CAPACITY WITH CHLOROPENTAFLUOROETHANE LOADING

Run No.	T_1	T_2	$-drift_1$	$-drift_2$	Mean Power	$\Delta\theta$	$\Delta T - \Delta T_{corr.}$	C_{gross}	T_{mean}
	°C	°C	°C/min.	°C/min.	Watts	min.	°C	cal/°C	°C
				Chloropentafluoroethane Loading No. 3. 592.52 gm. Recovered 592.43 gm.					
C-1	58.293	70.971	.0017	.0020	6.866	28.253	12.730	218.53	64.63
C-2	70.926	82.227	.0020	.0028	6.868	25.509	11.362	221.12	76.58
C-3	82.069	92.269	.0028	.0034	6.835	23.350	10.272	222.81	87.17
C-4	92.185	102.672	.0034	.0044	6.763	24.494	10.583	224.46	97.43
C-5	102.748	112.834	.0037	.0045	6.366	25.181	10.189	225.62	107.79
C-6	112.727	123.330	.0045	.0059	6.385	26.741	10.742	227.94	118.03
C-7	127.944	137.898	.0053	.0065	6.374	25.571	10.105	231.30	132.92
C-8	137.749	147.411	.0064	.0070	6.349	25.232	9.831	233.68	142.58
C-9	147.235	156.987	.0070	.0080	6.335	25.797	9.945	235.65	152.11
C-10	163.635	172.137	.0080	.0091	5.546	26.180	8.726	238.61	167.89
C-11	171.908	180.431	.0091	.0100	5.557	26.624	8.789	241.39	176.17
C-12	179.558	188.232	.0098	.0109	5.536	27.309	8.957	242.05	183.90
C-13	188.109	197.792	.0109	.0126	7.217	23.496	9.959	244.17	192.95
				Chloropentafluoroethane Loading No. 4. 791.79 gm. Recovered 791.40 gm.					
C-14	59.995	70.527	.0012	.0017	7.292	26.191	10.570	259.10	65.26
C-15	70.354	80.952	.0018	.0025	7.293	26.489	10.655	260.00	75.65
C-16	80.890	91.705	.0025	.0033	7.276	27.313	10.894	261.59	86.30
C-17	91.624	102.191	.0033	.0043	6.977	28.085	10.674	263.26	96.91
C-18	103.350	112.675	.0026	.0034	6.554	26.629	9.405	266.11	108.01
C-19	112.595	122.331	.0034	.0044	6.556	28.054	9.845	267.90	117.46
C-20	124.315	133.710	.0037	.0046	6.240	28.712	9.514	270.04	129.01
C-21	132.255	141.543	.0050	.0060	6.222	28.761	9.446	271.67	136.90
C-22	140.822	149.829	.0056	.0060	6.159	28.479	9.172	274.24	145.33
C-23	149.680	158.855	.0060	.0069	6.150	29.364	9.364	276.56	154.27
				Chloropentafluoroethane Loading No. 5. 981.10 gm. Recovered 980.75 gm.					
C-24	66.213	77.235	.0010	.0017	7.448	31.173	11.064	300.93	71.72
C-25	77.192	87.340	.0017	.0022	7.416	28.809	10.204	300.25	82.27
C-26	86.868	95.744	.0016	.0022	6.606	28.397	8.930	301.24	91.31
C-27	95.694	104.871	.0022	.0030	6.605	29.570	9.254	302.66	100.28
C-28	104.796	113.665	.0030	.0039	6.579	28.890	8.969	303.90	109.23
C-29	117.189	125.814	.0036	.0044	6.542	28.640	8.740	307.41	121.50
				Chloropentafluoroethane Loading No. 2. 393.11 gm. Recovered 392.26 gm.					
C-30	132.011	144.200	.0057	.0066	5.958	28.050	12.362	193.87	138.21
C-31	144.006	156.232	.0066	.0082	5.927	28.597	12.438	195.41	150.12
C-32	156.017	168.052	.0082	.0099	5.911	28.674	12.294	197.70	162.03
C-33	164.147	176.568	.0089	.0106	5.925	29.678	12.710	198.39	170.36
C-34	176.297	188.151	.0106	.0126	5.905	28.937	12.190	201.01	182.22
C-35	187.847	198.556	.0126	.0149	5.907	26.453	11.073	202.37	193.20
C-36	45.430	58.849	.0010	.0016	6.407	26.095	13.453	178.22	52.14
C-37	58.811	71.105	.0016	.0026	6.427	24.173	12.345	180.47	64.96
C-38	71.041	83.204	.0026	.0043	6.414	24.295	12.247	182.46	77.12
C-39	87.655	100.654	.0031	.0039	6.376	26.618	13.092	185.90	94.15
C-40	100.559	113.059	.0039	.0051	6.310	26.168	12.618	187.66	106.82
C-42	111.085	123.318	.0038	.0047	6.386	25.639	12.342	190.24	117.20
C-43	122.264	134.276	.0054	.0063	6.272	25.889	12.163	191.45	128.27
C-44	133.518	146.008	.0059	.0070	6.268	27.287	12.666	193.64	139.76
C-45	55.585	69.372	.0004	.0015	6.963	24.883	13.811	179.90	62.48
C-46	69.097	82.476	.0015	.0024	6.960	24.483	13.427	181.99	75.79
				Chloropentafluroethane Loading No. 1. 188.94 gm. Recovered 188.86 gm.					
C-48	54.796	68.344	.0025	.0038	6.790	20.022	13.611	143.24	61.57
C-49	68.039	81.038	.0023	.0039	6.766	19.595	13.060	145.57	74.54
C-50	80.933	93.688	.0039	.0056	6.727	19.661	12.848	147.62	87.31
C-52	100.790	112.112	.0045	.0056	5.904	20.163	11.426	149.40	106.45
C-53	111.776	123.002	.0056	.0068	5.881	20.307	11.352	150.87	117.39
C-54	122.838	134.652	.0068	.0079	5.860	21.742	11.974	152.59	128.75
C-55	138.327	149.435	.0079	.0091	5.486	22.145	11.296	154.23	143.88
C-56	149.228	160.826	.0091	.0102	5.472	23.578	11.826	156.45	155.03
C-57	159.402	170.742	.0105	.0118	5.452	23.319	11.600	157.17	165.07
C-58	170.390	183.314	.0118	.0137	5.447	26.846	13.266	158.07	176.85
C-59	182.705	194.476	.0137	.0155	6.777	19.852	12.061	159.96	188.59
C-60	37.367	51.516	.0006	.0022	6.632	20.969	14.178	140.66	44.44
C-61	51.247	63.684	.0017	.0028	6.624	18.726	12.479	142.54	57.47

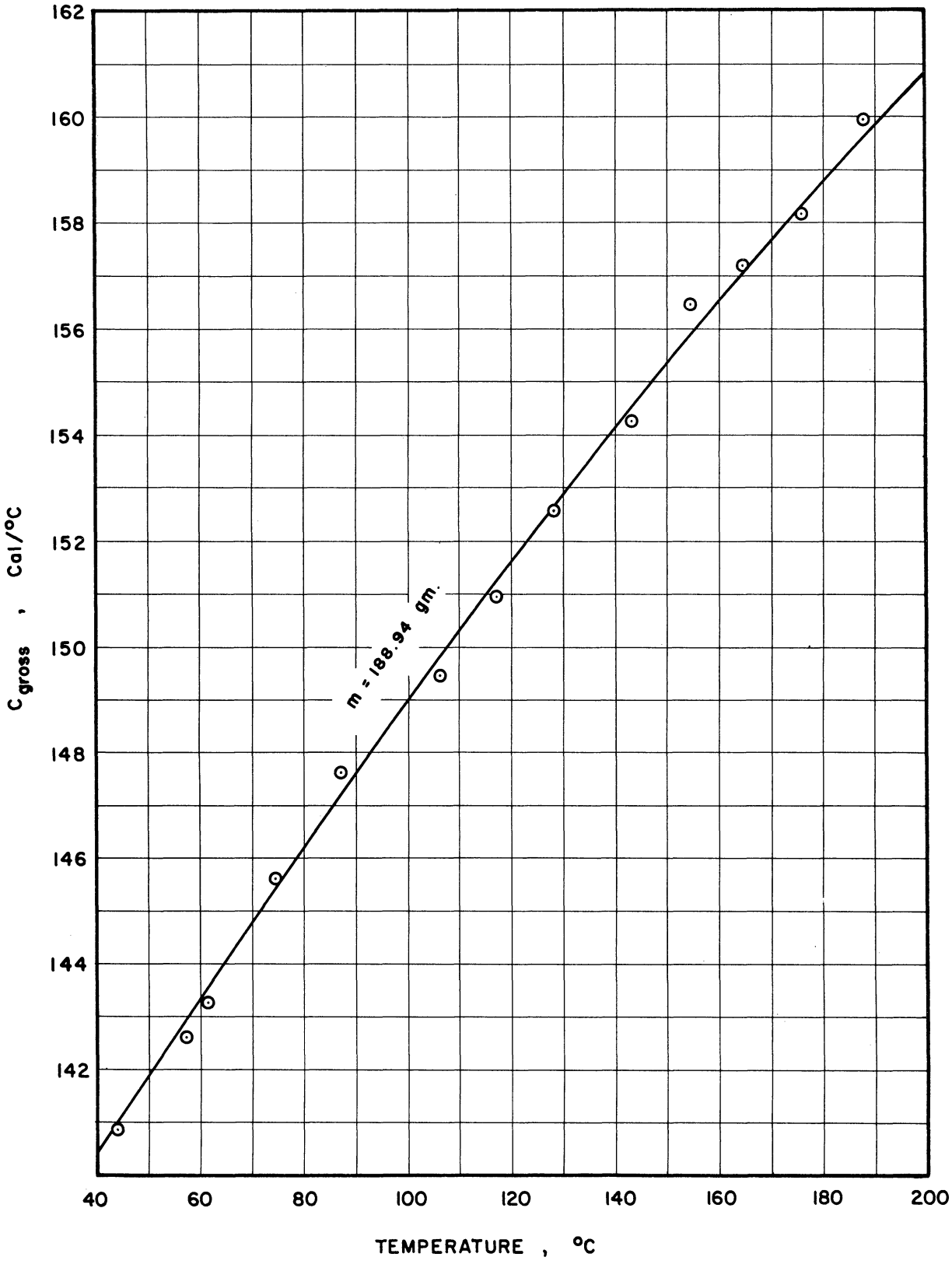

Figure D-6. Gross Heat Capacity with Chloropentafluoroethane Loading.

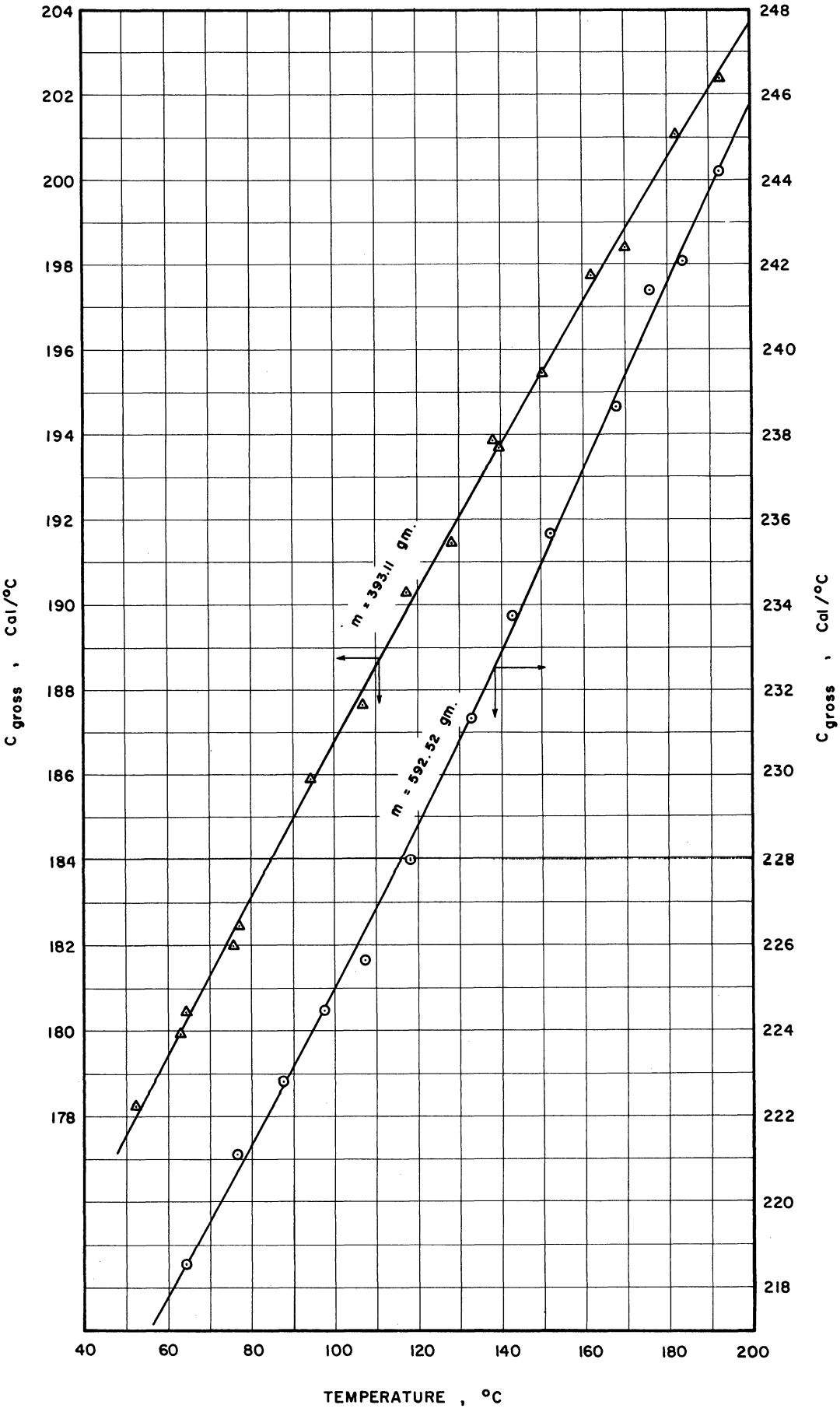

Figure D-7. Gross Heat Capacity with Chloropentafluoroethane Loading.

APPENDIX E

$C_v - C_v^*$ DERIVED FROM THE MARTIN-HOU EQUATION OF STATE

$$p = \sum_{i=1}^{i=5} \frac{A_i + B_i T + C_i \exp(-kT/T_c)}{(V - b)^i} \tag{E-1}$$

E-1 Derivation of the Basic Thermodynamic Relation

For the single phase of pure substance,

$$dA = -SdT - p\,dV$$

This leads to the following Maxwell relation

$$\left(\frac{dS}{dV}\right)_T = \left(\frac{dp}{dT}\right)_V \tag{E-2}$$

Differentiate (E-2) with respect to T at constant V, we have

$$\frac{d^2S}{dT_V dV_T} = \frac{d^2S}{dV_T dT_V} = \left(\frac{d^2p}{dT^2}\right)_V \tag{E-3}$$

Since

$$\left(\frac{dS}{dT}\right)_V = \frac{C_v}{T}$$

We obtain

$$\left(\frac{dC_v}{dV}\right)_T = \left(\frac{d^2p}{dT^2}\right)_V \tag{E-4}$$

or by substituting $V = 1/\rho$, we have

$$\left(\frac{dC_v}{d\rho}\right)_T = -\frac{T}{\rho^2}\left(\frac{d^2p}{dT^2}\right)_V \tag{E-5}$$

Integrating with respect to V or ρ, we obtain

$$C_v - C_v^* = -\int_V^\infty T \left(\frac{d^2p}{dT^2}\right)_V dV \tag{E-6}$$

or

$$C_v - C_v^* = -\int_0^\rho \frac{T}{\rho^2}\left(\frac{d^2p}{dT^2}\right)_\rho d\rho \qquad \text{(E-7)}$$

E-2 $C_v - C_v^*$ Formula for Martin-Hou Equation

The second derivative of Equation (E-1) with respect to T is

$$\left(\frac{d^2p}{dT^2}\right)_V = \left(\frac{k}{T_c}\right)^2 e^{-k\frac{T}{T_c}}\left\{\frac{C_2}{(V-b)^2} + \frac{C_3}{(V-b)^3} + \frac{C_4}{(V-b)^4} + \frac{C_5}{(V-b)^5}\right\} \qquad \text{(E-8)}$$

Combining this with Equation (E-6) we have

$$C_v - C_v^* = -\int_V^\infty T\left(\frac{k}{T_c}\right)^2 e^{-k\frac{T}{T_c}}\left\{\frac{C_2}{(V-b)^2} + \frac{C_3}{(V-b)^3} + \frac{C_4}{(V-b)^4} + \frac{C_5}{(V-b)^5}\right\} dV$$

$$= -\left[T\left(\frac{k}{T_c}\right)^2 e^{-k\frac{T}{T_c}}\left\{-\frac{C_2}{(V-b)} - \frac{C_3}{2(V-b)^2} - \frac{C_4}{3(V-b)^3} - \frac{C_5}{4(V-b)^4}\right\}\right]_V^\infty$$

$$= -T\left(\frac{k}{T_c}\right)^2 e^{-k\frac{T}{T_c}}\left\{\frac{C_2}{(V-b)} + \frac{C_3}{2(V-b)^2} + \frac{C_4}{3(V-b)^3} + \frac{C_5}{4(V-b)^4}\right\} \qquad \text{(E-9)}$$

or substituting $V = 1/\rho$, we have

$$C_v - C_v^* = -T\left(\frac{k}{T_c}\right)^2 e^{-k\frac{T}{T_c}}\left\{\frac{C_2\rho}{(1-b\rho)} + \frac{C_3\rho^2}{2(1-b\rho)^2} + \frac{C_4\rho^3}{3(1-b\rho)^3} + \frac{C_5\rho^4}{4(1-b\rho)^4}\right\} \qquad \text{(E-10)}$$

If $C_4 = 0$ as in case of "the improved Martin-Hou equation," we obtain

$$C_v - C_v^* = -T\left(\frac{k}{T_c}\right)^2 e^{-k\frac{T}{T_c}}\left\{\frac{C_2}{(V-b)} + \frac{C_3}{2(V-b)^2} + \frac{C_5}{4(V-b)^4}\right\} \qquad \text{(E-11)}$$

If $C_4 = 0$, $C_5 = 0$ as in the original Martin-Hou equation, we obtain

$$C_v - C_v^* = -T\left(\frac{k}{T_c}\right)^2 e^{-k\frac{T}{T_c}}\left\{\frac{C_2}{(V-b)} + \frac{C_3}{2(V-b)^2}\right\} \qquad \text{(E-12)}$$

APPENDIX F

CONSTANTS AND CONVERSION FACTORS

The constants and conversion factors used in this research are summarized here for convenience.

1 calorie = 1 thermochemical calorie = 4.1840 abs. joules

= 0.0412917 lit-atm.

1 Btu. = 1055.18 abs. joules = 5.4046 psi-cu ft

1 abs. watt minute = 14.3403 calories

$T^{\circ}K$ = $t^{\circ}C$ plus $273.16^{\circ}C$

$T^{\circ}R$ = $T^{\circ}K$ multiplied by 1.8 = $^{\circ}F$ + 459.69

1 atmosphere = 14.696 psi

R (the universal gas constant) = 1.985 Btu/lb mole-$^{\circ}R$

= 1.98719 cal/gm mole-$^{\circ}K$

= 0.0820544 lit. atm./gm mole-$^{\circ}K$

= 10.7315 psia-cu ft/lb mole-$^{\circ}R$

$h = 6.62377 \times 10^{-27}$ erg sec $(mol.)^{-1}$

$c = 2.997902 \times 10^{10}$ cm sec^{-1}

$k = 1.380257 \times 10^{-16}$ erg $(mol.)^{-1}$ $degree^{-1}$

$hc/k = 1.43868$

Molecular wt. of dichlorodifluoromethane = 120.924

Molecular wt. of chlorodifluoromethane = 86.476

Molecular wt. of tetrafluoromethane = 88.010

Molecular wt. of dichlorotetrafluoroethane = 170.936

Molecular wt. of chloropentafluoroethane = 154.477

The Martin-Hou equation's constants are as follows:

1. For chlorodifluoromethane:[26] P in psi, T in ^{o}R, V in cu ft/lb.

T_c = 664.5 deg.^{o}R., ρ_c = 32.76 lb/ft^3, P_c = 721.906 psia

A_1	= 0	B_1	= 0.12409802
A_2	= -3.7887702	B_2	= 1.2827656×10^{-3}
A_3	= 6.2780387×10^{-2}	B_3	= 1.1458314×10^{-6}
A_4	= $-1.0017004 \times 10^{-3}$	B_4	= 0
A_5	= 3.8423977×10^{-6}	B_5	= 3.8881629×10^{-9}
C_1	= 0	C_5	= $-7.5862255 \times 10^{-5}$
C_2	= -35.797897	b	= 6.5367861×10^{-3}
C_3	= 0.99056314	k	= 3.75
C_4	= 0		

2. For tetrafluoromethane:[8] Unites are the same as above.

T_c = 409.50^{o}R, P_c = 543.16 psia, ρ_c = 39.06 lb/cu ft

A_1	= 0	B_1	= 0.12193362
A_2	= -3.1553788	B_2	= 3.2480704×10^{-3}
A_3	= 0.05630627	B_3	= $-5.6586787 \times 10^{-5}$
A_4	= -3.157538×10^{-4}	B_4	= 0
A_5	= $-1.5210836 \times 10^{-6}$	B_5	= 6.6533754×10^{-9}
C_1	= 0	C_5	= $-3.5786565 \times 10^{-6}$
C_2	= -2.1911976	b	= 5.7104970×10^{-3}
C_3	= -0.052630252	k	= 5.0
C_4	= 0		

3. For dichlorotetrafluoroethane:[25] Units are the same as before.

T_c = 753.95°R, P_c = 473.187 psia, ρ_c = 36.32 lb/cu ft.

A_1	= 0	B_1	= 0.627808
A_2	= -2.3856704	B_2	= 0.0010801207
A_3	= 0.034055687	B_3	= $-5.3336494 \times 10^{-6}$
A_4	= -3.857481×10^{-4}	B_4	= 0
A_5	= 1.6017659×10^{-6}	B_5	= 6.263234×10^{-10}
C_1	= 0	C_5	= $-1.0165314 \times 10^{-5}$
C_2	= -6.564348	b	= 0.005914907
C_3	= 0.16366057	k	= 3.0
C_4	= 0		

4. For dichlorodifluoromethane:[34] Units are the same as before.

T_c = 699.3°R, P_c = 596.9 psia, ρ_c = 34.84 lb/cu ft

A_1	= 0	B_1	= 0.088734
A_2	= -3.409727134	B_2	= $1.59434848 \times 10^{-3}$
A_3	= 0.06023944654	B_3	= $-1.879618431 \times 10^{-5}$
A_4	= $-5.4873007 \times 10^{-4}$	B_4	= 0
A_5	= 0	B_5	= $3.46883400 \times 10^{-9}$
C_1	= 0	C_5	= $-2.54390678 \times 10^{-5}$
C_2	= -56.7627671	b	= 0.0065093886
C_3	= 1.311399084	k	= 5.475
C_4	= 0		

No Martin-Hou equation has been developed for chloropentafluoroethane. Martin et al.,[30] however, correlated PVT data in the following form:

$$P = -\frac{3.1857748}{V^2} - \frac{0.028919059}{V^3} - \frac{17.4448 \times 10^{-6}}{V^4}$$

$$+ T\left[\frac{0.06941}{V} + \frac{0.00267975}{V^2} - \frac{1.18424 \times 10^{-5}}{V^3} - \frac{1.67627 \times 10^{-7}}{V^4}\right]$$

$$- \frac{1}{T^3}\left[\frac{8343505}{V^2} - \frac{5984.903}{V^4}\right]$$

BIBLIOGRAPHY

1. Albright, L. F., Galegor, W. C. and Innes, K. K., J. A. C. S. 76 6017 (1954).

2. Amagat, E. H., Annales de Chimie et de Physique, 5^{e} series, xxii, 353-389 (1881).

3. American Society for Metals, Metal Handbook, Cleveland, 555 (1948).

4. Barcelo, J. R., J. of Research, N. B. S., 44, 521, RP 2099 (1950).

5. Beattie, J. A., and Bridgeman, O. C., Proc. Am. Acad. Arts and Sci. 63, 229-308 (1928).

6. Benedict, M., Webb, G. B., and Rubin, L. C., J. Chem. Physics, 8, 334 (1940) and 10, 747 (1942).

7. Bennewitz, K. and Splittgerber, E., Z. Phys. Chem., 124, 49-68 (1928)

8. Bhada, R. K., The Construction and Operation of a Variable Volume Isothermal Bomb for Determining the PVT Behavior of Gases and Liquids, Ph. D. thesis, Univ. of Mich. (1960).

9. Chari, N. C. S., Thermodynamic Properties of Carbon Tetrafluoride, Ph. D. thesis, Univ. of Mich. (1960).

10. Connolly, T. J., Sage, B. H. and Lacey, W. N., Ind. Eng. Chem. 43, 946 (1951). This is the most recent one in the long series.

11. Curtiss, C. F., Boyd, C. A., and Palmer, H. B., J. Chem. Phys., 19, 801 (1951).

12. de Nevers, N. H., The Constant Volume Heat Capacity of Gaseous Perfluorocyclobutane and Propylene, Ph. D. thesis, Univ. of Mich. (1958).

13. de Nevers, N. H. and Martin, J. J., A. I. Ch. E. J., 6, 43-49, (1960).

14. Dieterici, C., Ann. der Physik, 12, 145-185 (1903).

15. Dodge, B. F., Chemical Engineering Thermodynamics, McGraw-Hill, N. Y., p. 167 et seq. (1944).

16. Eucken, A. and Hauck, F., Z. Phys. Chem., 134, 161-189, (1928).

17. Gelles, E. and Pitzer, K. S., J. A. C. S. 75, 5259-5267 (1953).

18. Glockler, G. and Sage, C., J. Chem. Phys., 9, 387, (1941).

19. Goubeau, J., Bues, W. and Kampmann, F. W., Z. Anorg. Allgem. Chem., 283, 123 et seq. (1956).

20. Hoge, H. J., J. Res. NBS, 44, 321 (1950).

21. Hoge, H. J., Review Sci. Instrument, 20, 59-61 (1949).

22. Joly, J., Proc. Roy. Soc., 55, 390 (1894).

23. Keenan, J. H., Thermodynamics, John Wiley, N. Y., p. 409 (1941).

24. Kilpatrick, J. H. and Pitzer, K. S., J. of Res. NBS, 37, 163 (1946).

25. Martin, J. J., J. Chem. and Eng. Data, 5, 334-336 (1960).

26. Martin, J. J., Gifford, M. J., Welshans, L. M. and Gryka, G. E., Thermodynamic Properties of Chlorodifluoromethane, Univ. of Mich. Res. Inst. Project No. M777, Ann Arbor, Mich. (1953).

27. Martin, J. J. and Hou, Y. C., A. I. Ch. E. Journal, 1, 142-151 (1955).

28. Martin, J. J., Kapoor, R. M., Bray, B. G., Salive, M. L. and Bhada, R. K., Data and Equation for the Thermodynamic Properties of "Freon-C 318" Perfluorocyclobutane, Univ. of Mich. Eng. Res. Inst., Report No. 1777-29-T, Ann Arbor (1956).

29. Martin, J. J., Kapoor, R. M. and de Nevers, N., A. I. Ch. E., 5, 159-160 (1959).

30. Martin, J. J., Long, R. D., Marks, J. D., Service, W. J., Jr., Taylor, R. C. and Weaver, D. E., Thermodynamic Properties of "Freon-115", Univ. of Mich. Eng. Res. Inst. Report, Proj. No. M777, Ann Arbor (1951).

31. Martin, J. J., Long, R. D. and Service, W. J., Jr., Physical and Thermodynamic Properties of Various "Freons", Univ. of Mich. Eng. Res. Inst. Report, Proj. No. M777, Ann Arbor (1951).

32. Masi, J. F., JACS, 74, 4738 (1952).

33. McCullough, J. P., Finke, H. L., Hubbard, W. N., Good, W. D., Pennington, R. E., Messerly, J. F. and Waddington, G., JACS, 76, 2661 (1954).

34. McHarness, R. C., Eiseman, B. J., Jr., and Martin, J. J., Refrig. Eng. 63, 31 (1955).

35. Michels, A. and Strijland, J., Physica, 18, 613-628 (1952).

36. Osborne, N. S., Stimson, H. F. and Sligh, T. S., Jr., Sci. Papers of NBS, Number 503 (1924).

37. Pall, D. B., and Broughton, J. W., Canadian J. of Research, A-16, 230, 449 (1938).

38. Pitzer, K. S. and Gelles E., The Vibrational Frequencies of the Halogenated Methanes and the Substitution Product Rule API Res. Proj. No. 50, Univ. of Calif. (1952).

39. Reinganum, M., Ann. der Physik, 18, 1008 (1905).

40. Schaefer, K., Fortschritt Chem. Forsch., 1, 61-118 (1949).

41. Schneider, W. G. and Chynoweth, A., J. Chem. Phys., 19, 1607 (1951).

42. Smith, D. C., Alpert, M., Saunders, R. A., Brown, G. M. and Moran, N. B., Infrared Spectra of Fluorinated Hydrocarbons Naval Res. Lab. Report, 3924 (1949).

43. Smith, D. C., Nielsen, J. R., Berryman, L. H., Claasen, H. H., and Hudson, R. L., Spectroscopic Properties of Fluorocarbons and Fluorinated Hydrocarbons, Naval Research Laboratory Report 3567, (1949).

44. Trautz, M. and Grosskinsky, O., Ann. der Physik, 67, 462 (1922).

45. Weissman, H. B., Meister A. G. and Cleveland, F. F., J. Chem. Phys., 29, 72-77 (1958).

46. Young, S., Proc. Phys. Soc. London, 602 (1894-5).